



**University of
Zurich**^{UZH}

Department of Geography

Dryas octopetala L.:
Assessment of the dendrogeomorphological
potential for past debris-flow events
reconstruction in the Alps

GEO 511 Master's Thesis

Author

Giulia Fontana
10-928-471

Supervised by

Dr. Holger Gärtner

and

Prof. Dr. Markus Egli

Eidg. Forschungsanstalt WSL
Zürcherstrasse 111
CH-8903 Birmensdorf
holger.gaertner@wsl.ch

University of Zurich - Irchel
Winterthurerstrasse 190
CH-8057 Zurich
markus.egli@geo.uzh.ch

Faculty representative

Prof. Dr. Markus Egli

21. April 2017

Department of Geography, University of Zurich

LIST OF CONTENTS

ABSTRACT	7
INTRODUCTION	8
RESEARCH QUESTION AND HYPOTHESES.....	9
DEBRIS FLOWS, DENDROGEOMORPHOLOGY AND MOUNTAIN AVENS.....	11
DEBRIS FLOW IN DENDROCHRONOLOGY.....	11
DENDROCHRONOLOGY AND DENDROGEOMORPHOLOGY	13
DRYAS OCTOPETALA L.	16
STUDY SITE.....	18
THE RESEARCH AREA	18
GEOLOGY.....	22
SOIL.....	23
VEGETATION.....	24
CLIMATE	24
STUDY SITE	26
METHODS.....	27
SAMPLING.....	27
SAMPLE PREPARATION.....	29
ANALYSING DRYAS OCTOPETALA	32
<i>Visual analysis</i>	32
<i>Cross-Dating</i>	33
<i>Correlations and error calculation</i>	34
RESULTS	35
RELATIONSHIP BETWEEN AGE AND GROWTH PATTERN.....	35
CROSS-DATING	39
<i>Multi-radii cross-dating of the sample R1 RD 003a</i>	40
<i>R1LD</i>	41
<i>R1RD</i>	43
<i>Relationship between groups and the Dryas octopetala's growing positions</i>	45
CORRELATION BETWEEN RING GROWTH AND CLIMATIC FACTORS.....	46
DISCUSSION	49
CROSS-DATING THE DWARF SHRUB DRYAS OCTOPETALA	49
<i>Influences on the results</i>	49
<i>Cross-dating groups and correlating temperature/ precipitation records</i>	51
SPATIAL DISTRIBUTION OF DRYAS OCTOPETALA ON THE LEVEES	54
INFLUENCE OF SAMPLING AND SAMPLE QUANTITIES ON THE CROSS-DATING PROCESS	54
RECOSTRUCTION OF DEBRIS-FLOW EVENTS WITH DRYAS-OCTOPETALA	56
CONCLUSION	57
LITERATURE.....	59
APPENDIX.....	66
APPENDIX A – DATA OF THE COLLECTED SAMPLES IN R2 AND R3	66
APPENDIX B – SPECIFIC CROSS-DATING DATA OF R1	67
APPENDIX C – CLIMATE DATA	69
APPENDIX D – CDI-VALUES OF R1 BEFORE AND AFTER CROSS-DATING.....	71
APPENDIX E – GLK-VALUES OF R1 BEFORE AND AFTER CROSS-DATING.....	74
APPENDIX F – GSL-VALUES OF R1 BEFORE AND AFTER CROSS-DATING	78

ACKNOWLEDGMENTS82
PERSONAL DECLARATION83

IMAGE DIRECTORY

Image 1.	Dryas octopetala.....	17
Image 2.	The Marl-Graben North-West of Selden.....	18
Image 3.	Several end moraines show the retreat phases of the glacier.....	20
Image 4.	The Marl-Graben is located just below the moraines.....	21
Image 5.	Tectonic map of the Ortler-Region.....	22
Image 6.	Panorama of the eastern side of the Ortler.....	23
Image 7.	Four soil profiles that were taken during the field course.....	24
Image 8.	Channels R1, R2 and R3.....	26
Image 9.	Sampled Dryas octopetala shrubs.....	28
Image 10.	Sample preparation process.....	30
Image 11.	Dryas octopetala sample.....	31
Image 12.	Sample R1RD 003a with the three measured radii.....	33
Image 13.	Detail of the sample R2 RD 04.....	49

TABLE DIRECTORY

Table 1.	Monthly average of the amount of rainy days and precipitation in mm.....	25
Table 2.	Statistical parameters of the boxplot in figure 4	39
Table 3.	CDI-values of R1 LD group III.....	45
Table 4.	Data – R2LD.....	66
Table 5.	Data – R2RD	66
Table 6.	Data – R3LD.....	66
Table 7.	Data – R3RD	66
Table 8.	Cross-dating-data of the left levee of R1	67
Table 9.	Cross-dating-data of the right levee of R1	68
Table 10.	Monthly average temperature in Sulden.....	69
Table 11.	Monthly average volume in mm of precipitation in Sulden	70
Table 12.	CDI-values of group I R1LD.....	71
Table 13.	CDI-values of group II R1LD.....	71
Table 14.	CDI-values of group III R1LD.....	71
Table 15.	CDI-values of group 0 R1LD.....	72
Table 16.	CDI-values of group I R1RD	72
Table 17.	CDI-values of group II R1RD	72
Table 18.	CDI-values of group III R1RD	72
Table 19.	CDI-values of group IV R1RD.....	73
Table 20.	CDI-values of group V R1RD.....	73
Table 21.	CDI-values of group 0 R1RD	73
Table 22.	CDI-values of multiple radii of R1 RD 003a	73
Table 23.	GLK-values of group I R1LD	74
Table 24.	GLK-values of group II R1LD.....	74
Table 25.	GLK-values of group III R1LD.....	74
Table 26.	GLK-values of group 0 R1LD.....	75
Table 27.	GLK-values of group I R1RD	75
Table 28.	GLK-values of group II R1RD	75
Table 29.	GLK-values of group III R1RD	76
Table 30.	GLK-values of group IV R1RD	76
Table 31.	GLK-values of group V R1RD	76
Table 32.	GLK-values of group 0 R1RD	76
Table 33.	GLK-values of multiple radii of R1 RD 003a	77
Table 34.	GSL-values of group I R1LD	78
Table 35.	GSL-values of group II R1LD	78
Table 36.	GSL-values of group III R1LD	79
Table 37.	GSL-values of group 0 R1LD	79
Table 38.	GSL-values of group I R1RD.....	79
Table 39.	GSL-values of group II R1RD.....	80
Table 40.	GSL-values of group III R1RD.....	80
Table 41.	GSL-values of group IV R1RD	80
Table 42.	GSL-values of group V R1RD	81
Table 43.	GSL-values of group 0 R1RD.....	81
Table 44.	GSL-values of multiple radii of R1 RD 003a.....	81

FIGURE DIRECTORY

Figure 1.	Distribution of the age of the shrub on the levees before and after the cross-dating.....	35
Figure 2.	Relationship between age and growth position of the thin sections with piths. .	37
Figure 3.	Samples in the two sampling sites (A and B) of the channel R1	38
Figure 4.	Age distribution in the different channels levees.....	39
Figure 5.	Cross-dating between multiple radii of the sample R1RD 003a	41
Figure 6.	Cross-dated group I of the levee R1LD	42
Figure 7.	Cross-dated group II of the levee R1LD	42
Figure 8.	Cross-dated group III of the levee R1LD	42
Figure 9.	Cross-dated samples of group I in R1RD.....	43
Figure 10.	Cross-dated samples of group II in R1RD.....	43
Figure 11.	Cross-dated samples of group III in R1RD.....	44
Figure 12.	Cross-dated samples of group IV in R1RD	44
Figure 13.	Cross-dated samples of group V in R1RD	44
Figure 14.	Distribution of the grouped samples on the levee	46
Figure 15.	Correlation of R1LD group-means and the precipitation	47
Figure 16.	Correlation of R1RD group-means and precipitation	47
Figure 17.	Correlation of R1LD group-means and temperatures	48
Figure 18.	Correlation of R1RD group-means and temperatures.....	48
Figure 19.	Cross-dated groups of the left levee	52
Figure 20.	Cross-dated groups of the right levee	52

ABSTRACT

Debris flows are natural hazards endangering human life and infrastructure in alpine areas. It is therefore important to gain a detailed understanding of these events by reconstructing the frequency of past debris flows. The aim of the study presented is to analyse as to what extent the pioneer dwarf shrub mountain avens (*Dryas octopetala* L.) can be used to reconstruct debris flow events in the alpine site of the Marlt-Graben.

The Marlt-Graben is situated at the foot of the Ortler mountain peak, north of the village of Suldén in South Tyrol (Italy). The site is highly affected by debris-flows and avalanche events. Consequently the mountain slope shows a series of very distinct debris flow channels composed of mostly calcareous moraine material, which are partly covered by vegetation such as mountain pine (*Pinus mugo*) and mountain avens. This dwarf shrub species is restricted to calcareous substrates and is widely spread in respective high mountain and arctic regions. Within three debris flow channels with differing vegetation cover densities, 150 mountain avens plants were sampled and their distance to the channel bed was measured. One thin section per plant was cut from the main stem using a GSL1-microtome. The samples were bleached, stained, embedded in Canada balsam and then each section was photographed under a microscope. Thereafter, ring-width measurement was performed using WinDendro. In a further step the cross-dating of the samples of each levee of one channel was attempted using TsapWin.

First results show a relation between the mean age of the plants on the levees and the respective density of the vegetation cover. Unfortunately, no common growth pattern on the levees could be observed relating to the distance of the plant to the channel bed and the age of the plant. While determining a minimal plant age was possible, the cross-dating was difficult. The plants did not show a common growth signal. However, groups of plants with similar growth patterns were found. Nevertheless, precise cross-dating was not possible based on single sections of each plant.

These results indicate that while *Dryas octopetala* can be used to define the minimum number of years since the last erosive event happened, a precise dating of events within the channels based on cross-dating of these shrubs is hardly possible.

INTRODUCTION

In the past years, the topic of natural hazards, such as mass movements, has repeatedly been the centre of discussions in scientific publications. Natural hazards remain a current topic of interest not only due to their dangerous destructive potential but also because of the close connection between triggering events and climate change (Dowling and Santi 2014, 204; Raetzo et al. 2002, 263; Stoffel and Huggel 2012, 421-423). Many authors have linked their studies of mass movements to environmental changes (Collison et al. 2000; Damm and Felderer 2013; Dehn et al. 2000; Dietrich and Krautblatter 2016; Jomelli et al. 2009; Pavlova et al. 2014; Stoffel and Huggel 2012; Sewell et al. 2015 and van den Heuveln et al. 2016).

Debris flows are some of the most important and dangerous natural hazards in high mountain regions. The increasing mountain tourism as well as difficulties in the prediction of such events render debris-flow events a serious threat to human life and infrastructure (Arbellay et al. 2010, 399; Baumann and Keiser 1999, 128; Beniston and Stephenson 2004, 1). The prediction of such events is deemed extremely difficult due to differences in local conditions. If the observation of some of the primary factors allows in one place a correct prediction of a debris flow, the same favourable conditions in a different location might not lead to a similar event. The disparities in predictions are possibly due to varying interplays with local factors. Nevertheless, a higher content of water in the soil is seen as one of the fundamental triggers for debris flow events (Bollschweiler und Stoffel 2010, 186; Bollschweiler et al. 2006, 337-338; Chen 2006, 3-14; Owczarek et al. 2013, 75; Saemundsson et al. 2013, 171).

Predictions and mitigation strategies of hazardous debris flows gain further importance in connection with studied probable impacts of climate change. The latest Intergovernmental Panel on Climate Change (IPCC) report outlines a change in the intensity and frequency of rainfall. An increase of above average precipitation promotes a higher probability of natural hazards such as debris flows. The degradation of permafrost and glaciers in high mountains because of rising climate temperatures also influences the probability of such an event. The retreat of permafrost in the depth of sediment reservoirs (e.g. moraines) in high mountains induces a loss of cohesion in sediments and a negative effect on slope stability. These newly formed loose sediment layers serve as perfect material input for debris-flow events (Baumann

and Keiser 1999, 128; Beniston and Stephenson 2004, 1-8; Bollschweiler and Stoffel 2010, 186, 191; Johnson and McCuen 1996, 161-162; IPCC 2014, 6-7; Stoffel and Hugel 2012, 429-430).

Arbellay et al. (2010, 399) emphasise the importance of studying relicts from past events to improve the still-lacking prediction of debris flow. Whereas Bollschweiler und Stoffel (2010, 186) stress further the importance of giving priority to gain a deeper understanding of past and present events before switching to the future. The reconstruction of former debris-flow activity is, however, difficult due to a scarcity of historical record. The reconstruction of past events has attempted by applying different methods such as the analysis of arial images, discontinuity distributions, the observation of typical geometric characteristics in the landscape, lichenometry, cosmogenic nuclides analysis and dendrogeomorphology (Corominas et al. 1996 166-172).

Dendrogeomorphology implements vegetation (tree rings, scars, etc.) as an information archive of unusual and interfering influences such as natural hazards. The majority of studies in dendrogeomorphology as well as dendrochronology concentrated mostly on conifers and only in infrequent cases on broadleaved trees. However, in the past decade the interest in shrubs and dwarf shrubs has increased significantly (Au and Tardif 2007, 585; Gärtner et al. 2004, 198; Hopp et al. 1987, 1-2; Szymczak et al. 2010, 107-108; Trappmann et al. 2013, 704). This master thesis will make a contribution to the research area based on dwarf shrubs *Dryas octopetala* L. The aim is to investigate how this dwarf shrub is suited for dendrogeomorphological reconstructions.

RESEARCH QUESTION AND HYPOTHESES

As indicated, in this master thesis the potential in dendrogeomorphological reconstruction of past debris flow events of the dwarf shrub *Dryas octopetala* L. (mountain avens) will be evaluated. This aim will be archived by analysing the growing *Dryas octopetala* in three adjacent debris-flow channels in the “Marlt”-debris fan near Sulden (IT). The age and ring growth of the dwarf shrubs will be investigated along the largest sample radius by analysing thin sections of the stems. The cross-dating of the samples of one channel will be attempted and the results analysed.

The master thesis will be subdivided into the following chapters: Firstly, an introduction on debris flows, dendrogeomorphology and *Dryas octopetala* will be presented. In a second step the field site will be specifically introduced. In the description of the methodological procedure a more precise description of the sampling location, sampling criteria, sample preparation and analyse proceedings will follow. Further, the results of the analyses will be presented. Thereby the following hypotheses will be tested:

- a) A growth pattern on the channel levees channels exists.
- b) The age distribution of the dwarf shrubs in the different levee correlate to the vegetation cover density.
- c) Further, it is hypothesised that debris flows events and avalanches are recorded as disturbances in the tree rings and therefore measurable. Moreover, it is presumed that the age of the oldest *Dryas octopetala* corresponds to the minimum time since the last great erosive event process (Anderson 1967; Bär et al. 2006; Elkington 1971, 889-890; Jay et al. 2012).
- d) The ring widths correlate with climate data (temperature and precipitation).

Concluding the research question, as to what extent tree rings and the anatomical analyses of *Dryas octopetala* trunks permit the deduction of the activity and history of debris flow events in the southern Alps, this will be discussed and answered.

DEBRIS FLOWS, DENDROGEOMORPHOLOGY AND MOUNTAIN AVENS

DEBRIS FLOW IN DENDROCHRONOLOGY

Debris flows are difficult to define exactly. Many authors have tried to classify different flowing mass movements, such as mud flows, hyperconcentrated flows, landslides and debris flows. Each classification had different foci. Furthermore, the difference between specific mass movements is very small (Coussot and Meunier 1996, 209-211).

Costa (1984, 268) uses a broader general definition for debris flows, which includes mudflow, lahars and debris avalanches. He describes further the movement as a gravitation induced transport of water, air and granular debris. Corominas et al. (1996, 161) define a debris flow as a melange of solid material (with a wide range of grain size) and a variable content of water. These two components are blended into a muddy-slurry mass. Similarly, Johnson and McCuen (1996, 161) describe a debris flow as a voluminous muddy mix of air, granular debris and water, which moves downslope with varying velocities. Debris flows occur in form of a sequence of surges, which in varying intervals flow downslope. These impulses of debris flows are caused by brief damming (e.g. remnant channels in their path) in the upperpart of the flow track. A debris flow has an elongated shape with a front rich in coarse debris. It moves as a viscous debris-water package. Nearly no difference in velocities within the flow and amongst the solid and fluid components exist. The only exception exists at the sides of the flow, where the mass of debris and moisture becomes shallower and the friction influences the velocity as well as the debris deposition. The lateral levees of a debris flow, besides the lateral displacement of debris during the flow, might be built up due to erosion at the sides or the overflowing of already existing channel levees (Costa 1984, 273; Coussot and Meunier 1996, 211-214; Corominas et al. 1996, 163-177).

Debris flows have a wide manifestation spectrum. These events differentiate in size, velocity and sediment content. Debris flows can be very slow, but can also reach high velocities. Coussot and Meunier (1996, 213) specify a velocity range between 0.5m/s and 10m/s. They also add that some authors accredit debris-flow speeds of even 20m/s. Johnson and McCuen compare velocities of avalanches (12m/s) as an upper limit for debris-flows. The speed of a debris flow depends on the "...character of the debris – the size, concentration and sorting of material, and because of channel geometry including shape, slope, width and sinuosity" (Costa

1984, 273) (Owczarek 2010, 51; Takahashi 1991, 63, 105; Johnson and McCuen 1996, 161-162; Malik and Owczarek 2009, 57).

Johnson and McCuen (1996, 162-167) defined primary factors, which have an influence on the potential occurrence of debris flows: "...geology and the topography of the watershed, soil type, climate, run-off, antecedent moisture conditions and ground cover...". A further important factor is the availability of loose and poorly sorted sediments to initiate the solid part of the debris flow. Moraine deposits and weathered rocks are possible sediment sources (Corominas et al. 1996, 173). Further, as a requirement, the deposited sediment should be on steep bare slopes ($>20^{\circ}$ - 30°), which are connected with a source of water such as "...rainfall, snowmelt, [...] glacial outburst flood and rapid drainage of volcanic crater lakes" (Costa 1984, 269-270). Corominas et al. (1996, 172-173) as well Costa emphasise the importance of a higher influx of water as a trigger for debris flows. They specify amongst other causes, the role of intensity and duration of precipitation as uncommon higher water input. Coussot and Meunier (1996, 214-215) differentiate mostly between two processes, which lead to debris-flow events. Firstly, a debris flow will occur through evolution of another flowing mass movement, such as a landslide or slope failure. This happens by increasing the slope of the flow or the water content. Secondly, by "...a conjunction of small-scale bank slides or collapses, bed erosion and solid transport" (Coussot and Meunier 1996, 215) in a catchment areas (Corominas et al. 1996, 173; Costa 1984, 269).

Debris-flow relicts can be found either at the end of valleys and gullies in the form of accumulated debris cones and debris fan. They can be recognised by the channel forming ridges with a lobe-shaped end. The occurrence of debris flow forms a channel with a V-shaped cross section. The levees are composed by non-sorted deposited material. The heads of past debris flows are formed like lobes. The levees as well as the lobes give evidence of the direction of the flow. However, lobes can additionally indicate an intersection and break-up of a younger debris-flow through the deposits of an older event. This geomorphological shapes can be often observed in high mountain regions and arctic regions (Bollschweiler et al. 2006, 337; Corominas et al. 1996, 161-165; Costa 1984, 271, 292; Gärtner et al. 2003, 211; Owczarek et al. 2013, 75; Owczarek 2010, 51).

Debris flows as destructive events are considered a main threat for human life, infrastructure, villages, agriculture and economy in high mountain areas in many parts of the world. Therefore, an overall interest on studying how a such mass movement takes place and how it could be stopped or predicted exists (Arbellay et al. 2010, 399; Baumann and Keiser 1999, 128; Beniston and Stephenson 2004, 1; Corominas et al. 1996, 178; Costa 1984, 268).

One of several analysis approaches of past debris-flow events is the dendrogeomorphological approach. Dendrogeomorphology is based on the principle that vegetation can be used as an in situ information archive to reconstruct the magnitude, the date, direction of the flow and frequency of mass movements (Arbellay et al. 2010, 399; Dietrich and Krautblatter 2016; Hopp et al. 1987, 3; Owczarek et al. 2013, 77; Stoffel et al. 2005; Stoffel et al. 2008; Youberg et al. 2014).

DENDROCHRONOLOGY AND DENDROGEOMORPHOLOGY

Andrew Ellicott Douglas was the first scientist to examine the potential of using tree rings for dating and gathering of climate information. In 1904 he discovered the process of cross-dating thus starting the scientific field of study dendrochronology. In the 1970's dendrochronological research evolved from a practice consisting mostly of dating into an environment-analysing study area. Dendrochronology, however, is still based on the same principle: each year a tree produces during its "...vegetation period..." (Stoffel and Bollschweiler 2008, 187) new cells. These grow in a cell zone between the bark and wood. They form consequently a new ring with the pith in the middle (assuming a concentric growth). In conifers it is easy to recognise that there are two types of new cells. In the beginning of the vegetation period the cells are rather large (early wood). Their purpose is mostly the transport of water and nutrients. Additionally, broadleaved trees also show a varying number of vessels with the same function. In autumn, plants need more stability to prepare for the winter and therefore they produce cells that are smaller but equipped with thicker cell walls (late wood). When the vegetation period comes to an end the growth ceases until the coming springtime. A new tree ring is formed. Tree rings are not only observed in conifers and broadleaved trees but also in shrubs and dwarf shrubs and are influenced by similar factors to trees. Analogically comparable reactions to externalities (e.g. wounding) were observed in trees, shrubs and dwarf shrubs. These visible

reactions are implemented in the research field of dendrogeomorphology (Au and Tardif 2007, 586; Robinson et al. 1990, 1-2; Stoffel and Bollschweiler 2008, 187-189; Szymczak et al. 2010, 107).

Dendrogeomorphology is a discipline, which aims to study geomorphological forms and processes by taking advantage of the information recorded by the vegetation. It is a cross between earth science (geomorphology) and ecology (dendrochronology). By mixing geomorphological and dendrochronological methods a new two-focus approach was developed. Firstly, the study site is to be observed and geomorphic processes have to be recognised and mapped. Secondly, for the dendrochronological analysis the “right” species and individuals depending on the research question should be located and sampled. The samples are then analysed employing dendrochronological, dendroanatomical or other approaches (Gärtner et al. 2004, 198-205; Gers et al. 2001, 164).

Dendrogeomorphology draws upon the fact that each disturbance caused by a landslide, a rock fall, an avalanche or a debris flow is reflected in some way by the vegetation (Trappmann et al. 2013, 704). Shroder (1980, 165) speaks of the “Process-event-response system”. He describes seven basic events (“... inclination, [...] shear of root wood, [...] corrosion, [...] burial of stem wood, [...] exposure of root wood inundation and [...] nudation” (Shroder 1980, 165)) and to them belonging responses (“... reaction wood growth, [...] growth suppression, [...] growth release, [...] ring termination and [...] new callus growth, sprouting, succession and miscellaneous structural changes in external and internal wood character” (Shroder 1980, 165)). The relationship between effect and counter effect has been observed, recorded and interpreted by many authors.

Trappmann et al. (2013) give in their paper an overview of the application of tree wounds and growth disturbance analysis in the reconstruction of rock fall events. A similar approach was used by Stoffel (2006), who analysed wounding on stem disks and cores caused by rock fall. Other studies such as Baumann and Keiser (1999), who implemented wounding analyses for the reconstruction of events on the Muletta debris fan, and Malik and Owczarek (2009) also base their dating of debris-flow or avalanche events on tree injury analysis. If a tree or a shrub is injured by moving debris the plant will react by compartmentalizing an area around the wound. Compartmentalization is a reaction in which a plant will build a barrier like isolation

zone near a wound to protect itself from penetrating insect and pest attacks. The production of "...chaotic callus tissue at the edges of the injury..." (Stoffel and Bollschweiler 2008, 188) will begin as soon the wounding is detected by the plant (Shroder 1980, 166; Stoffel and Bollschweiler 2008, 188; Stoffel and Bollschweiler 2009, 1015-1017).

Other studies concentrate on the dating of rapid flowing mass movements such as debris flows, which could cause a part-burial of the tree stem by deposited material. This might have two main responses. If the trunk of a tree is buried by debris the plant grows adventitious roots to become acclimatised to the new situation. During his research, Strunk (1997) dated these roots to determine when the burying mass movement took place and to build a better chronology of the events. However, he highlights with his work, that adventitious roots enable only a vague minimum-age dating due to missing rings (Shroder 1980, 166-167; Stoffel and Bollschweiler 2009, 1018; Strunk 1997).

Research on landslides and other slower mass movements are usually investigated with the help of reaction wood response. A moving landslide might incline, even if only slightly, a tree. Tilted trees produce as a counter reaction wood to correct their shifted growing axes. The production of either compression or tension wood results into an eccentric growth pattern of the rings. The changing ring width and the presence of reaction wood records the direction of the movement, the "... beginning as well as the length, amplitude and frequency..." (Strunk 1997, 138). Braam et al. (1987) and Gers et al. (2001) take advantage of this reaction to reconstruct and date landslide activities. The study of reaction wood was also used when the tilting was caused by a boulder impact, by an avalanche or another type of mass movement (Butler 1987, 65; Shroder 1980, 165-166; Stoffel and Bollschweiler 2009, 1017).

The basic event of nudation takes place when mass movements, for example a debris flow, erode the former vegetation cover and part of the top soil horizons. Owczarek et al. (2013) implemented pioneer dwarf shrubs to reconstruct such events. As an example, a freshly eroded debris-flow track needs time before first new pioneer plants and later bigger trees repopulate the area. The recolonization depends on different factors such as soil properties, climate and the forthcoming of seeds. Therefore, this method results often in a minimal date for the last erosive, burial or disruption event (Shroder 1980, 167-168; Stoffel and Bollschweiler 2008, 188-192; Strunk 1997, 138, 149).

DRYAS OCTOPETALA L.

Dryas octopetala L., also commonly known as mountain avens, appertains to the *Rosaceae* family (see image 1.). This family entails about 100 genera and 3000 species. The *Dryas octopetala* is per se a plant, which can be easily recognised due to its characteristic appearance. As a dwarf shrub it grows up to 5 cm in height above the ground under favourable conditions. It has long branches, which wind on and below the soil surface between the rocks and boulders. The usual short stem, the adventitious and the long roots grow also underground. Its phenotype resembles a pillow consisting of numerous small toothed, sometimes evergreen, leaflets. In high mountains, and northern sub-arctic and arctic regions the occurrence of *Dryas octopetala* is plentiful. This dwarf shrub can be found in mountain ranges as the Alps, the Pyrenees, the Apennines, the Caucasus and the Rocky Mountains. Furthermore, it has been located in colder climate regions such as Greenland, Iceland, Ireland, Britain, Scandinavia, Siberia, North Korea and Alaska. Their distribution and growth is mainly restricted by a maximum temperature isotherm. This isotherm differs slightly with the latitude and varies between 23°-27°C. The influence of temperature on the establishing potential of *Dryas octopetala* has been studied and observed by different authors such as Wada and Nakai (2004). This plant also prefers locations with free drainage, a yearly precipitation higher than 1000mm/yr and calcareous ground. As a pioneer dwarf shrub, *Dryas octopetala* grows mostly on immature soil, such as a lithosol, often covered by rocks and rough debris. The soils has usually a relatively basic pH, which, similarly to the isotherm, varies between locations (Elkington 1971, 887-900; Vasari 1999, 250; Pigott and Walters 1954, 99; Schweingruber et al. 2011, 383).



Image 1. Dryas octopetala (Lauber 2012).

While this plant was repeatedly used to investigate climate change influences in the arctic or the competitive behaviour in ecosystems, it has been used more rarely to analyse geomorphic processes (Eichel et al. 2015; Elkington 1971, 889-890; Henry and Molau 1997; Isselin-Non-dedeu and Bédécarrats 2007; Jay et al. 2012; Klanderud and Totland 2004; Klanderud and Totland 2005; Kozłowska and Rączkowska 2002; Vasari 1999, 250; Welker et al. 1997).

STUDY SITE

THE RESEARCH AREA

Sulden is a small village at the end of the Sulden-valley in Vinschgau, South Tyrol, North Italy. This area is situated in the south west of the Ortler-zone (see image 2.). The Sulden-valley was shaped by several glaciers still influencing the landscape. In the past the glacier “End der Welt-Ferner” represented a potential danger for Sulden while advancing. At that time, the village featured very few households. Mostly poor farmers and a priest. Today the glaciers “Suldener-Ferner”, “Ende der Welt-Ferner” and “Marlt-Ferner” have retreated. Meanwhile Sulden has grown and has become a tourist spot for hiking, climbing and skiing (Keppler 1938, 10; Langhans 1913, 32-34; Stötter et al. 2003, 244).

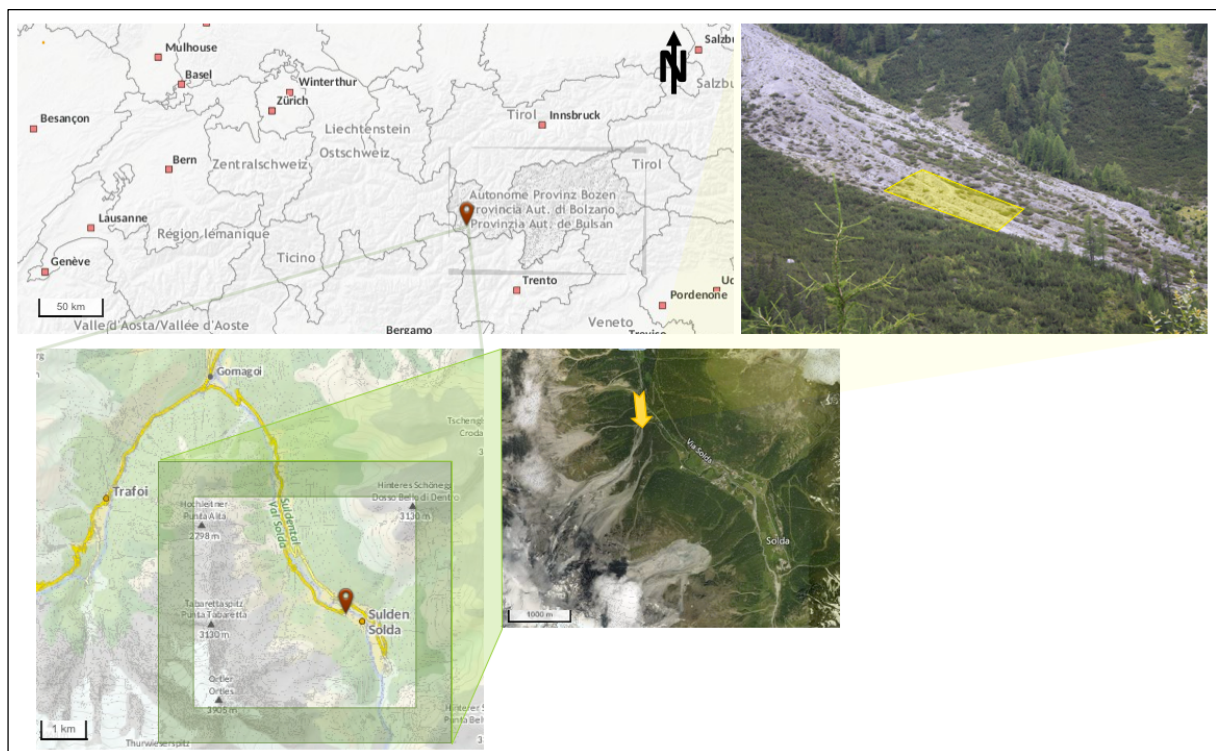


Image 2. The Marlt-Graben North-West of Sulden. In yellow the study site with the channels R3, R1 and R2 (Autonome Provinz Bozen-Südtiroler Informatik AG 2007; author 2017).

There is a large debris fan to the north-west of the village, at the foot of the Ortler mountain. This fan is known as the “Marlt-Graben”. In the past the Marlt-Ferner covered the Marlt-Graben. When the glacier retreated it left behind large end and lateral moraines. At present the

glacier has retreated just below the extremely steep East-wall of the mountain (see image 3.). This area is well known for avalanches and debris flows, transporting material from the upper moraines downwards. This area has been a subject of interest for some scientific studies on hazard protection management. For instance, Zischg et al. (2005) focussed on the success potential of the winter road. This second access road to Sulden aims to protect travellers from the hazardous processes of the Marlt-Graben. The area has also been part of studies on the effect of climate change on glacier activity and permafrost distribution. Stötter et al. (2003) analyzed past glacial retreat, advance and volumetric changes in the upper Sulden-valley. Furthermore, they focussed on the retreating area of discontinuous permafrost in the region. (Zischg et al. 2005, 235-23; Stötter et al. 2003, 245-262).

The Marlt-debris fan was accumulated at the bottom of large end moraines of the Marlt-Ferner (see image 4.). The massive glacial sediment deposits mould themselves in a curve along the sides of the "Marltberg" (Payer 1865) and lead to the debris fan. Higher up smaller end moraines are reflecting different retreat phases of the glacier. These end-moraine walls show a breakthrough in the middle, where the main flowing path is. This path is directly connected with the outermost channel (main channel) in the orographic left direction. The remaining areas of the debris fan are mostly cut off from the main channel by its levees and past deposits. Small channels show that a few events have overflowed the levees at certain locations. These more isolated parts of the fan are composed of a series of intersecting, overflowing and merging debris-flow channels as well as tongue shaped debris lobes. These geomorphological deposits correspond to Corominas et al. (1996, 177) and Costa (1984, 292) descriptions of typical debris flow relicts. The outer channels, on the orographic right side, have on average a lower vegetation cover than the ones in the centre of the fan. Additionally, the density of the vegetation seems to increase more downslope. At the sides of the fan several tall larches ("*Larix decidua* Mill." (Pignatti and Pignatti 2014, 159)) can be seen. On the orographic right side the fan is delimited by a slope with a dense cover of mountain pines. A small stream flows through the channel adjacent to the mountain pine "forest". This stream represents the only surface water discharge in the fan. Besides discharge variations of the small stream, the Marlt debris fan is also influenced by snow avalanches, debris-flow events, hikers, wild animals, livestock and students of the annual geochronological field course. The actual

research site of this master thesis is a segment of three channels, which run at the west border of the Marlt-Graben.



Image 3. Several end moraines show the retreat phases of the glacier. In the background the Marlt-Ferner can be seen (author 2016)



Image 4. The Marlt-Graben is located just below the moraines (author 2016)

GEOLOGY

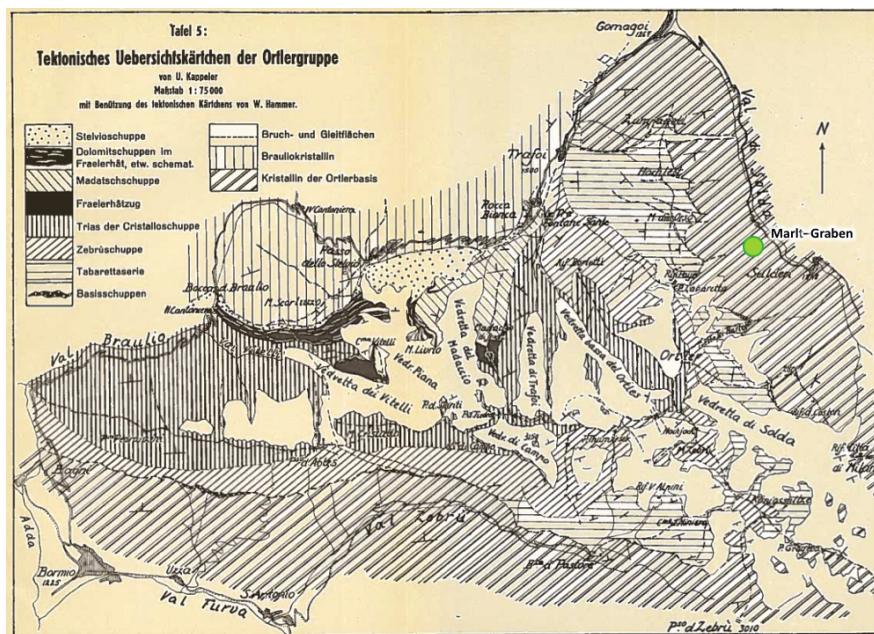


Image 5. Tectonic map of the Ortler-Region (Kepler 1938).

The debris fan of the Marlt-Graben has a maximum width of about 110m, and consists mostly of calcareous sediments of different sizes. Grain sizes of the material building up the fan vary from boulders of several metres in height to gravel of a few centimetres in diameter. However, the debris varies predominantly in coarseness from boulders and finer gravels with smaller particles in sand grain size (Blott and Pye 2001, 1239) or from boulders to coarse-medium sand grain (Wentworth 1922, 381). According to Stötter et al. (2003, 268) the origin of the material composing the fan are the moraines as well as material fallen from the upperpart of the Ortler and surrounding ridges like the Tabrettaspitze. The top of the Ortler massive is composed of mighty Dolomite banks, which lie above the crystalline bedrock. In the upper part of the Ortler, near the Tabretta pass, several tectonic faults were observed by Kepler (1938, 12-18, 99-101, 106, 131-134). Near sliding and shearing surfaces of the faults breccia were observed by Kepler (1938), which were influenced by metamorphic processes. At the boundary between the sediment deposits of the Trias and the underlying crystalline bedrock, Kepler identified a sharp fault. On this fault the Dolomite banks were pushed in the North/North-East direction above the bedrock. This fault extends from the Bärenkopf, just under the Marlt-Ferner and further west (see image 5. and image 6.). The bedrock below the Trias-sediments at the Marlt-Graben consists of "Orthogneiss-layers" (Kepler 1938, 16). At the northern border of the debris fan, at the edges of the Marltberg, the crystalline bedrock of the mountain

can be found on the surface. This is why occasional blocks of crystalline material are scattered between the calcareous moraine debris (Keppler 1938, 15-31, 99-101, 131-134).

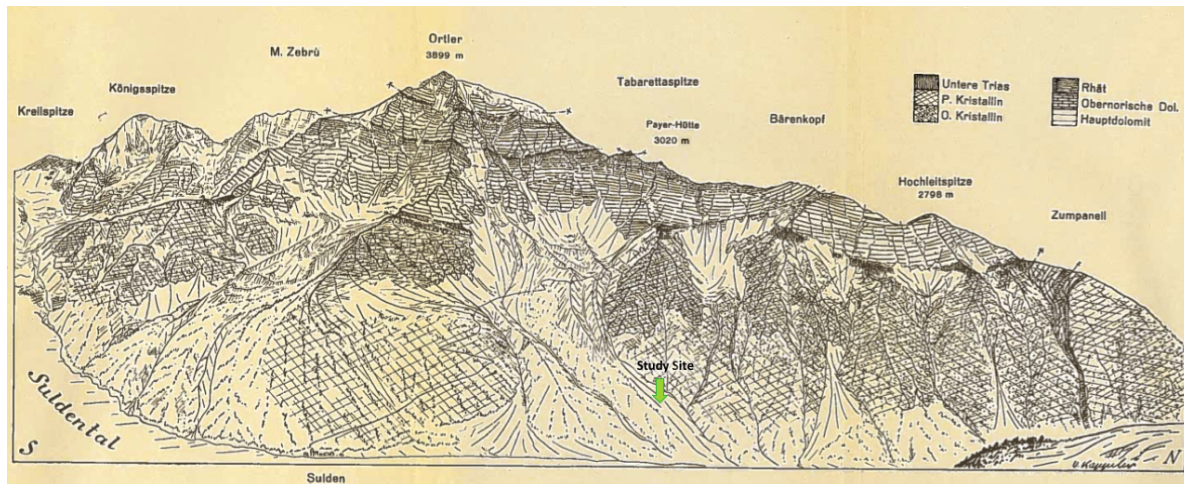


Image 6. Panorama of the eastern side of the Ortler. This image shows beside an overview of the study area the different geological layers. Further it is possible to see where the tectonic faults run through (see dashed lines) (Keppler 1938).

SOIL

This master thesis is associated with the field course of GEO 417 Environmental Archives of the University of Zurich. Therefore, some of the work, mostly the soil analyses and part of the sampling, originates from a group work during the course. Within the framework of the field course four soil profiles in three different channels of the study site were dug and analysed. The three channels analysed are located on the outermost part of the fan on the orographic right side. The first channel is the only one directly influenced by the stream. On this channel, a profile was taken on the orographic left levee. Furthermore, a soil profile on each levee of the adjacent channel were dug. The last profile was situated on the left levee in the next channel (see image 7.). The profiles displayed sequences of an O-C-horizon. The thickness of the O-horizon decreased the further the profile was situated away from the central zone of the fan. In the case of the last profile even a transition CA-horizon was seen between the O- and the C-horizon. These different observed soil development states, were mirrored by the PDI (Profile Development Index) values of the single profiles. The PDI-Values were the highest in the innermost sampled channel and the lowest in the outer channel. The chemical analysis of the soil samples showed a C-horizon rich of calcareous material with a pH between 7.19 and 8, which increased by increasing depth (Aus der Au et al. 2016, field report, 11-25).

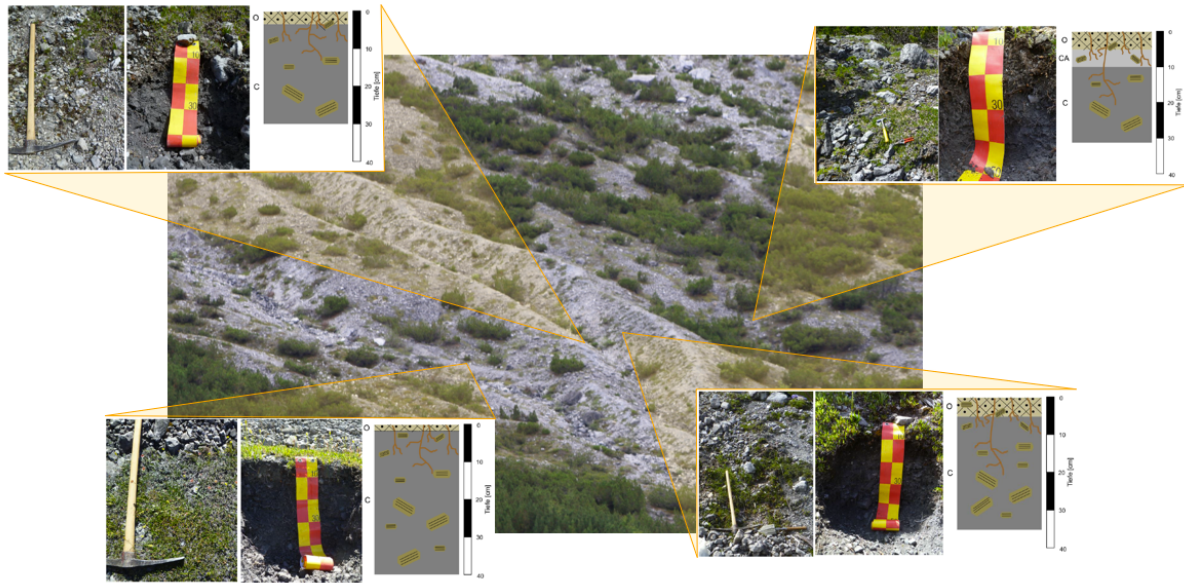


Image 7. Four soil profiles that were taken during the field course (author 2016; Aus der Au et al. 2016, field report, 11-25).

VEGETATION

The main vegetation covering the fan are mountain avens ("*Dryas octopetala* L." (Info Flora 2017b)), mountain pine ("*Pinus mugo* Turra s.l." (Info Flora 2017c)), different grasses, heather ("*Calluna vulgaris* (L.) Hull" (Info Flora 2017a)), different type of moos and willow ("*Salix appendiculata* Vill" (Info Flora 2017d)). As mentioned above the vegetation cover varies from channel to channel. The outer channels mainly show shrubs, grasses and willows. The further central the more numerous and taller are the mountain pines. The occurrence of moss also increases as the mountain pine vegetation becomes denser.

CLIMATE

Langhans (1913, 32) hints that the climate around Suldén in winter is particularly cold and dry. Looking at the climate data registered from the University of Bolzano the winter in Suldén is indeed showing low precipitation values. Table 1. shows the average amount of rain days and the amount of rainfall for each month. December, January and February show similar values in the amount of precipitation (24-29mm) and days (3.6-4.6) as well as mean temperatures (around -4°C). Comparably close average values can also be observed in the springtime as well

as the summer and autumn months. The precipitation averages display higher values during the summer months, but the winter months are the driest. While the temperatures do not seem to be exceedingly low the average temperatures remain overall relatively low not surpassing 12°C even in summer. However, this average data should be carefully analysed. Taking a closer look at the whole dataset (see appendix C) it is noticeable that the temperatures have a wider range than indicated by the mean values. For instance, the minimum temperatures recorded in winter are relatively often around -10°C and similarly in summer the maximum range is often between 15° and 22°C. Still the average values reflect the main trend. From the precipitation data it is possible to notice that, while the values mostly correspond to or, at least do not deviate much from the average, several exceptions can be seen. As an example, in February 1925 110.7 mm precipitation was registered by the weather station in Suldén (46.5159 ° / 10.5953 °, 1904 m a.s.l.). This value exceeds the average value.

Months	Rainy Days	Precipitation [mm]	Mean Temperatures [°C]
January	3.6	24.3	-4.4
February	4.6	28.8	-3.8
March	5.2	33.2	-1.5
April	7.9	56.7	1.5
May	9.2	73.5	6.0
June	10.9	89.3	9.4
July	10.7	99.4	11.8
August	10.8	105.7	11.6
September	7.7	80.6	7.9
October	7.3	73.0	4.1
November	6.1	56.8	-1.0
December	4.2	28.2	-3.9
Annual Mean	88.3	749.3	3.1

Table 1. Monthly average of the amount of rainy days, precipitation in mm during a period of 65 years and temperatures during 33 years. The mean values were calculated from time series beginning in 1921. However, the dataset is relatively incomplete and fragmented. Information was recorded only during 65 Years within the time interval [1921, 2016]. Analogous is the situation for the mean temperatures. This recording however is younger and only began in 1971 (see appendix C) (Data: University of Bolzano 2017a; University of Bolzano 2017b).

STUDY SITE

Within the Marl-debris fan a section of three different channels was chosen; The channel with the river (R3) and the next two beside it (R1 and R2) (see image 8.). The three channels differentiate themselves by vegetation cover, degree and shape. The outermost debris-flow channel shows a lower amount of plants while the innermost of the three is overgrown with several fully-grown mountain pines. The channel in the middle displays a higher vegetation cover than R3, however, the mountain pines are only sporadically located in the centre. Smaller pines are beginning to grow on the levees. The channel R3 is mainly overgrown by mountain avens and willows. In the upper part of this channel, however, single mountain pines can be found where the small stream flowing through the channel takes a large curve. In this area a kind of channel-free plateau has been formed. The relatively plain area is merely interrupted by tongue-like deposits of debris-flow heads. The channel R1 is directly adjacent to the R3. The single designations of the channels reflect the order in which the channels were sampled for the first time during the field course. R1 is a relatively long curved channel. It has been cut off from the main channel by several debris-flow head stoppages, which are accumulated one above the other and build up quite a large debris-hill. Some of the heads were deflected on their sides and then flowed into R3. At the lower border of the segment of interest R1 and R3 merge. The channel R2, however, starts midway on the orographic left side of R1 and runs with a relatively straight path downslope.



Image 8. Channels R1, R2 and R3 (author 2016).

METHODS

SAMPLING

As outlined in the site description, *Dryas octopetala* dwarf shrubs were sampled in three channels. The sampling was done during two periods: First samples were collected during the field course between the 4th and the 8th of July 2016 by the participants of the course. The sampling locations were, however, not exactly on the same transect (see image 8.). The samples of the channels R2 and R3 were sampled slightly further downslope (site B) than the ones of the channel R1 (site A).

The second sampling period was between the 29th of August and the 2nd of September 2016. The sampling location was determined by going to the same site as during the field course and looking for traces of the first sampling. Clearly visible were many previously dug holes and parts of cut plant in R2 as well as in R3 which helped for orientation.

The aim of sampling was to have at least 30 plants from each levee. So the plants were partly dug around until the stem of the plant was visible. The long intersecting main branches, which were below the surface, were gently excavated at first and then followed until they reached a common junction. Then the main stem was carefully excavated, paying attention not to damage or break it. This process occurred mostly with the use of a geologist's hammer. When the stem was secured, and wide tape was wrapped around it for stabilization as well as labelling, the shrub was either completely pulled out of the soil or moved in such a way that the tape on the plant was exposed and clearly visible. The plant was then left in situ and the next *Dryas octopetala* was tackled. When all samples were marked with the tape, the distance from the centre of the channel to the plant was measured. At the same time the samples were labelled. The labels indicated the name of the channel (R1/R2/R3) followed by an L for the left levee or an R for the right levee, the initial of the sampled plant name (D for *Dryas octopetala* and F for mountain pines) and finally two digits for the plant number. For dwarf shrubs that were not sampled during the field course an additional "0" before the two digits were added. This indicated on which day the sample was taken (see image 9.). If several shrubs were found extremely close to one another and almost in the same position, the same number assigned and an additional letter (a, b, c, d,...) was added.

After the stem was taped, labelled and its position measured, the plant was cut with garden scissors. The branches were separated from the stem and the roots at their intersection with the stems. For the investigation of this thesis only the stem was needed. However, to be sure to have enough sample material, the upperpart of the root, which was just connected to the stem, was also included in the sample. As the roots were sometimes astonishingly long they were appropriately cut to have a sample with a maximum length of about 20 cm. Only these samples were collected while the rest of the plant was left in the field. This whole process was recorded with pictures and notes.



Image 9. Sampled *Dryas octopetala* shrubs (author 2016).

During sampling several conditions were observed: Because an aim of the thesis is to analyse if a common growing pattern exists, plants were sampled over a wider area of the levee. Special attention was given to find samples from different distances to the middle of the channel, to investigate any possible growth pattern on the levee. A pattern could help to draw a conclusion on the drainage process of the levee after an erosive debris flow and the repopulation pattern of the plant *Dryas octopetala*. Thinner and thicker stems were sampled equally in order to have a wide spectrum of samples. Furthermore, stems which were broken or had major damage caused by the sampling were not collected. Moreover, only living shrubs were sampled.

The samples were finally collected and stored into paper bags, which were left open to prevent rotting.

SAMPLE PREPARATION

On all 190 stem samples collected, one small section by the stem was cut off to a length of a few centimetres for further analysis. Careful attention was given to correctly label all the parts of the same plant. Then the smaller parts were sorted by levee and the remainder stored as before in paper bags.

Thin sections were taken of the samples: For this, the methods described by Bär et al. (2006) and Gärtner and Schweingruber (2013) were applied. The samples were sliced with a WSL-Lab-microtome (Gärtner and Nievergelt 2010). Before cutting, the sample was immersed in a beaker full of water for at least 3 minutes. After moistening, the samples were fixed in the holder. The main blade-holder was positioned at a horizontal angle of 45° to the sample. Firstly, a few rough slices were cut off to gain a smooth surface. Then the slice thickness was decreased. With the help of a fine paintbrush and a needle the sliced thin section was transferred onto the prepared microscopic slide. The slide was prepared in advance with a few drops of glycerol to prevent the section from drying and to simplify the placement of the sample on the glass. The section was then examined under a microscope. While observing the samples special care was taken to achieve a clear visibility of all cells and that by slightly shifting the zoom no additional cell layers were present. If the sections were too thick, sectioning was repeated with a reduced thickness. The best cuts were achieved with a thickness of between 5-15µm and the usage of normal NT Japan cutter blades instead of specific microtome blades. Broken samples or sections with missing pith were also repeated. However, many samples showed a compartmentalized zone around the pith and proved to be extremely brittle. Even with the help of 95% ethanol or starch, the compartmentalized area was very difficult to cut. As a result, some of the samples were either very fragmented near the pith or they were incomplete. Furthermore, if the sample was partially twisted, the thin section had to have most of the area with the longest radius cut as a clear transect. 3 to 5 good thin sections were cut from each sample. Each was covered with glycerol and stored in a slide holder.

When all samples were sectioned the process of staining and permanently fixing the thin sections began. The samples were first washed with water to remove the glycerol. In a second step, the samples were bleached with sodium hypochlorite. This step helped to clear all brownish areas of the compartmentalisation process and enabled a better viewing of the cells. The samples were left for just a few moments under the influence of the bleach. As soon as

most of the brown colour had vanished the samples were washed very carefully. After the second flushing the thin sections were covered by a staining-liquid for at least 3-4 minutes. This colour was a 1:1 mixture of Safranin and Astrablue solutions. The first stains lignified parts of the section red, while the latter stains lignified structures blue. Then the stain was washed away with water, thereafter, they were carefully dehydrated with three different ethanol concentrations (75%, 96% and dehydrated ethanol). The washing process finished when the ethanol had removed almost all surplus Safranin-Astrablue solution. The coloured samples were then finally flushed with xylene. This substance helps the fixation of the sample with Canada balsam, in which the samples were embedded. The coloured thin section and balsam were covered with a covering glass. The covered microscope slides were placed between two layer “...heat-resistant plastic strips on an iron plate” (Gärtner and Schweingruber 2013, 65) and fixed on the plate with several magnets. After this the samples were placed in an oven at 60°C for at least 24 hours. After the samples cooled down and the Canada balsam hardened the magnets together with the plastic sheets could be removed. With the help of cutter blades the microscope slides were cleaned from the leaked balsam (Gärtner and Schweingruber 2013).

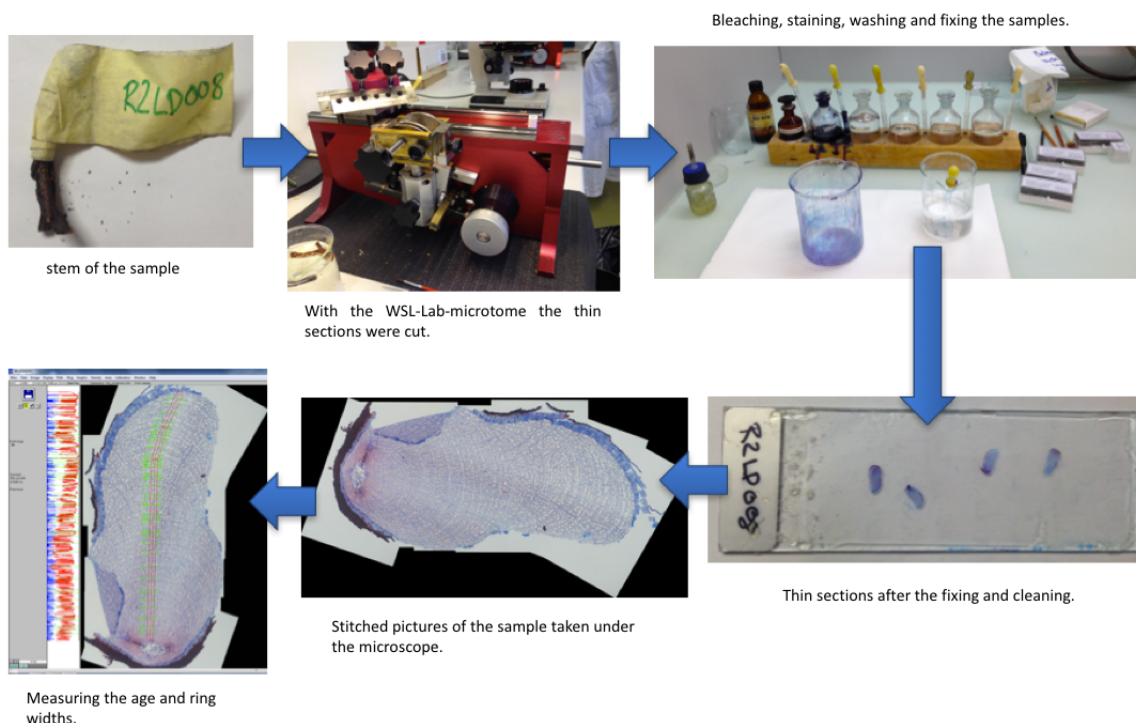


Image 10. Sample preparation process (author 2017).

For further analysis of the thin sections, the best looking section had to be chosen and photographed. The pictures were taken under a microscope (100x magnification), which was connected with a photo camera (CANON EOS 700D) and a computer. Depending on the magnification used, various pictures had to be taken. The pictures were taken beginning from the bark following the xylem rays along the largest radius to the pith. While photographing the direction of the camera was always positioned as to have the imaginary largest radius in the middle of the picture and vertical to the growth rings. Also the camera was permanently moved to maintain a landscape image. Finally, the pictures were stitched with PT-Gui to one image, which was optimized and saved.

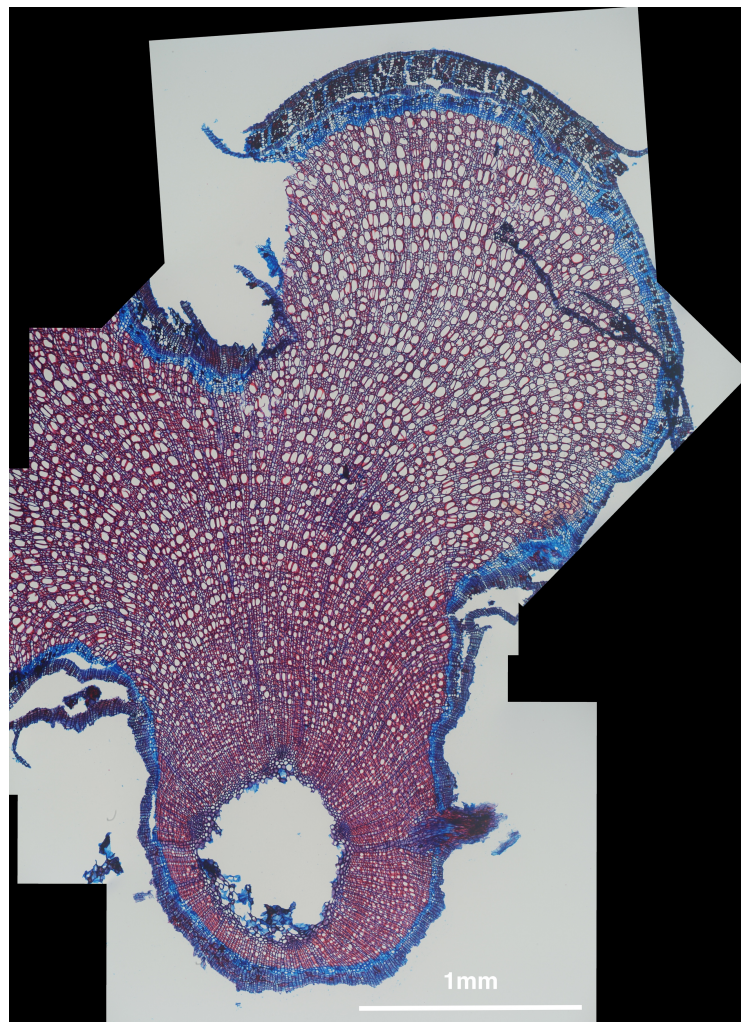


Image 11. *Dryas octopetala* sample (R2 RD 04) (author 2016).

Visual analysis

Ring-width measurements of the samples were carried out on the images using WinDendro software. To do so, the stitched pictures were opened in the programme and a path to measure the longest radius had to be defined. Beginning from the pith following the xylem rays as consequently as possible a measuring track was determined. The track was set to begin at the first earlywood-pith transition of the ring and end by the latewood of the outermost ring, in this case 2015. This was done because the plant was cut in July 2016, when the latewood was incomplete. Even though some samples were taken in September 2016, this procedure was applied to all samples to analyse them all in the same way. After setting the radius path, the boundaries between late- and earlywood (ring boundaries) were marked manually. As an indicator for a growth ring boundary an investigation was made to look for smaller and flattened cells rows but with thicker walls. Furthermore, as *Dryas octopetala* is a semi-ring-porous wood, the rows of vessels in the earlywood helped to define the border. partially missing rings (PMR), which could be found at other positions however not appearing in the track, were marked as missing rings. During the beginning of the visual analysis a problem emerged for some of the samples. The WinDendro programme was not able to open some of the images. Therefore, the number of analysed samples was reduced to 153. For each thin section one radius was measured. For only one sample three radii were measured as an exception (see image 12.). This plant should then give more insight into approximately how many missing rings might be expected (Buchwal et al. 2013, 1308; Schweingruber et al. 2011, 387; Stoffel and Bollschweiler 2008, 188).

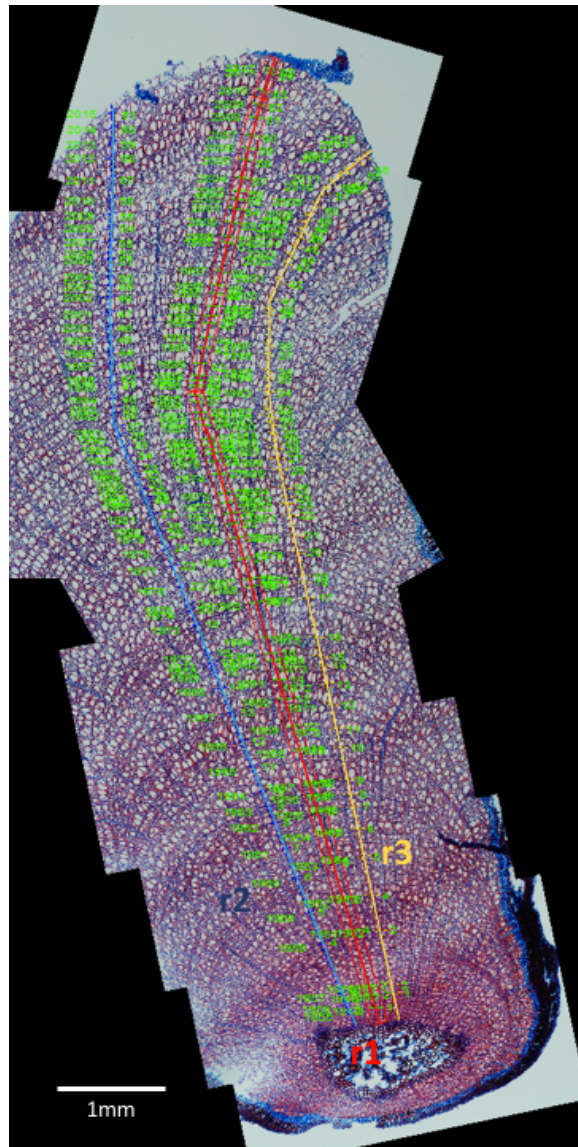


Image 12. Sample R1RD 003a with the three measured radii (author 2017).

Cross-Dating

The cross-dating of the ring-width series was attempted by using TSAP-Win. To arrange the curves a search of the best combinations of pairs based on CDI-values was conducted. The CDI-Value, or Cross-Dating Index, is an important statistical indicator for the level of correspondence between two cross-dated curves. It incorporates several T-values, which describes the influence of extreme values, and the Gleichläufigkeit, which is a dimension for matching growth trends (Rinn 2012, 26).

Measured curves were then split into clusters of samples, which had a CDI value higher than or at least 18. Many clusters could contain the same sample. These samples were then compared with each other and after that a first cross-dating was performed. If the samples could

be cross-dated without adding more than 5-6 missing rings, they were permanently classified in the same group (e.g. group I, group II, ...). This condition was added due to two difficulties met while the cross-dating process: (i) often only small sections (5-15 years) matched. However, these corresponding sequences frequently might suit in one section as well as in another. Longer and unequivocally fitting sequences were seldom; (ii) missing rings have rarely a clear insertion point. Due to these observations, it became obvious that without a specific limit the cross-dated curve could be easily constructed just by adding enough rings. To prevent the involuntarily assembling of a compatible curve, an upper limit was appointed. This limit was defined by cross-dating multiple radii of one sample and taking into consideration that relatively often the cross-dated samples do not begin in 2015. After the first cluster was cross-dated, the samples were either assigned to a group or set aside for further testing, to be allocated into a group. The attention shifted towards a next cluster, which contained already assigned samples. The samples in these clusters were either successfully or unsuccessfully cross-dated with the already existing group-samples. The non-assigned samples were then cross-dated with each other: If the cross-dating could be done while maintaining the above described conditions, new groups were formed. This process continued until all samples were put under the cross-dating trial. The samples, which were not assigned to a group, were collected under the group name "group 0".

Correlations and error calculation

The relationship between the growth position on a levee and the age as well as the relationship between the channels and the ages of *Dryas octopetala* were graphically analysed. The correlation between the cross-dated curves was calculated via TSAP-Win. The CDI-values and as well the Gleichläufigkeits-values (GLK and GLS) were analysed. Furthermore, the relationship between climate factor (annual temperature and precipitation) and the group means were calculated by implementing a correlation test using R.

Finally an actual error could not be calculated, due to the lack of references on the amount of missing rings and other comparable values. However, the percentage of added missing ring was calculated.

RESULTS

RELATIONSHIP BETWEEN AGE AND GROWTH PATTERN

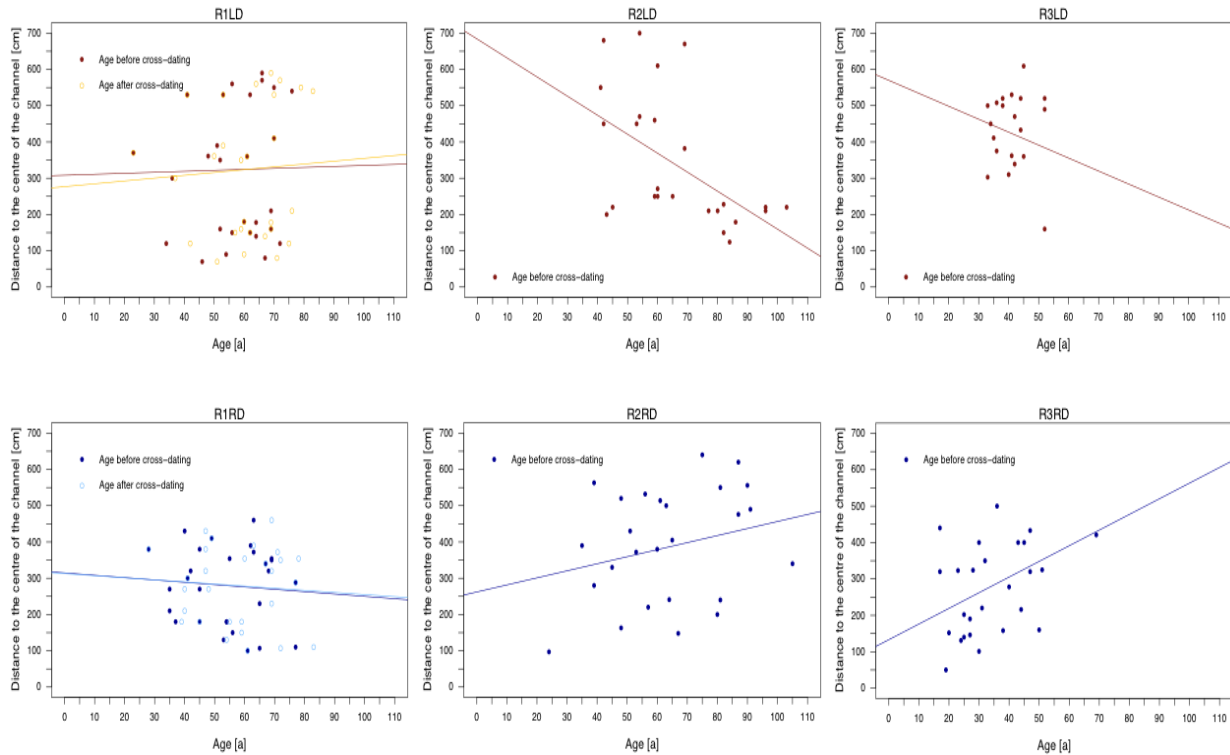


Figure 1. Distribution of the age of the shrub on the levees before and after the cross-dating. R1LD before cross-dating: p -value = 0.6007, $r = 0.1034$, R1LD after cross-dating: p -value = 0.4421, $r = 0.1513$, R1RD before cross-dating: p -value = 0.6089, $r = -0.1010$, R1RD after cross-dating: p -value = 0.7477, $r = -0.0636$, R2LD: p -value = 0.003183, $r = -0.5660488$, R2RD: p -value = 0.3564, $r = 0.1885$, R3LD: p -value = 0.0032, $r = -0.5660488$, R3RD: p -value = 0.02197, $r = 0.4390095$ (author 2017).

In figure 1 the relationship between the age of all measured samples and their growth position on the levees is illustrated. The plots were arranged in such a way to display a channel for each column while the upper row represents the left and the lower row the right levees. This structure has been consequently applied throughout this chapter. The points in the plots represent the samples. Full coloured points represent the original measured age in WinDendro. The coloured circle circumferences represent cross-dated samples. The lines in the plots show the regression lines calculated by R.

Observing the plots of figure 1. It is clearly noticeable that there is no clear trend. The points-clouds seem to be randomly arranged. However, the points in R1LD, R1RD, R3LD and R3RD are displayed close to each other forming relatively dense point-clouds. This fact signifies firstly that the plants sprouted during a set time interval and secondly that the sampled shrubs were not so widely scattered as expected.

The age intervals, in which most of the points are found, are in both R1 plots about 50 years long ($]30a, 80a[$). In R3 the intervals are more narrow; $]30a, 50a[$ on the left and $]20a, 50a[$ on the right levee.

The sampling in R1LD seem to have been limited at three height intervals ($]50cm, 200cm[$, $]300cm, 400cm[$ and finally $]525cm, 625cm[$). R1RD, R3LD and R3RD mostly lack samples near the centre. However, in R3 the flowing stream in the centre of the channel has to be taken into consideration. The shortage of samples in the lower parts of the levees can also be observed in the plots of R2LD and R2RD. Nevertheless, the upper levee heights seem to have been equally sampled. In R2 RD the samples display in different heights a wide range of age. The points are widely scattered.

In R2 most of the oldest plants were found. In R2 LD the more aged plants were found in a stripe between 100 cm and 250cm. R2RD does not display a pattern where the older dwarf shrubs were found.

The cross-dated samples in R1LD and R1RD have a similar behaviour than not cross-dated levees: While some of the samples are a bit older, no pattern in the point cloud has been recognised.

Looking at the regression lines it is possible to see appositve trend for R2RD, R3RD and R1LD. The remaining levees however seem to have a negative trend line. Though the regression lines of R1LD, R1RD, R2RD and R3LD have a relatively low slope. Additionally, it is probable that the regression lines were influenced by singular points, which lie farther from the main concentration of points. The p-values of the Spearman correlation test it can be seen that only in the levees R2LD, R3LD, R3RD the age and the growing position of the shrubs have a significant correlation (p-value < 0.05) (Artusi et al. 2002, 150).

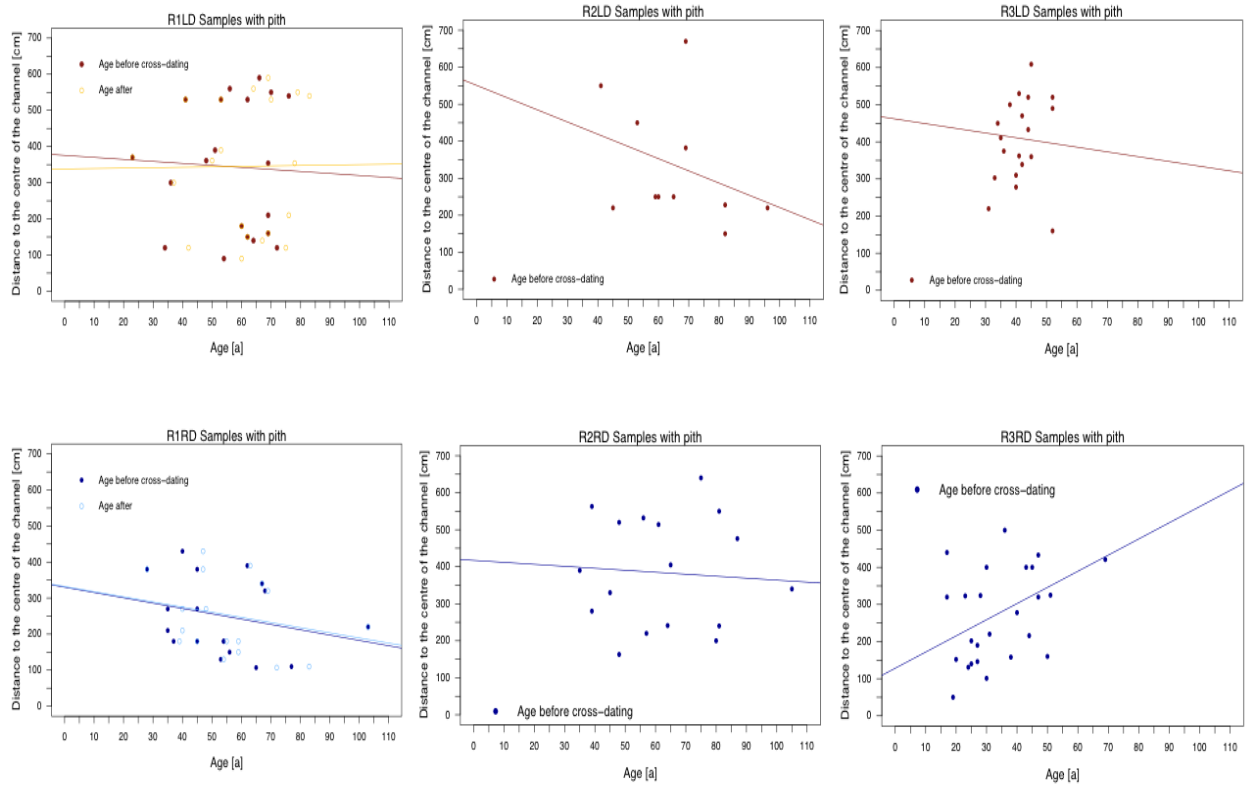


Figure 2. Relationship between age and growth position of the thin sections with piths. R1LD all samples before cross-dating: p -value = 0.8055, r = 0.0588, R1LD all samples after cross-dating: p -value = 0.553, r = 0.1411, R1RD all samples before cross-dating: p -value = 0.3637, r = -0.2276, R1RD all samples after cross-dating: p -value = 0.3713, r = -0.2241, R2LD all samples: p -value = 0.1647, r = -0.4502, R2RD all samples: p -value = 0.7111, r = -0.0970, R3LD all samples: p -value = 0.1647, r = -0.4502, R3RD all samples: p -value = 0.0268, r = 0.4339 (author 2017).

To control a possible influence of compartmentalized samples, which could not be cut with a pith, only the age and positions of the thin sections with pith were plotted in figure 2. By just observing the plots, no obvious difference in the observed pattern of figure 1. could be found. Looking at the result of the statistical tests it can be seen that less significant relationships between age and distance to the channel bed exist. The test showed a significant correlation only for the R3RD levee.

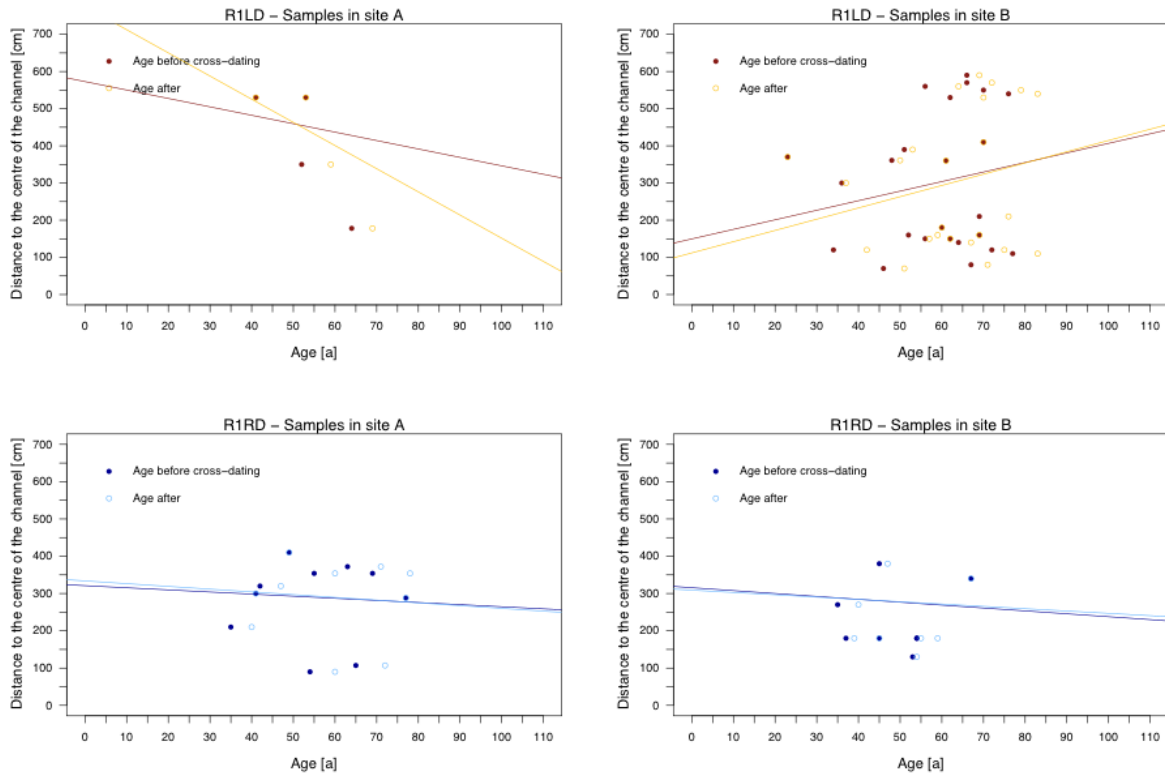


Figure 3. Samples in the two sampling sites (A and B) of the channel R1 (author 2017).

In figure 3, the possible influence of the sampling in two different sites has been represented in the plots. As can be observed the samples are in similar positions and of comparable age in both sites. The most noticeable difference is the amount of sampled stems.

Furthermore, the distribution of the age in the different channels has been illustrated in figure 4 and table 2. In the plots the mean values of the channel R3 (R3LD and R3RD) are clearly the lowest and show that the channel R3 is most likely the latest channel. Looking at the other two channels the determination of which channel is earlier it is possible to note that R1 has a more narrow range of age between the first and the third quantile. Also the maximum values are clearly higher in R2 than in R1. However, if the means are taken into account, while R2 shows the higher mean, the means of R2RD and R1LD are close together. The gap between the mean-values of R1 and R3 is wider than those among the channels R2 and R1. Rather interesting is the fact that in R1 and R2 the mean values of the right levee are lower than the mean values of the left levee.

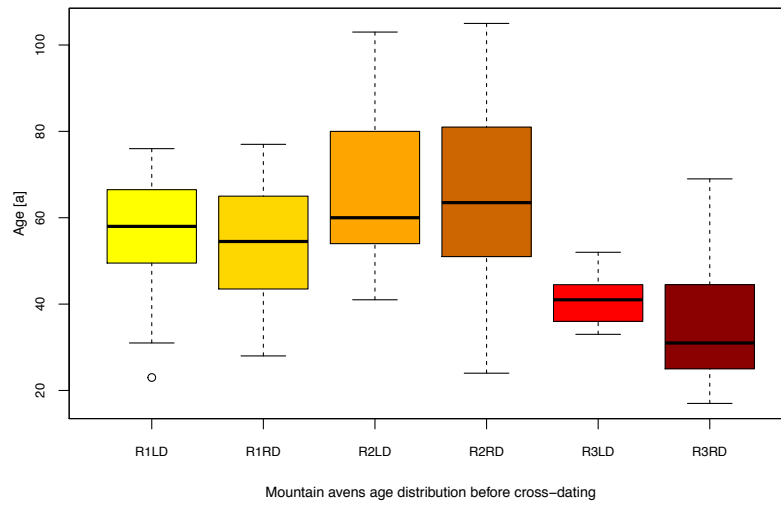


Figure 4. Age distribution in the different channels levees (author 2017).

	R1LD	R1RD	R2LD	R2RD	R3LD	R3RD
Min.	23	28	41	24	33	17
1st Quantil	50.25	44.25	54	51.5	36	25
Median	58	54.5	60	63.5	41	31
Mean	55.96	54.39	65.6	64.96	40.8	34.7
3rd Quantil	66.25	65	80	81	44.25	44.5
Max.	76	77	103	105	52	69

Table 2. Statistical parameters of the boxplot in figure 4 (author 2017).

CROSS-DATING

During the cross-dating groups were formed. The left levee has three groups and the additional reserve group 0. Group I contains the samples R1 LD 004, R1 LD 05, R1 LD 08, R1 LD 11, R1 LD 19, R1 LD 21b and R1 LD 27b. Group II consists of R1 LD 001, R1 LD 02, R1 LD 03b, R1 LD 04, R1 LD 06, R1 LD 10a, R1 LD 18 and R1 LD 23b, while group III has the samples R1 LD 09, R1 LD 13, R1 LD 17, R1 LD 21a and R1 LD 26b. The remaining samples R1 LD 002a, R1 LD 002b, R1 LD 03a, R1 LD 12a, R1 LD 14, R1 LD 15, R1 LD 23a and R1 LD 27a were placed in group 0.

Other than R1LD the right levee has two additional groups. The first two groups (I and II) are rather large, while the last three contain fewer samples. In group I the samples R1 RD 001, R1 RD 002, R1 RD 003a, R1 RD 00005, R1 RD 05, R1 RD 08, R1 RD 12 and R1 RD 13 were grouped together. R1 RD 00001, R1 RD 01b, R1 RD 00003, R1 RD 03, R1 RD 00006, R1 RD 11 and R1 RD

15b were arranged under group II. The group III contains the plants R1 RD 02 and R1 RD 15c. R1 RD 09, R1 RD 14 and R1 RD 15a which were assigned to group IV. R1 RD 06 and R1 RD 07 were placed in the last group, group V. The reserve samples R1 RD 00002, R1 RD 04, R1 RD 00009, R1 RD 00011, R1 RD 15e and R1 RD 16, which could not be matched under the set cross-dating condition, were gathered together and named group 0. During this chapter a distinction between partially missing rings, inserted rings and refilling rings will be applied. Partially missing rings or PMR, following Buchwal et al. (2013, 1308) definition, are irregular rings that appear and disappear in different position of the sample. Therefore a PMR might be found in one radius while in a second radius the same ring can not be spotted. These PMRs were counted as missing rings when they were found in other locations but not in the measuring radius. They were given the value $1\mu\text{m}$. Inserted rings are missing rings, which were integrated within the growing curve during the cross-dating. They were also given the width-value $1\mu\text{m}$ and were extra marked in Tsap-Win. Not counting as inserted rings as such that were inserted to fill the gap up to the sampling year 2015 after the curve was shifted in a more suitable position for the cross-dating. These rings are defined as refilling rings. In table 9. and 8. of the appendix more details on which and how many years were added.

Multi-radii cross-dating of the sample R1 RD 003a

To determine a limit of inserting rings, three radii of the sample R1 RD 003a were cross-dated (see figure 5.). During the cross-dating several rings had to be inserted: in radius 1 (r1) only a partially missing ring was detected in 1981. In the radii 2(r2) and 3 (r3) four and five rings respectively were inserted within the curves. Additionally, one ring for r2 as well two rings for r3 had to be inserted.

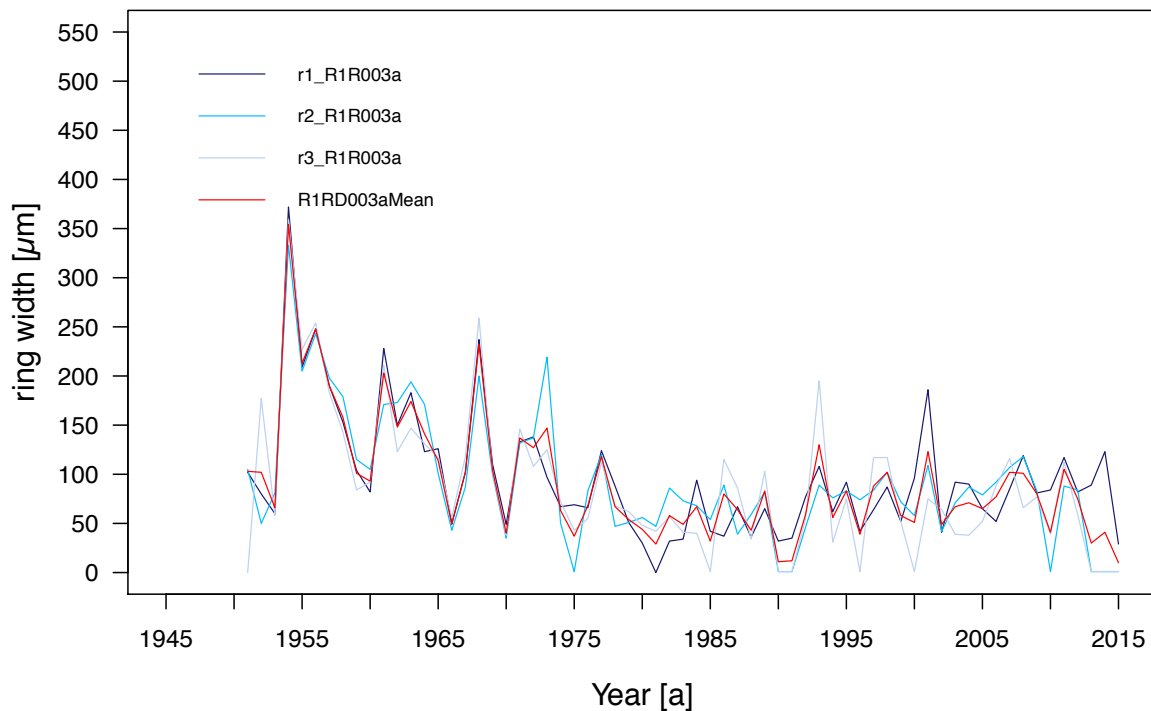


Figure 5. Cross-dating between multiple radii of the sample R1RD 003a (author 2017).

R1LD

In group I (see figure 6.) seven samples were visually cross-dated and put together in the same group. All samples in addition to number 08 were refilled in the front to reach the sampling year (2015). The refilling years reach between one and five, such as in R1LD27b. The sample R1LD19 shows most inserted missing rings (1957, 1976, 1987, 1996, 2004), while R1LD08 the lowest (1996). Group II (see figure 7.) contains a sample more than group I. It also retains the sample with the most added missing rings of the left levee. To the curve of R1LD001 (1983, 2001, 2003) were inserted three rings, but due to beginning in year 2008, after being moved into the best position, five refilling rings were added to the overall missing rings. A similar situation could be observed for the other samples, beside R1LD23a. The amount of actual inserted missing rings are at the most three in group II. An equal situation can be found in group I, where the quantity of inserted missing rings is mostly around 1-2. Only in the sample R1LD19 five missing rings had to be inserted. In group III however, the number of missing rings in the curve is in several samples somewhat higher, mostly around three rings per sample (see

figure 8.). R1LD17 having 6 (1965, 1972, 1974, 1982, 1992, 2005) inserted missing rings representing the maximum. "...[P]artially missing rings (PMR)..." (Buchwal et al. 2013, 1308) were only found in the samples R1LD002b (1980, 1981), R1LD13 (2006, 2013), R1LD14 (1951, 2002), R1LD19 (1965) and R1LD27a (1977, 1982). However, in R1LD13 one of the PMRs (2006) was cancelled during the cross-dating process. Overall in the left levee the percentage of missing rings (including refilling rings but counting partially missing rings as normal rings) has a range of between 24.4% and 0%.

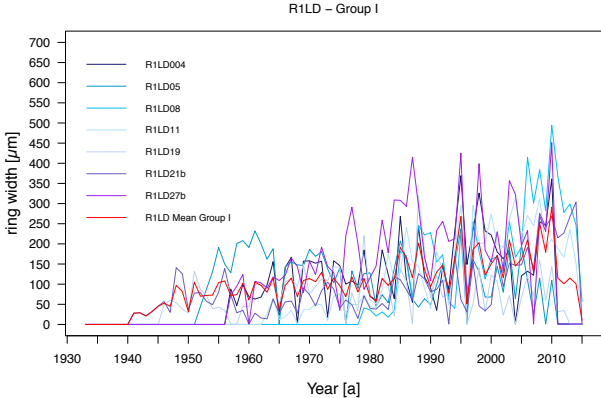


Figure 6. Cross-dated group I of the levee R1LD (author 2017).

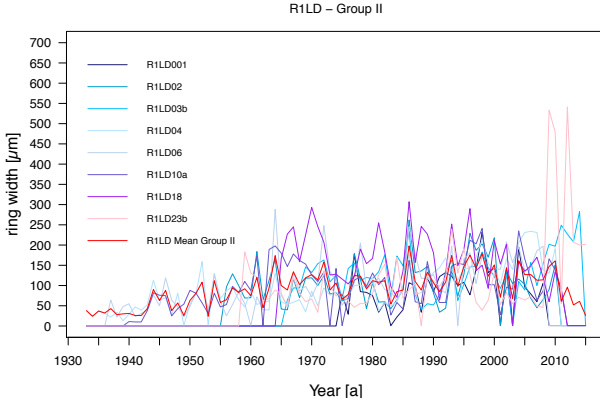


Figure 7. Cross-dated group II of the levee R1LD (author 2017).

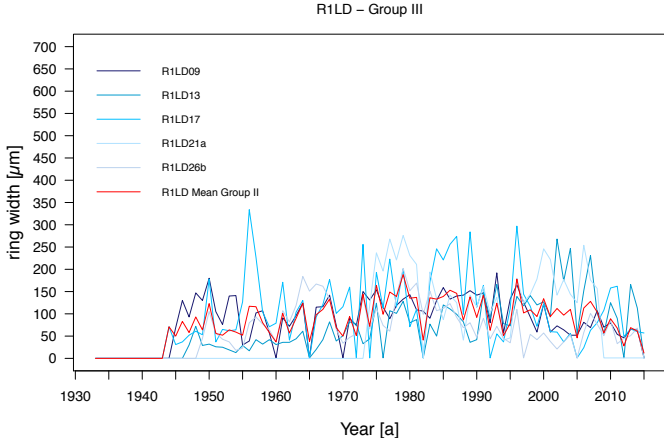


Figure 8. Cross-dated group III of the levee R1LD (author 2017).

Analysing the curves, following sequences were particularly of interest, due to being either peaks or lows found in all curves of a group or even in other groups. In group I three sequences stand out; the first sequence is between 2003 and 2001, the second is a longer rise and fall sequence in the years 1995-1992 and the last is a peak in 1985. The groups II and III have similar sequences nearly at the same time intervals: The sequences 1995-1993, 1988-1983

and the peak in 2004 cancel the most in group II. In group III only two apparent sequences attracted interest: 1994-1990 and 1951-1948.

R1RD

In the right levee of the channel R1 five groups were found. In group I eight samples were collected. In group II seven samples showed similar patterns. In the group IV three samples fit best together, while both groups III and V include only two samples each.

In comparison of the levee R1LD the sample with the most missing rings (R1 RD 00005) has an amount of nine rings and only three of them are inserted rings (1972, 1984, 2005). The sample with the most inserted rings is R1 RD 00001 in group I (1974, 1978, 1980, 1994, 2003). Analysing all the groups the amount of inserted rings ranges from zero to four while the amount of refilling rings does not surpass four. The samples of this levee show more PMRs than the left levee: in group I the samples R1 RD 002 (1995*, 2000), R1 RD 003a (1981), R1 RD 00005 (1992) and R1 RD 08 (1983*) show the presence of PMR. R1 RD 00003 (1992) and R1 RD 00006 (1982) are the only two samples with partially missing rings while group III has R1 RD 02 (1996, 2007) as a single PMR containing sample. In group IV the samples R1 RD 14 (2003), R1 RD 15a (2002) have also PMR. However, the samples R1 RD 06 (1973, 1977, 2000) and R1 RD 07 (1986, 2008, 2010, 2013) in group V have the most partially missing rings. The PMRs marked with a star are the ones, which were cancelled while cross-dating but were still measured with WinDendro. Nevertheless, the overall percentage of missing rings (PMR excluded) range from 15% to 0%.

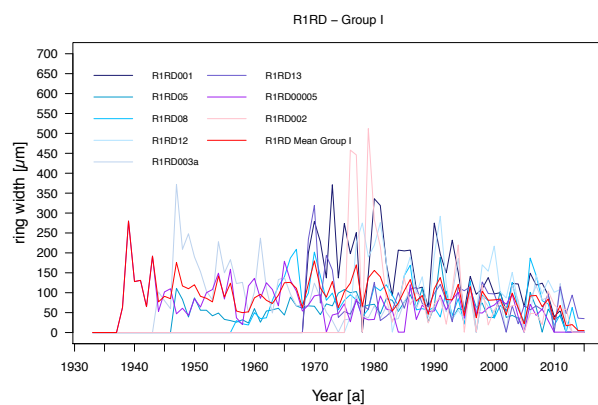


Figure 9. Cross-dated samples of group I in R1RD (author 2017).

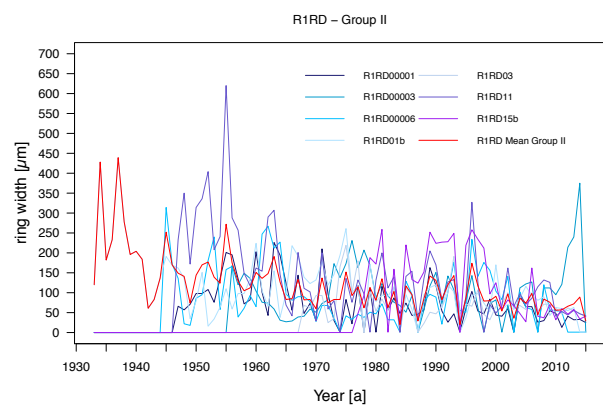


Figure 10. Cross-dated samples of group II in R1RD (author 2017).

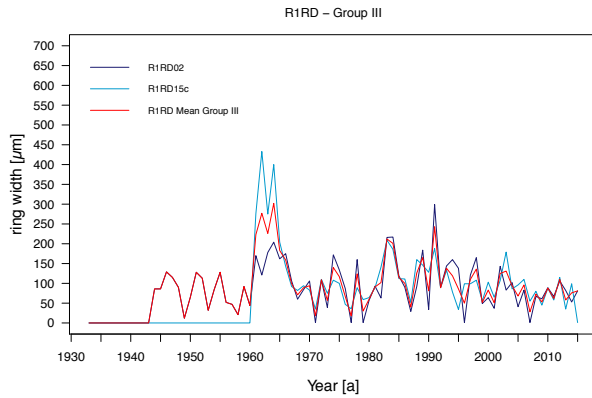


Figure 11. Cross-dated samples of group III in R1RD (author 2017).

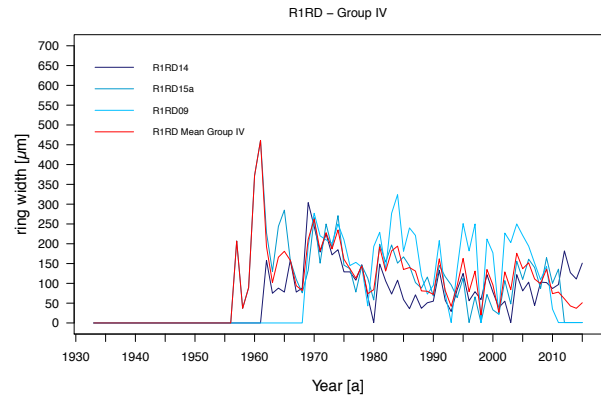


Figure 12. Cross-dated samples of group IV in R1RD (author 2017).

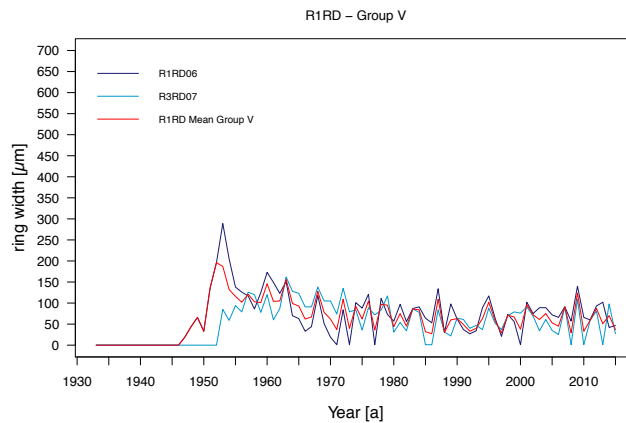


Figure 13. Cross-dated samples of group V in R1RD (author 2017).

Observing the curves similarly as in R1LD, repeating sequences in the curves within the groups might be found. In group I such sequences are 1986-1990, 1994-1998, 2001-2004 and 2009-2010. The sequences in group II (1985-1986, 1995-1997 and 2001-2003) intersect with the same time intervals as in group I. The last three groups of the number of samples in one group is very low. The curves within the groups fit very well and have therefore longer sequences of equal growth behaviour. In group III 1971-1978, 1989-1993, 1997-2003 and 2006-2013 contained the sequences, which stood out. In group IV a long interval (1990-2005) was found, during which the curves matched exceptionally well. Finally, the sequences of group V (1963-1978, 1990-1993 and 2004-2010) cross with the ones from group III.

Looking at the correlation-index CDI and the Gleichläufigkeits-indices (GLK and GLS) (see tables 12.-44. in the appendix) it is clear, that the cross-dating process has improved the correlation between the samples. Furthermore, a confirmation of the grouping was given through comparing group means with samples and means of different groups. However, some

grouped samples might show high CDIs only in combination with individual samples rather than all the sample in the same group. As an example, in table 3., just below, the CDI-values for the samples in group III of the left levee are displayed. The cells in bright grey show the CDIs after the cross-dating (refilling rings included). Most of the values are high. Though the CDI-value of the sample R1 LD 21a are for R1 LD 09 and R1 LD 13 far lower in comparison to the one with R1 LD 17. These samples are either not in the right group or they need to be further edited.

To see the influence of the refilling rings on the CDI-values a comparison between the samples with refilled beginning (bright grey) and samples with only inserted rings (darker grey). It is noticeable that some of the CDIs increase, whilst others decrease after the refilling.

	R1 LD 09	R1 LD 13	R1 LD 17	R1 LD 21a	R1 LD 26b	MeanGroupIII
R1 LD 09	8	20	8	16	44	
R1 LD 13	10	9	5	11	24	
R1 LD 17	18	8	34	32	89	
R1 LD 21a	5	4	24	16	51	
R1 LD 26b	24	14	28	12	53	
MeanGroupIII	53	27	74	32	65	

Table 3. CDI-values of R1 LD group III (author 2017).

Relationship between groups and the *Dryas octopetala*'s growing positions

Figure 14. shows the already observed relationship between the age and the growing position of the samples. This time the samples were divided into the groups to see if a spatial relationship between the grouped samples exists. Looking at the plots however, no clear pattern or clustering of the grouped samples can be recognised.

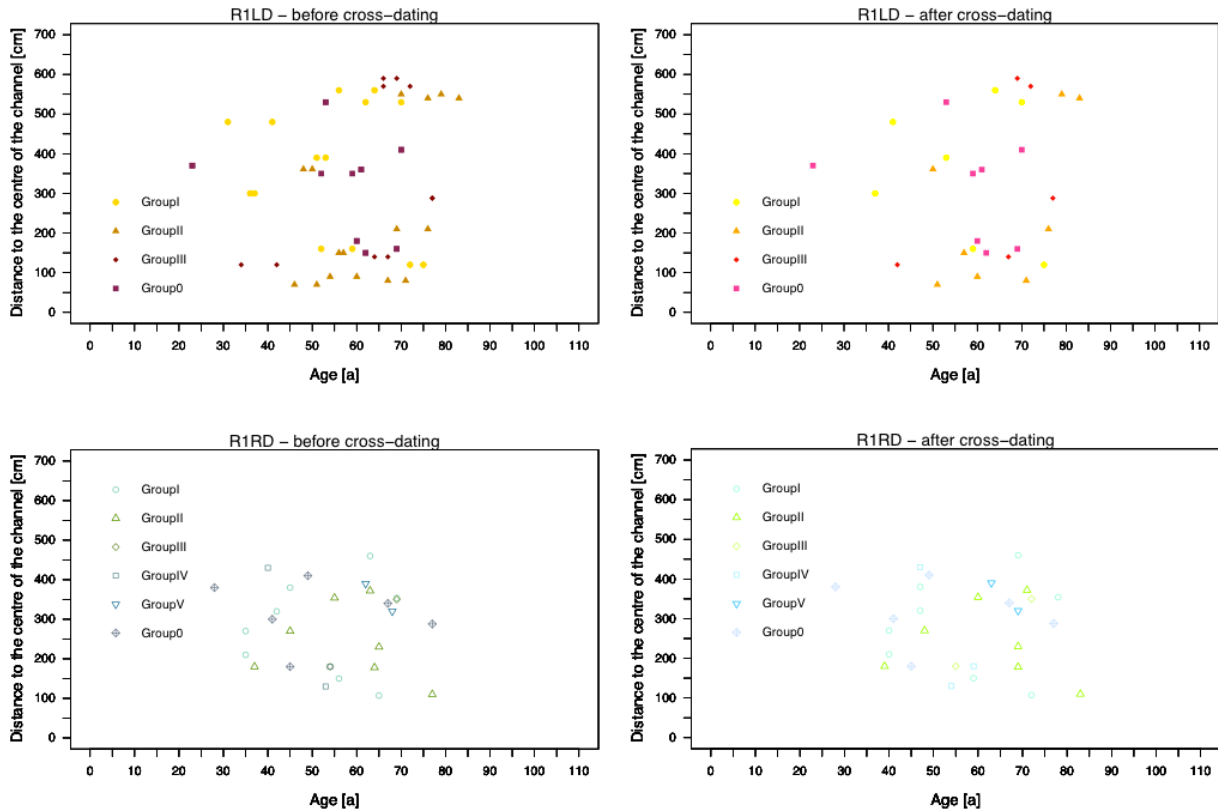


Figure 14. Distribution of the grouped samples on the levee (author 2017).

CORRELATION BETWEEN RING GROWTH AND CLIMATIC FACTORS

The figures 15.-18. show the relationship between the cross-dated group means curves and either the temperatures or the precipitation-values in Suldén. It is noticeable that the measurements of climate data are very fragmented. While the precipitation records reach back until the 1933, the temperature measurements started in 1971. The main data-gaps are in the 80's and in the 40's.

Comparing the curves, it is apparent that neither the temperatures nor the precipitation curves match the means. The only exception represents the mean of R1RD group II with the precipitation. The statistical p-values of the Spearman correlation test confirm a significance in the relationship between the two curves. However, another correlation was deemed significant by the statistical test. The R1 LD group II mean is statically significant with the temperature. Yet visually analysing the curve a relationship would not be expected.

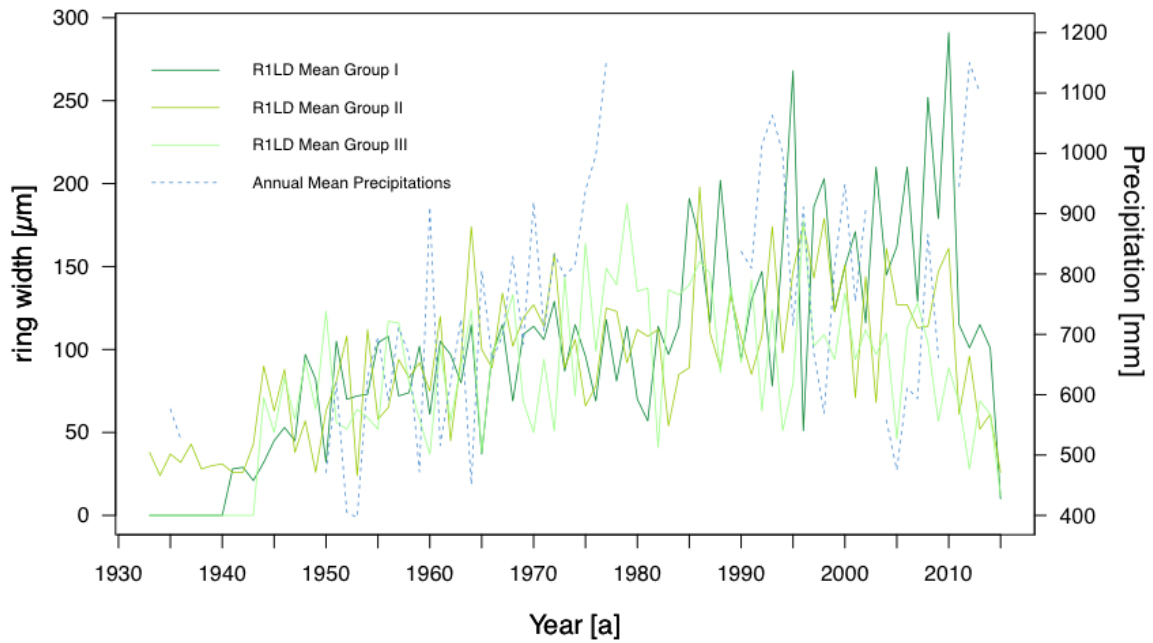


Figure 15. Correlation of R1LD group-means and the precipitation. R1LD Mean group I, p -values = 0.3122, ρ = 0.1401, R1LD mean group II, p -values = 0.4816, ρ = 0.0978, R1LD mean group III, p -values = 0.22, ρ = 0.1697 (author 2017).

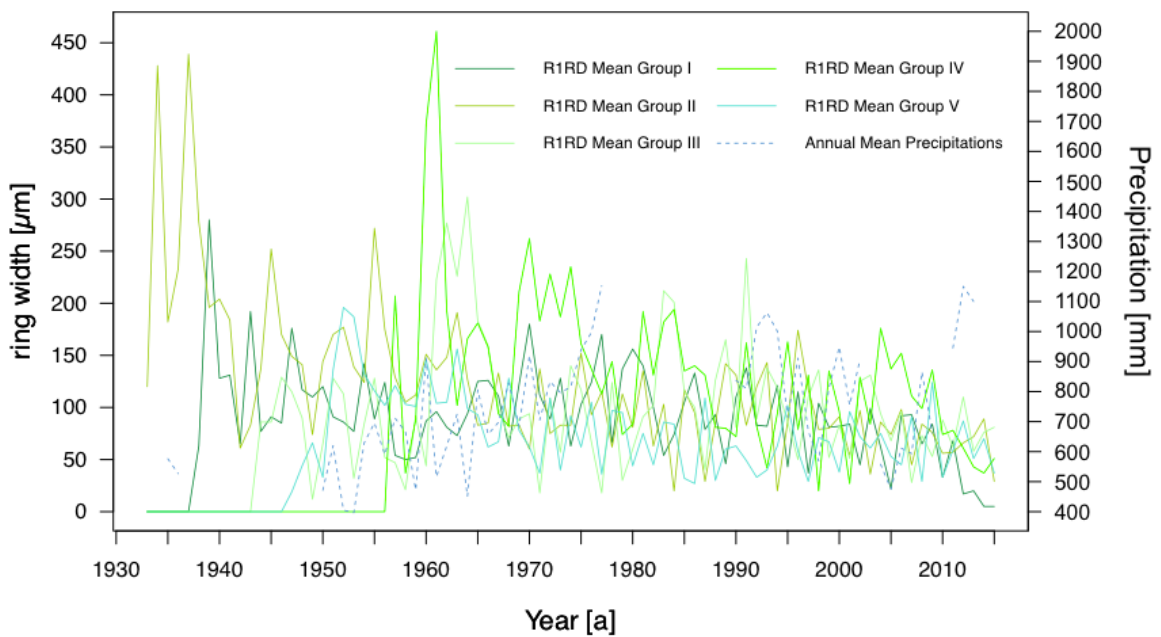


Figure 16. Correlation of R1RD group-means and precipitation. R1RD mean group I, p -values = 0.5309, ρ = 0.0872, R1RD mean group II p -values = 0.0097, ρ = -0.3488, R1RD mean group III, p -values = 0.8789, ρ = -0.0212, R1RD mean group IV, p -values = 0.2026, ρ = 0.1762, R1RD mean group V, p -values = 0.2131, ρ = -0.1722 (author 2017).

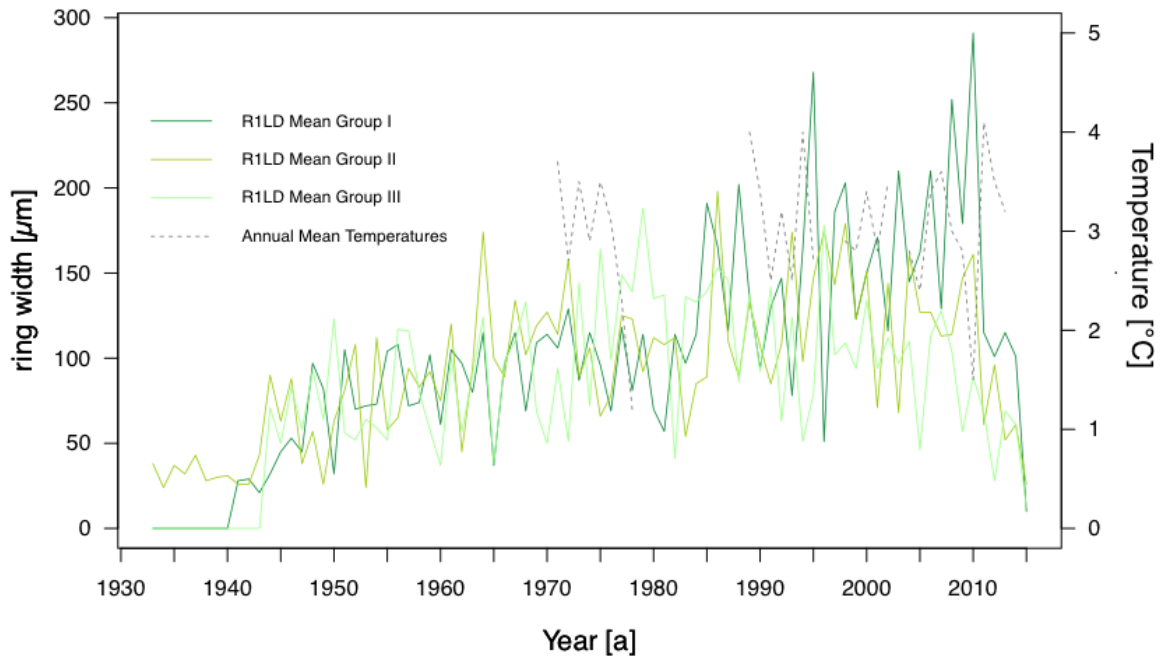


Figure 17. Correlation of R1LD group-means and temperatures. R1LD mean group I, p -values = 0.257, ρ = -0.2099, R1LD mean group II, p -values = 0.0194, ρ = -0.4176, R1LD mean group III, p -values = 0.9578, ρ = -0.0099 (author 2017).

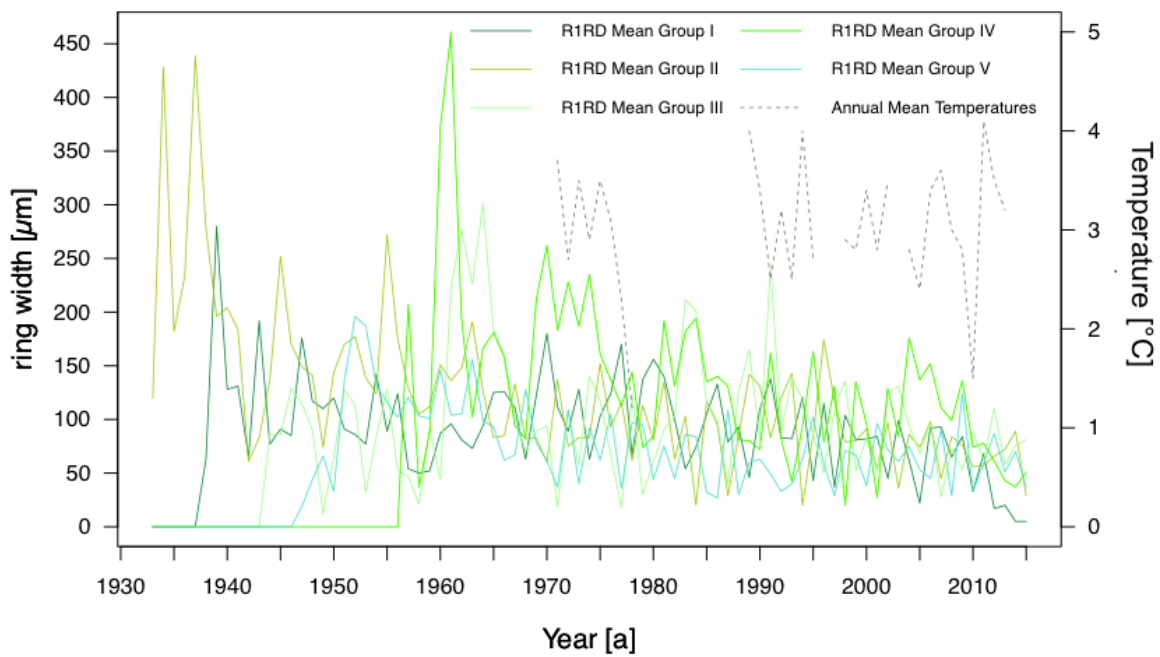


Figure 18. Correlation of R1RD group-means and temperatures. R1RD mean group I, p -values = 0.5116, ρ = 0.1225, R1RD mean group II, p -values = 0.571, ρ = 0.1058, R1RD mean group III, p -values = 0.7531, ρ = -0.0589, R1RD mean group IV, p -values = 0.4778, ρ = -0.1324, R1RD mean group V, p -values = 0.6216, ρ = -0.0922 (author 2017).

DISCUSSION

CROSS-DATING THE DWARF SHRUB DRYAS OCTOPETALA

Influences on the results

As can be seen from the results, the building of a chronology for an entire channel or even a levee was not achieved. During the cross-dating process the matching between two samples was relatively easy as rarely more than five inserted rings had to be added. However, as soon as a third, or fourth, or fifth, or even more samples were added the number of missing rings increased. To ensure a proper fit of all the curves fit each, other many more rings would have to be inserted. The danger of doing this would be the construction of a fictionally perfect chronology, which would be extremely influenced by missing rings. This procedure was attempted to see how many additional rings would have to be added to match all the curves of one levee in R3. The result was that summing together refilling and inserted rings, the single curves consisted to more than 50% of inserted (missing) rings. The chronology was a sequence of rise and fall, which after every few years had a missing ring inserted.

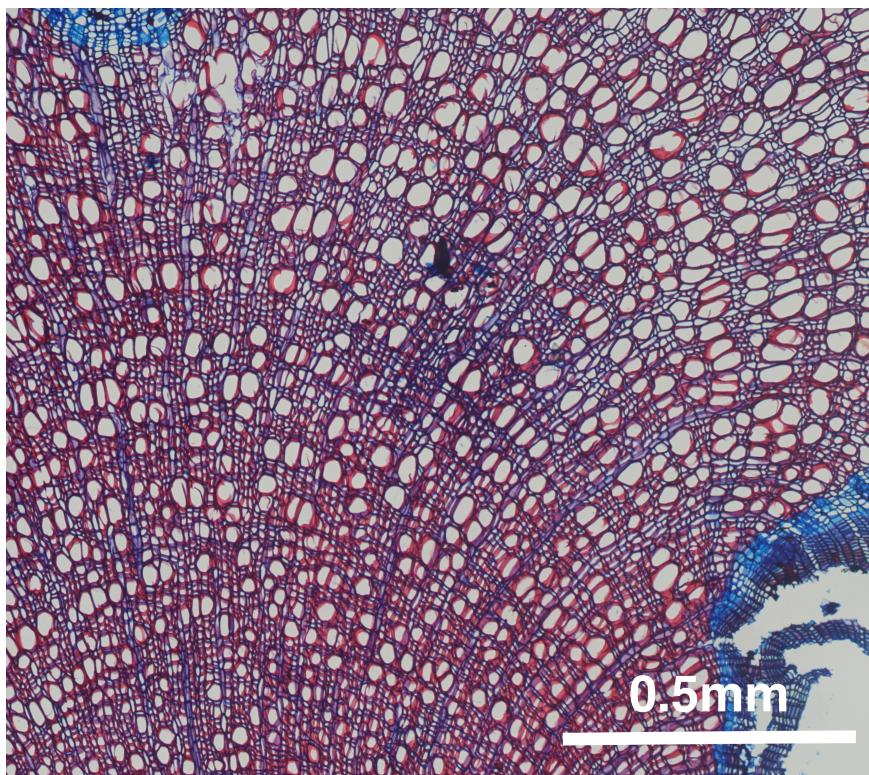


Image 13. Detail of the sample R2 RD 04. The rings are irregular and sometimes the boundaries difficult to determine (author 2017).

A second attempt was started by cross-dating the samples of different plants and looking for any possibly overlooked missing ring. However, the problem in this approach was that the idea, in which specific rings had to be found, lead to an influence of the perception and often to finding “rings” that normally would have not been classified as rings. Due to the structure of *Dryas octopetala* this mistake was relatively facilitated. The sometimes extremely narrow and irregular ring sequences often seem to hide very slim PMR. The semi ring porous arrangement of the vessels also might sometimes mislead the recognition of ring boundaries (see image 12.). Similar difficulties were already described by Au and Tardif (2007, 593), Bär et al. (2006, 20-23) and Schweingruber and Poshold (2005, 287).

A frequent change of zoom perspectives was implemented to avoid similar mistakes. These changes helped to focus to remain on both the overall picture of the rings and the boundaries in smaller scales rings. However, in some situations mistakes might have occurred due to the above mentioned closeness, tightness and irregular form of the rings.

The *Dryas octopetala* samples are very eccentric. The pith is positioned on one side close to the bark. Therefore, the annual rings are well developed only in the few directions of growth. On the sides of these main growth directions they come together and the single rings are extremely difficult to remain recognisable.

These described problems have surely influenced the creation of growth curves and the counting of the rings. Different samples were influenced by these difficulties to various extents. Usually such challenges were more present in older samples.

A further influencing factor regarding cross-dating is the position from where the thin section was taken. Owczarek (2010, 47) described in his paper how shrubs have a location between the roots and the branches where the maximum amount of rings are displayed. Schweingruber and Poshold (2005, 287) describe the perfect location as “...the transition zone between the shoot and the root collar...”. Therefore, if the thin section taken does not correspond to the described location, the measurement is underrated. However there is no possibility of recognising from the habitus of a stem where this specific location is. So there is a high probability that the analysed samples do not show the maximum age of the plants. Furthermore, during preparation attention was given only to cut samples from the stem. As a result, the slides originate from different position on the stem. While it is not known how much the ring variation within the stem is, it is possible that this ring-difference between the

various stem slides had an influence on the cross-dating results. This stem characteristic has an impact on the amount of missing rings. Consequently, the amount of missing rings might be higher than the set limit of rings, which could have been inserted. Owczarek (2010, 47) resolved this problem by taking 4-7 thin sections from all points along the branches, stem and roots of the studied shrub as well measuring along multiple radii.

Similarly, as observed with the cross-dating of the R1RD 003a radii, a variation between measuring tracks, which are relatively close to each other, exist. Therefore, if only one radius is taken into consideration, the choice of its path has an influence on the measurements and in consequence on the cross-dating. Bär et al. (2006, 20) applied the B.A.I. (basal area increment) method to synchronize the rings and resolve the problem of the eccentricity of the rings, while utilizing the whole sample area for measurements.

Cross-dating groups and correlating temperature/ precipitation records

All these described factors have an influence on age measurement and the cross-dating. Still interesting is that, while not all samples could be arranged regarding chronology, eight separate different “smaller” chronologies could be built. These chronologies were produced by cross-dating smaller groups of samples. While a connection and the matching of the singular groups-mean-values did not seem possible on the first sight, single similar features could be found in multiple curves of different groups (see figures 19. and 20.). As an example, the peak of 1994 (marked in red) in the plot R1LD - Group I might also be found in the samples of Group II and III, whereas the position of the peak has moved in the different graphs. Analogously, the sink of 2003 in R1RD – Group I (marked in yellow) and the peak directly after red marked one (blue arrow) can be observed in all plots of both levees. Not just the singular peaks and the low are recurrent. Looking attentively at the pattern of the curves similar segments, containing multiples years, might be recognised. The fact that these recurrent patterns in the curves are not exactly in the same position but have moved, strengthen the above mentioned hypothesis that more “missing rings” had to be added. If the ring difference between the position of relocated features is due to actually missing rings or the missed optimum thin section position in the stem or, even due to the variable sampling location on the stem is, however, not clear. The answer of this question requires a deeper understanding of the plant and the ring distribution within it.

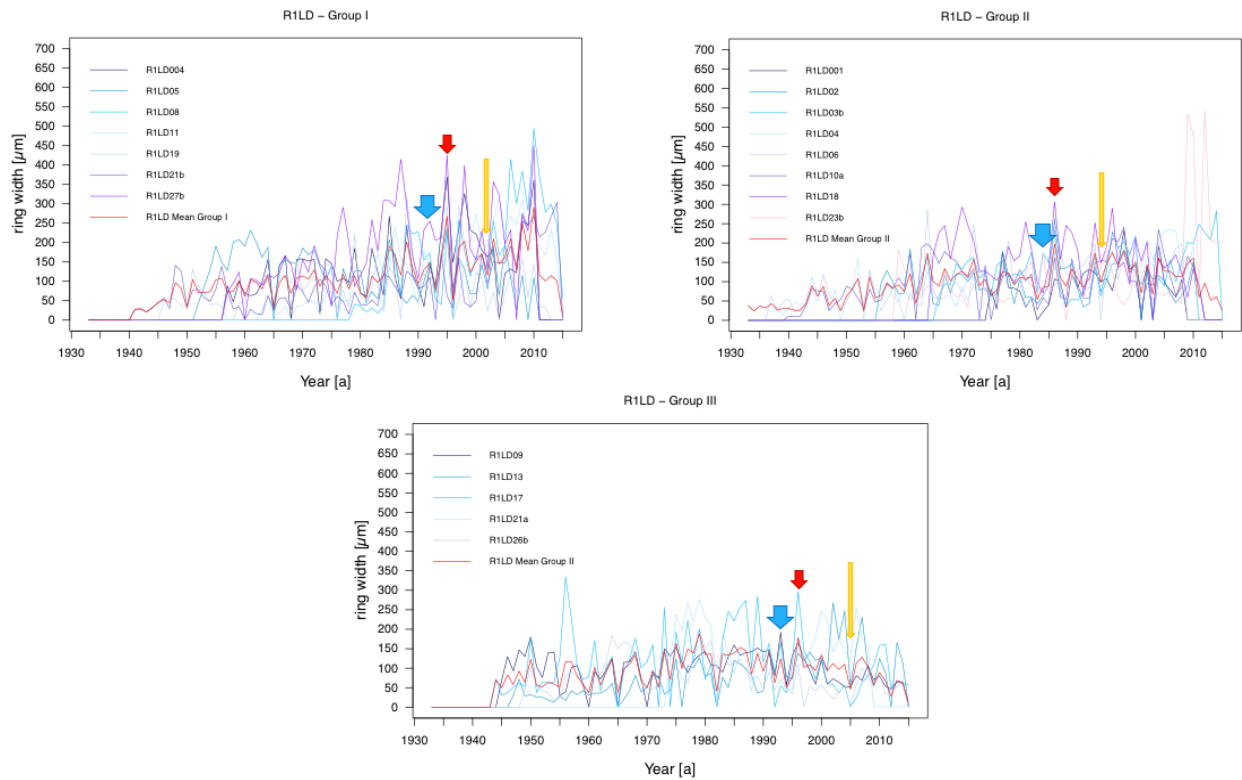


Figure 19. Cross-dated groups of the left levee. With colored arrows, three of the recurrent peaks or rather low were marked (author 2017).

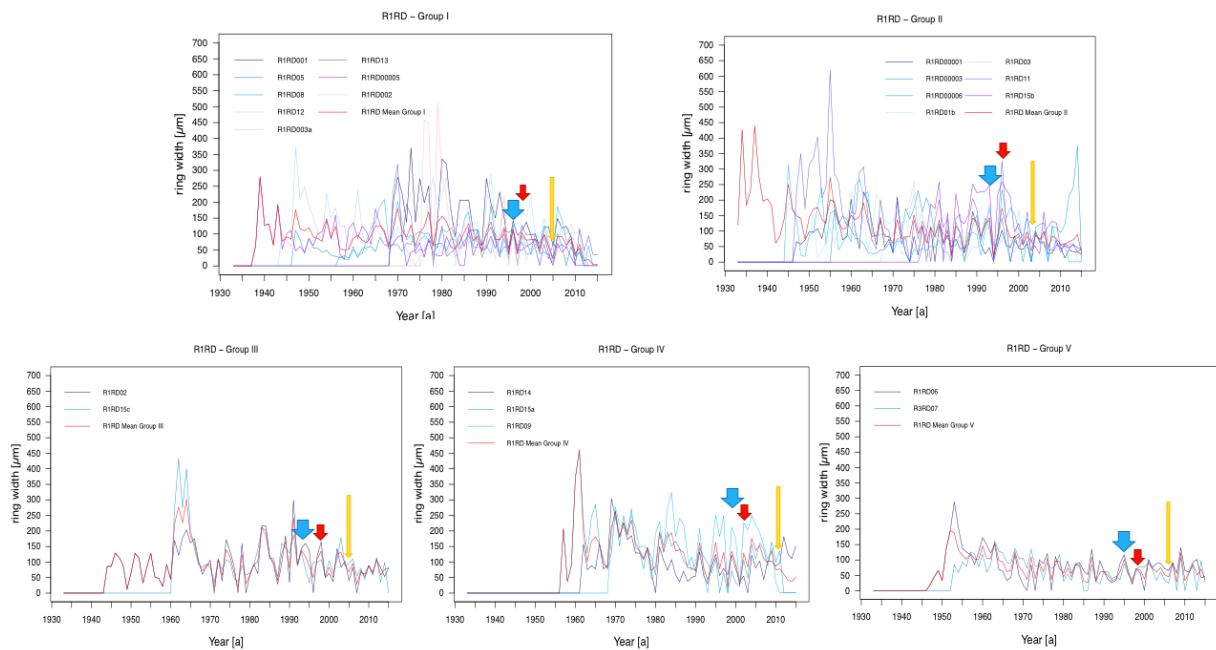


Figure 20. Cross-dated groups of the right levee. With colored arrows, three of the recurrent peaks or rather low were marked (author 2017).

It is interesting that most of the recurring shapes might be observed in the sequences of same direction described in the results. The interpretation of the features varies. As the area is prone to be affected by avalanches, it might be that the common sinks represent an interference that affected all the plants, such as an avalanche. Particularly low temperatures could

also be a reason. The peaks could, therefore, be a sign of common favourable condition. Comparing the maximum and minimum temperatures with the common sinks and peaks is difficult. Around the time of movement date of the peaks/lows, years of exceptionally high precipitation in winter 1992, 1993, 1996, 1997 and 2000 as well max. and min. temperatures registered in that decade showed signs of exceptionally cold winters (min. temperature lower than -10°C) in the years 1991, 1993, 1994 and 1999. Also high temperatures in summer 1991, 1992 and 1994 were recorded. These years could match the peaks/lows.

However, the result of the correlation test showed an insignificant relationship between most of the means and the annual mean temperatures during the past 55 years. Only one of the means curves showed a statistically significant correlation. However, analysing the plots visually, it was noticed that some peaks-low-sequences might fit better if relocated a few years. This hypothesis was, however, not followed because it would inquire further intensive detailed analyses which would go beyond the scope of this Master Thesis. Such a hypothesis could further confirm that the number of missing rings was set too low and further cross-dating might improve the chronologies.

A different explanation for the finding of groups is the influence of microclimate. Bär et al. (2006, 25) explained the variation in their results with the influence of a change in microtopography conditions change. Owczarek (2010, 47) also propose the influence of microsite conditions, such as inclination, exposure and snow cover period as an important cross-dating affecting factor.

Temperature, rainfall, nutrients and soil characteristic differences on small scales might influence the growth of the plants. Dwarf shrubs of the same group could have similar microclimate conditions. While one of the group means showed a statistically significant relationship with the temperature, the source of the climatic data should be taken into consideration while considering a microclimate. The weather station is located in Suldén a few kilometres from the study site. So it could be possible that the data does not entirely correspond the conditions in the site. Therefore, the climate data can only be taken as a rough approximation of the temperatures and the precipitation in the channels. The data is, however, possibly not suitable, due to uncertainties on the degree of concordance between the climate in Suldén and the climate in the Marl-Graben, to draw any conclusion on the effects of microclimate.

SPATIAL DISTRIBUTION OF *DRYAS OCTOPETALA* ON THE LEVEES

The results of the spatial-age distribution of the groups would oppose the microclimate hypothesis. The *Dryas octopetala*, which were arranged in the same groups do not show similar growing positions. The sampled plants seem to grow randomly on the levee.

Observing the spatial distribution of the sampled *Dryas octopetala* on all levees a further possible influence must be taken into consideration. A debris-flow event might not only influence the growth of the shrubs on its levees but also those on the adjacent channel. This question arises mostly in connection with the channels R1 and R2. As mentioned in the site description the channel R2 must have been cut off from the debris flow which created the ridges of R1. The question was raised if R2 might be a result of the overflowing of the levees of R1 due to a relict debris-flow head found at the intersection between R2 and R1. This question, however, was answered by the age of the sampled plants. The oldest samples in the channel R2 are much older than the one in R1. However, this fact does not exclude that the upperparts of the right levee of R2, directly next to the channel R1 might be influenced by the debris flow. Such a situation might have an effect on the plant distribution on the levees.

INFLUENCE OF SAMPLING AND SAMPLE QUANTITIES ON THE CROSS-DATING PROCESS

Besides all the challenging facts already described, which might affect the cross-dating, two further methodical aspects, which could also influence the choice of *Dryas octopetala* as the centre of a dendrogeomorphological study, will be presented i.e. the amount of sampled dwarf shrubs and the condition of the samples.

The mountain avens predominantly grow in sites full of coarse debris. Having to wind its way between rocks the stem, roots and branches are often twisted or have assumed very irregular transverse section shapes (Owczarek 2010, 54). Additionally, due to the influence of smaller "rock falls", hiker activity, animals or even after avalanche events the debris around the *Dryas octopetala* might be set into motion and consequently the shrubs might become damaged. As

already explained, damage to the stem and the roots leads to compartmentalisation. This preventive process leads to challenging samples to cut into thin sections, possibly with the compartmentalised area. As such situations (compartmentalised as well as twisted samples) were experienced relatively often, a high number of stem slides resulted in not optimal thin sections. Furthermore, during the process of digitalization of the section, a further amount of samples was sampled out due to technical difficulties. By the time the cross-dating could be started, a little more than a fifth of all samples could not be implemented in the analysis. Further, during the cross-dating it became clear that a high quantity of samples were needed to form the groups and to be compared between each other.

Owczarek (2010, 47) analysed only 10 samples of *Salix polaris* and *Salix reticulata* per debris-flow ridge. He encountered similar conditions as the one found in *Dryas octopetala*. Missing, partially missing and irregularly shaped rings have a challenging impact on the cross-dating. Additionally, his samples showed an irregular growth.

Bär et al. (2006) analysed in their work a higher quantity (12-15 per levee) of plants. They studied the *Empetrum hermaphroditum* Hagerup (crowberry), which displays similar anatomical features to *Dryas octopetala* and is a dwarf shrub. Their serial sectioning cross-dating, would confirm the above stated expectation that the placement of the sectioning is indeed of great importance for the cross-dating. A similar statement was completed by Myers-Smith et al. (2015, 7-9).

Myers-Smith et al. (2015) further discussed the importance for the minimum-age-dating to find the oldest plant in the site and how this endeavour is not trivial, as shrubs often display a not correlating height or stem thickness with the age of the plants. This observation matched the findings of *Dryas octopetala*. Often the older samples, belonged to the ones with a smaller diameter. The fact that it was impossible to ensure to have sampled the oldest shrub without counting the rings, also confirmed the requirement of a great number of sampled plants.

A further aspect is that the *Dryas octopetala* is a pioneer plant, which has a high initial growth, but which is also affected by a high mortality of these first seedlings (Karlisdóttir and Aradóttir 2006, 29-30). Furthermore, weather conditions (mostly frost and wind) during the settling period have a further influence on the population of the levee. Mountain avens plants have difficulties to settle in especially windy areas (Scott 1986, 95; Sjögren 1980, 85; Wada and Nakai 2004, 68-69).

For these given reasons a high amount of sampling material has to be collected and analysed. The main drawback of the major amount of sampling material is that the sample preparation procedure is composed of many time consuming steps. A large amount of samples take a long time to cut, bleach, stain, fix and clean. For this reason, the dwarf shrub *Dryas octopetala* is probably more suited for smaller study sites.

RECONSTRUCTION OF DEBRIS-FLOW EVENTS WITH DRYAS-OCTOPETALA

During this master thesis the potential of the dwarf shrub *Dryas octopetala* for reconstructing debris-flow events was evaluated. As assessed, a minimal date since when the last erosive flow occurred could be measured (Owczarek et al. 2013, 81); the channel R2, which was assumed to be the oldest due to its denser vegetation cover, was created at least before 1910. The oldest plant recovered in the channel was 105 years old (counted rings, without cross-dating). This age is close to the oldest recorded *Dryas octopetala* plant (108 years) reported by Schweingruber and Poshold (2005, 264). The dwarf shrub with the most rings in the middle-channel, R1, contained 77 annual rings before and 83 following cross-dating. In the last channel R3 a 69 year old *Dryas octopetala* stem was collected and dated. This dating allowed the determination of a probable chronology of the three events. Firstly, at the beginning of the 20th century the debris flow, which created channel R2, occurred. At the end of the 30's a second debris flow "pushed" its way downslope and probably broke through channel R2 cutting it off. About 10 years later, a final debris-flow shaped the channel R3 and, breaking through the right ridge of R1, created a connection between the two adjacent channels.

This chronology is further supported by the density of the vegetation cover. As shown in the site description showed, the vegetation density increased in the sampling area from the channel R3 to R2. This order corresponds to the determined age-order of the channels. Stoffel and Bollschweiler (2008, 192) further reminds us that the dating approach remains an approximation of the event date due to the unknown time period between the event and the repopulation of the newly bared soil.

Further, it was attempted to validate this sequence of events by cross-dating the growth time-series. However, as just described above, the cross-dating was only partly successful.

CONCLUSION

The dwarf shrub species *Dryas octopetala* is a pioneer plant, which grows on calcareous young soils. It is a widely spread species found in high mountain areas and in the northern subarctic zones. Due to its easily recognizable characteristics and its common frequency in areas bare of trees, the mountain avens potentially is a suitable plant for dendrogeomorphologic studies. This thesis aimed to assess the extent of the suitability of *Dryas octopetala* for dendrochronological methods and its ability to reconstruct debris-flow events. This analysis was conducted on mountain avens samples that originated from a section of three debris-flow channels in the debris fan Marlt-Graben by Sulden in South Tyrol. 154 stem thin sections of *Dryas octopetala* were examined. The annual growth rings were counted along the longest radius. The resulting growth curves were cross-dated for one channel. The resultant cross-dating was, however, successful for some selected samples only. Small chronologies (groups) with 2 to 8 shrubs were built. These chronologies were then tested on correlations to annual mean temperatures and mean precipitation. Beside two group-means, neither the temperatures nor the precipitation volumes seem to have a significant relationship to the growth of the plants. Furthermore, no spatial distribution trends were found on the levee by plotting the distance of the sprouting position and the age of the samples.

These results might be influenced by the following factors:

During sample preparation slides were cut until the section was satisfactory, but the position of the section in the stem was not noted. As a ring amount variation within the stem exists, the samples should, under the best conditions, be all cut in the same stem position. This ring discrepancy has not only an influence on the amount of counted rings but also on the amount of missing rings. The extent of inserted missing rings represented the main challenge in this work. How many rings are missing? How many rings might be inserted before the curve is not over influenced by them resulting into a construct? These questions were constantly present. In this work, an answer was found by the cross-dating of multiple radii. While this procedure resulted as a guiding value, the result could have been further improved and confirmed by cross-dating multiple radii in all samples. Also a wider understanding of the ring distribution within the plant might help gain a deeper knowledge on the difference of the sampling position in the plant and the number of missing rings. This can be achieved by taking several thin

sections from many different positions on the plant. Further studies in these directions might help improve the cross-dating results as well as the building of a full chronology.

Concluding following further results of this master thesis must be highlighted. The *Dryas octopetala* can be used for the minimal age and process sequence determination of debris-flow events. This was achieved with the evaluation and investigation of a large amount of mountain avens samples. This work suggests that more samples might improve the results, as many plants have a compartmentalized area or are partly twisted. Furthermore, the analysis of the dwarf shrubs is challenging due to the eccentric, extremely narrow and partially missing structure of the rings. Additionally, the sample preparation process is relatively time intensive. However, the *Dryas octopetala* is a pioneer plant which is a common sight in former glacier influenced mountain and arctic areas with a calcareous ground material. With further studies this dwarf shrub might show a greater potential within the field of dendroecology, and more specifically dendrogeomorphology.

LITERATURE

ANDERSON D.J. (1967): Studies on Structure in Plant Communities: IV. Cyclical Succession in *Dryas* Communities from North-West Iceland. In: *Journal of Ecology*, 55(3), 629–635.

ARBELLAY E., BOLLSCHWEILER M. and STOFFEL M. (2010): Dendrogeomorphic reconstruction of past debris-flow activity using injured broad-leaved trees. In: *Earth Surface Processes and Landforms*, 35(), 399–406.

ARTUSI R., VERDERIO P. and MARUBINI E. (2002): Bravais-Pearson and Spearman correlation coefficients: meaning, test of hypothesis and confidence interval. In: *The International Journal of Biological Markers*, 17(2), 148–151.

AU R. and TARDIF J.C. (2007): Allometric relationships and dendroecology of the dwarf shrub *Dryas integrifolia* near Churchill, subarctic Manitoba. In: *Canadian Journal of Botany*, 85(), 585–597.

AUS DER AU R., FONTANA G. and SCHÄRER C. (2016): GEO 417.3 Feldkurs in Geochronologie. 04. – 08. Juli 2016. field report. University of Zurich, 1–33.

AUTONOME PROVINZ BOZEN-SÜDTIROLER INFORMATIK AG (2007): GeoKatalog. <http://geokatalog.buergernetz.bz.it/geokatalog/#!> (Accessed: 29.03.2017).

BÄR A., BRÄUNING A. and LÖFFLER J. (2006): Dendroecology of dwarf shrubs in the high mountains of Norway – A methodological approach. In: *Dendrochronologia*, 24(), 17–27.

BAUMANN F. and KEISER K.F. (1999): The Muletta Debris Fan, Eastern Swiss Alps: A 500-Year Debris Flow Chronology. In: *Arctic, Antarctic, and Alpine Research*, 31(2), 128–134.

BENISTON M. and STEPHENSON D.B. (2004): Extreme climatic events and their evolution under changing climatic conditions. In: *Global and Planetary Change*, 44(), 1–9.

BLOTT S.J. and PYE K. (2001): Gradistat: A grain size distribution and statistics package for the analysis of unconsolidated sediments. In: *Earth Surface Processes and Landforms*, 26(), 1237–1248.

BOLLSCHWEILER M. and STOFFEL M. (2010): Variations in debris-flow occurrence in an Alpine catchment — A reconstruction based on tree rings. In: *Global and Planetary Change*, 73(), 186–192.

BOLLSCHWEILER M., STOFFEL M., EHMISCH M. and MONBARON M. (2006): Reconstructing spatio-temporal patterns of debris-flow activity using dendrogeomorphological methods. In: *Geomorphology*, 87(), 337–351.

BRAAM R.R., WEISS E.E.J. and BURROUGH P.A. (1987): Spatial and temporal analysis of mass movement using dendrochronology. In: *CATENA*, 14(), 573–584.

BUCHWAL A., RACHLEWICZ G., FONTI P., CHERUBINI P. and GÄRTNER H. (2013): Temperature modulates intra-plant growth of *Salix Polar* from a high Arctic site (Svalbard). In: *Polar Biology*, 36(), 1305–1318.

BUTLER D.R. (1987): Teaching General Principles and Applications of Dendrogeomorphology. In: *Journal of Geological Education*, 35(), 64–70.

CHEN H. (2006): Controlling factors of hazardous debris flow in Taiwan. In: *Quaternary International*, 147(), 3–15.

COLLISON A., WADE S., GRIFFITHS J. and DEHN M. (2000): Modelling the impact of predicted climate change on landslide frequency and magnitude in SE England. In: *Engineering Geology*, 55(), 205–218.

COROMINAS J., REMONDO J., FARIAS P., ESTEVAO M., ZÉZERE J., DÍAZ DE TERÁN J., DIKAU R., SCHROTT L., MOYA J. and GONZÁLEZ A. (1996): Debris Flow. In: Dikau R., Brunsden D., Schrott L. and Ibsen M. (eds.). *Landslide Recognition. Identification, Movement and Courses*. Bath: John Wiley & Sons Ltd, 161–180.

COSTA J.E. (1984): Physical Geomorphology of Debris Flow. In: Costa J.E. and Fleisher P.J. (eds.). *Developments and Applications of Geomorphology*. Heidelberg: Springer-Verlag Berlin Heidelberg, 268–312.

COUSSOT P. and MEUNIER M. (1996): Recognition, classification and mechanical description of debris flows. In: *Earth-Science Reviews*, 40(), 209–227.

DAMM B. and FELDERER A. (2013): Impact of atmospheric warming on permafrost degradation and debris flow initiation – A case study from the eastern European Alps. In: *Quaternary Science Journal*, 62(2), 136–149.

DEHN M., BÜRGER G., BUMA J. and GASPARETTO P. (2000): Impact of climate change on slope stability using expanded downscaling. In: *Engineering Geology*, 55(), 193–204.

DIETRICH A. and KRAUTBLATTER M. (2016): Evidence for enhanced debris-flow activity in the Northern Calcareous Alps since the 1980s (Plansee, Austria). In: *Geomorphology*, 1–15.

DOWLING C.A. and SANTI P.M. (2014): Debris flows and their toll on human life: a global analysis of debris-flow fatalities from 1950 to 2011. In: *Natural Hazards*, 71(), 203–227.

EICHEL J., CORENBLIT D. and DIKAU R. (2015): Conditions for feedbacks between geomorphic and vegetation dynamics on lateral moraine slopes: A biogeomorphic feedback window. In: *Earth Surface Processes Landforms*, 1–14.

ELKINGTON T.T. (1971): *Dryas Octopetala* L.. In: *Journal of Ecology*, 59(3), 887–905.

GÄRTNER H., ESPER J. and TREYDTE K. (2004): Geomorphologie und Jahrringe – Feldmethoden in der Dendrogeomorphologie. In: *Schweizerische Zeitschrift für Forstwesen*, 155(6), 198–207.

GÄRTNER H. and NIEVERGELT D. (2010): The core-microtome: A new tool for surface preparation on cores and time series analysis of varying cell parameters. In: *Dendrochronologia*, 28(), 85–92.

GÄRTNER H. and SCHWEINGRUBER F.H. (2013): *Microscopic Preparation Techniques for plant Stem Analysis*. Remagen-Oberwinter: Verlag Dr. Kessel.

GÄRTNER H., STOFFEL M., LIÈVRE I., CONUS D., GRICHTING M. and MONBARON M. (2003): Debris-flow frequency derived from tree-ring analyses and geomorphic mapping, Valais, Switzerland. In: *Debris Flow Hazards Mitigation: Mechanics, Prediction, and Assessment*, 1(), 207–217.

GERS E., FLORIN N., GÄRTNER H., GLADE T., DIKAU R. and SCHWEINGRUBER F.H. (2001): Application of shrubs for dendrogeomorphological analysis to reconstruct spatial and temporal landslide movement patterns. A preliminary study. In: *Zeitschrift für Geomorphologie*, 125(), 163–175.

HENRY G.H.R. and MOLAU U. (1997): Tundra plants and climate change: The International Tundra Experiment (ITEX). In: *Global Change Biology*, 3(1), 1–19.

HOPP C.R., OSTERKAMP W. R and THORNTON J. L. (1987): Dendrogeomorphic evidence and dating of recent debris flows on Mount Shasta, Northern California. U.S. geological survey professional paper 1396-B. Washington: United States Government Printing Office.

INFO FLORA (2017a): *Calluna vulgaris* (L.) Hull. <https://www.infoflora.ch/de/flora/836-calluna-vulgaris.html#map> (Accessed: 01.04.2017).

INFO FLORA (2017b): *Dryas octopetala* L.. <https://www.infoflora.ch/de/flora/1023-dryas-octopetala.html#map> (Accessed: 01.04.2017).

INFO FLORA (2017c): *Pinus mugo* Turra s.l.. <https://www.infoflora.ch/de/flora/9993-pinus-mugo-sl.html#map> (Access: 01.04.2017).

INFO FLORA (2017d): *Salix appendiculata* Vill. <https://www.infoflora.ch/de/flora/627-salix-appendiculata.html#map> (Accessed: 01.04.2017).

INTERGOVERNMENTAL PANEL ON CLIMATE CHANGE (IPCC) (2014): *Climate Change 2014. Synthesis Report. Summary for Policymakers*. https://www.ipcc.ch/pdf/assessment-report/ar5/syr/AR5_SYR_FINAL_SPM.pdf (Accessed: 16.01.2016).

ISSELIN-NONDEDEU F. and BÉDÉCARRATS A. (2007): Influence of alpine plants growing on steep slopes on sediment trapping and transport by runoff. In: *CATENA*, 77(), 330–339.

JAY F., MANEL S., ALVAREZ N., DURAND E.Y., THUILLER W., HOLDEREGGER R., TABERLET P. and FRANÇOIS O. (2012): Forecasting changes in population genetic structure of alpine plants in response to global warming. In: *Molecular Ecology*, 21(), 2354–2368.

JOHNSON P.A. and MCCUEN R.H. (1996): Mud and Debris Flow. In: Singh V.P.(ed.). Hydrology of Disasters. Dordrecht: Kluwer Academic Publishers, 161–181.

JOMELLI V., BRUNSTEIN D., DÉQUÉ M., VRAC M. and GRANCHER D. (2009): Impacts of future climatic change (2070–2099) on the potential occurrence of debris flows: A case study in the Massif des Ecrins (French Alps). In: Climatic Change, 1–21.

KARLSDÓTTIR L. and ARADÓTTIR Á. (2006): Propagation of *Dryas octopetala* L. and *Alchemilla alpina* L. by direct seeding and planting of stem cuttings. In: Icelandic Agricultural Sciences. 19(), 25–32.

KEPPLER U. (1938): Zur Geologie der Ortlergruppe und zur Stratigraphie der Ortlerzone. Zwischen Sulden und dem Endagin. Zürich: Buchdruckerei Fluntern.

KLANDERUD K. and TOTLAND Ø. (2004): Habitat dependent nurse effects of the dwarf shrub *Dryas octopetala* on alpine and arctic plant community structure. In: Écoscience, 11(4), 410–420.

KLANDERUD K. and TOTLAND Ø. (2005): Simulated Climate Change Altered Dominance Hierarchies And Diversity Of An Alpine Biodiversity Hotspot. In: Ecology, 86(8), 2047–2054.

KOZŁOWSKA A. and RAÇZKOWSKA Z. (2002): Vegetation as a tool in the characterization of geomorphological forms and processes: an example from the abisko mountains. In: Geografiska Annaler: Series A, Physical Geography, 84(3–4), 233–244.

LANGHANS J.E. (1913): Ins Ortlergebiet. Meran–Naturns–Schmalstal. Schlanders–Laas–Spondoring. Gomagoi–Sulden–Ortler. Frankfurt am Main: Expedition von Hendschels Telegraph.

LAUBER K. (2012): *Dryas octopetala* L.. <https://www.infoflora.ch/de/flora/1023-dryas-octopetala.html> (Accessed: 19.04.2017).

MALIK I. and OWCZAREK P. (2009): Dendrochronological records of debris flow and avalanche activity in a mid-mountain forest zone (Eastern Sudetes – Central Europe). In: Geochronometria, 34(), 57–66.

MYERS-SMITH I.H., HALLINGER M., BLOK D., SASS-KLAASSEN U., RAYBACK S.A., WEIJERS S., TRANT A.J., TAPE K.D., NAITO A.T., WIPF S., RIXEN C., DAWES M.A., WHEELER J.A., BUCHWAL A., BAITTINGER C., MACIAS-FAURIA M., FORBES B.C., LÉVESQUE E., BOULANGER-LAPOINTE N., BEIL I., RAVOLAINEN V. and WILMKING M. (2015): Methods for measuring arctic and alpine shrub growth: A review. In: Earth-Science Reviews, 140(), 1–13.

OWCZAREK P. (2010): Dendrochronological dating of geomorphic processes in the High Arctic. In: Landform Analysis, 14(), 45–56.

OWCZAREK P., LATOCHA A., WISTUBA M. and MALIK I. (2013): Reconstruction of modern debris flow activity in the arctic environment with the use of dwarf shrubs (south-western Spitsbergen) – A new dendrochronological approach. In: Zeitschrift für Geomorphologie, 57 (3), 75–95.

PAYER J. (1865): Originalkarte des Sulden-Gebietes. 1:48'000. <http://nbn-resolving.de/urn:nbn:de:bvb:355-ubr03803-0021-8> (Accessed: 30.03.2017).

PAVLOVA I., JOMELLI V., BRUNSTEIN D., GRANCHER D., MARTIN E. and DÉQUÉ M. (2014): Debris flow activity related to recent climate conditions in the French Alps: A regional investigation. In: *Geomorphology*, 219(), 248–259.

PIGNATTI E. and PIGNATTI S. (2014): *Plant Life of the Dolomites. Vegetation structure and ecology*. Heidelberg: Springer-Verlag.

PIGOTT C.D. and WALTERS S.M. (1954): On the Interpretation of the Discontinuous Distributions Shown by Certain British Species of Open Habitats. In: *Journal of Ecology*, 42(1), 95–116.

RAETZO H., LATELTIN O., BOLLINGER D. and J.P. TRIPET (2002): Hazard assessment in Switzerland –Codes of Practice for mass movements. In: *Bulletin of Engineering Geology and the Environment*, 61(), 263–268.

RINN F. (2012): TSAP-Win™ Professional. Zeitanalyse und Präsentation für Dendrochronologie für verwandte Anwendungen. Version 4.5 für Microsoft Windows. Benutzerhandbuch. Heidelberg: Rinntech.

ROBINSON W.J., COOK E., PILCHER J.R., ECKSTEIN D., KAIRIUKSTIS L., SHIYATOV S. and NORTON D.A. (1990): Some Historical Background on Dendrochronology. In: Cook E.R. and Kairiukstis L.A. (eds.) (1990): *Methods of Dendrochronology. Applications in the Environmental Sciences*. Dordrecht: Kluwer Academic Publishers, 1–21.

SAEMUNDSSON T., PETURSSON H.G. and DECAULNE A. (2013): Triggering factors for rapid mass movements in Iceland. In: Rickenmann D. and Chen C. (eds). *Debris-Flow Hazards Mitigation: Mechanics, Prediction, and Assessment*. Rotterdam: Millpress, 167–178.

SCOTT A.I.(1986): Factors Influencing Soil Moisture and Plant Community Distribution on Niwot Ridge. In: *Arctic and Alpine Research*, 18(1), 83–96.

SCHWEINGRUBER F.H., BÖRNER A. and SCHULZE E. (2011): *Atlas of Stem Anatomy in Herbs, Shrubs and Trees*. Heidelberg: Springer-Verlag Berlin Heidelberg.

SCHWEINGRUBER F.H. and POSHOLD P. (2005): Growth Rings in Herbs and Shrubs: life span, age determination and stem anatomy. In: *Forest Snow and Landscape Research*, 79(3), 195–415.

SHRODER Jr. J.F. (1980): Dendrogeomorphology: Review and new tree-ring dating. In: *Progress in Physical Geography*, 4(2), 161–188.

SJÖGREN E. (ed.) (1980): *Studies in Plant Ecology. Dedicated to Hugo Sjörs*. In: *Acta Phytographica Suecica*, 68(),1–192.

STÖTTER J., FUCHS S., M. KEILER M. and ZISCHG A. (2003): Oberes Suldental - Eine Hochgebirgsregion im Zeichen des Klimawandels. In: Steinecke E. (ed.) (2003): Geographischer Exkursionsführer Europaregion Tirol, Südtirol, Trentino. Band 3: Spezialexcursionen in Südtirol, Innsbrucker Geographische Studien, 33(3), 239–281.

STOFFEL M. (2006): A Review of Studies Dealing with Tree Rings and Rockfall Activity: The Role of Dendrogeomorphology in Natural Hazard Research. In: *Natural Hazards*, 39(), 51–70.

STOFFEL M. and BOLLSCHWEILER M. (2008): Tree-ring analysis in natural hazards research? an overview. In: *Natural Hazards and Earth System Science*, 8(2), 187–202.

STOFFEL M. and BOLLSCHWEILER M. (2009): What Tree Rings Can Tell About Earth-Surface Processes: Teaching the Principles of Dendrogeomorphology. In: *Geography Compass*, 3(3), 1013–1037.

STOFFEL M. and HUGGEL C. (2012): Effects of climate change on mass movements in mountain environments. In: *Progress in Physical Geography*, 36(3), 421–439.

STOFFEL M., LIÈVRE I., CONUS D., GRICHTING M.A., RAETZO H., GÄRTNER H.W., and MONBARON M. (2005): 400 Years of Debris-Flow Activity and Triggering Weather Conditions: Riti-graben, Valais, Switzerland. In: *Arctic, Antarctic, and Alpine Research*, 37(3), 387–395.

STOFFEL M., CONUS D., GRICHTING M.A., LIÈVRE I. and MÂÎTRE G. (2008): Unraveling the patterns of late Holocene debris-flow activity on a cone in the Swiss Alps: Chronology, environment and implications for the future. In: *Global and Planetary Change*, 60(), 222–234.

STRUNK H. (1997): Dating of geomorphological processes using dendrogeomorphological methods. In: *CATENA*, 31(), 137–151.

SEWELL R.J., PARRY S., MILLIS S.W., WANG N., RIESER U. and DEWITT R. (2015): Dating of debris flow fan complexes from Lantau Island, Hong Kong, China: The potential relationship between landslide activity and climate change. In: *Geomorphology*, 248(), 205–227.

SZYMCZAK S., BOLLSCHWEILER M., STOFFEL M. and DIKAU R. (2010): Debris-flow activity and snow avalanches in a steep watershed of the Valais Alps (Switzerland): Dendrogeomorphic event reconstruction and identification of triggers. In: *Geomorphology*, 116(), 107–114.

TAKAHASHI T. (1991): *Debris Flow*. Rotterdam: A.A. Balkema Publishers.

TRAPPMANN D., CORONA C. and STOFFEL M. (2013): Rolling stones and tree rings: A state of research on dendrogeomorphic reconstructions of rockfall. In: *Progress in Physical Geography*, 37(5), 701–716.

YOUBERG A.M., WEBB R.H., FENTON C.R. and PEARTHREE P.A. (2014): Latest Pleistocene–Holocene debris flow activity, Santa Catalina Mountains, Arizona; Implications for modern debris-flow hazards under a changing climate. In: *Geomorphology*, 219(), 87–102.

UNIVERSITY OF BOLZANO (2017a): Valori mensili e annui delle Precipitazioni. Solda-Sulden.

UNIVERSITY OF BOLZANO (2017b): Temperature mensili e annue. Solda-Sulden.

WADA N. and NAKAI Y. (2004): Germinability of Seeds in a Glacial Relict *Dryas octopetala* var. *asiatica*: Comparison with a Snowbed Alpine Plant *Sieversia pentapetala* in a Middle-Latitude Mountain Area of Central Japan. In: *Far Eastern Studies*, 3(), 57–72.

WELKER J.M., MOLAU U., PARSONS A.N., ROBINSON C.H. and WOOKEY P.A. (1997): Responses of *Dryas octopetala* to ITEX environmental manipulations: a synthesis with circumpolar comparisons. In: *Global Change Biology*, 3(1), 61–73.

WENTWORTH C.K. (1922): A Scale of Grade and Class Terms for Clastic Sediments. In: *The Journal of Geology*, 30(5), 377–392.

VAN DEN HEUVLEN F, GOYETTE S., RAHMAN K. and STOFFEL M. (2016): Circulation patterns related to debris-flow triggering in the Zermatt valley in current and future climates. In: *Geomorphology*, 272(), 127–136.

VASARI Y. (1999): The history of *Dryas octopetala* L. in eastern Fennoscandia. In: *Grana*, 38(), 250–254.

ZISCHG A., FUCHS S., KEILER M. and STÖTTER J. (2005): Temporal variability of damage potential on roads as a conceptual contribution towards a short-term avalanche risk simulation. In: *Natural Hazards and Earth System Sciences*, 5(), 235–242.

APPENDIX

APPENDIX A – DATA OF THE COLLECTED SAMPLES IN R2 AND R3

Sample name	Distance to the centre [m]	Age before cross-dating	pith
R2 LD0001	100	61	no
R2 LD001	100	-	-
R2 LD001	150	82	yes
R2 LD0002	200	43	no
R2 LD002	220	103	yes
R2 LD002	-	-	-
R2 LD003	210	80	no
R2 LD003	680	42	no
R2 LD004	300	-	-
R2 LD004	450	53	yes
R2 LD005	382	69	yes
R2 LD005a	210	96	no
R2 LD005b	210	77	no
R2 LD006	179	86	no
R2 LD006	-	-	-
R2 LD007	271	60	no
R2 LD007	670	69	yes
R2 LD008	220	45	yes
R2 LD008	220	96	yes
R2 LD009	250	59	yes
R2 LD009	250	65	yes
R2 LD010	330	-	-
R2 LD010	450	42	no
R2 LD011	433	-	-
R2 LD011	250	60	yes
R2 LD012	460	59	no
R2 LD012	610	60	no
R2 LD013	470	54	no
R2 LD013	700	54	no
R2 LD014	124	84	no
R2 LD014	550	41	yes

Table 4. Data – R2LD (author 2017).

Sample name	Distance to the centre [m]	Age before cross-dating [a]	pith
R3 LD00001	300	-	-
R3 LD001	350	-	-
R3 LD00002	330	45	yes
R3 LD002	530	41	yes
R3 LD00003	470	42	yes
R3 LD003	609	45	yes
R3 LD00004	310	40	yes
R3 LD004	433	44	yes
R3 LD00005	160	52	yes
R3 LD006	508	36	no
R3 LD007	470	-	-
R3 LD008	200	-	-
R3 LD009	156	-	-
R3 LD010	450	-	-
R3 LD011	520	44	yes
R3 LD012	520	38	no
R3 LD013	500	33	no
R3 LD014	500	38	yes
R3 LD015	362	41	yes
R3 LD016	265	-	-
R3 LD017	244	-	-
R3 LD018	339	42	yes
R3 LD019	490	52	yes
R3 LD020	450	34	yes
R3 LD021	375	36	yes
R3 LD022	411	35	yes
R3 LD023	303	33	yes
R3 LD024	380	-	-
R3 LD025	360	45	yes

Table 6. Data – R3LD (author 2017).

Sample name	Distance to the centre [m]	Age before cross-dating [a]	pith
R2 RD0001	228	82	yes
R2 RD001	240	81	yes
R2 RD001	520	48	yes
R2 RD0002	380	60	no
R2 RD002	200	80	yes
R2 RD0003	405	65	yes
R2 RD003	220	57	yes
R2 RD003	340	105	yes
R2 RD0004	241	64	yes
R2 RD004	410	-	-
R2 RD004	280	39	yes
R2 RD0005	372	53	no
R2 RD005	570	-	-
R2 RD005	490	91	no
R2 RD0006	97	24	no
R2 RD006	563	39	yes
R2 RD006	390	35	yes
R2 RD0007	148	67	no
R2 RD007	476	87	yes
R2 RD007	-	-	-
R2 RD0008	163	48	yes
R2 RD008	514	61	yes
R2 RD008	-	-	yes
R2 RD0009	532	56	yes
R2 RD009	360	-	-
R2 RD009	550	81	yes
R2 RD0010	500	63	no
R2 RD0011	556	90	no
R2 RD0012	620	87	no
R2 RD0013	640	75	yes
R2 RD0014	550	-	-
R2 RD0014	430	-	-
R2 RD0014	430	51	no
R2 RD0014	120	-	-
R2 RD0014	310	-	-

Table 5. Data – R2RD (author 2017).

Sample name	Distance to the centre [m]	Age before cross-dating [a]	pith
R3 RD00001	520	52	yes
R3 RD001	140	25	yes
R3 RD001	320	17	yes
R3 RD00002	220	31	yes
R3 RD002	152	20	yes
R3 RD002	400	30	yes
R3 RD00003	278	40	yes
R3 RD003	131	24	yes
R3 RD003	500	36	yes
R3 RD00004	202	25	yes
R3 RD004	324	28	yes
R3 RD004	440	17	yes
R3 RD00005	-	-	-
R3 RD005	160	50	yes
R3 RD005	-	-	-
R3 RD00006a	400	43	yes
R3 RD00006c	400	45	yes
R3 RD006	146	27	yes
R3 RD006	50	19	yes
R3 RD007	350	32	no
R3 RD007	190	27	yes
R3 RD008	323	23	yes
R3 RD009	417	-	yes
R3 RD010	421	69	yes
R3 RD011	433	-	yes
R3 RD012	433	47	yes
R3 RD013	216	44	yes
R3 RD014	325	51	yes
R3 RD015	158	38	yes
R3 RD016	101	30	yes
R3 RD017	320	47	yes
R3 RD018	-	-	-

Table 7. Data – R3RD (author 2017).

APPENDIX B – SPECIFIC CROSS-DATING DATA OF R1

Sample name	Distance to the centre [m]	Age before cross-dating [a]	Age after cross-dating [a]	Age without refill years [a]	missing ring	missing ring sum without PMR	PMR	cancelled rings	Group	plith	Years of missing rings	years on Null-rings before cross-dating	years on Null-rings after cross-dating	years cancelled rings	birth-year	Death-cross-year	death-year	Missing ring percentage [%]
R1 RD 00001	178	64	69	69	5	5	0	0	2	no	1974, 1978, 1980, 1994, 2003	-	-	-	1947	2015	2015	7.2
R1 RD 001	320	42	47	43	1	5	0	0	1	no	1978	-	-	-	1969	2011	2015	10.6
R1 RD 01a	110	-	-	-	-	-	-	-	-	-	-	-	-	-	-	-	-	-
R1 RD 01b	110	77	83	81	4	6	0	0	2	yes	1978, 1984, 1987, 1994	-	-	-	1933	2013	2015	7.2
R1 RD 00002	288	77	77	77	0	0	0	0	0	no	-	-	-	-	1939	2015	2015	0.0
R1 RD 002	210	35	40	37	3	6	1	1	1	yes	1978, 1997, 2005	1995, 2000	1995	-	1976	2012	2015	15.0
R1 RD 02	350	69	72	72	3	3	2	0	3	no	1971, 1977, 1979	1996, 2007	-	-	1944	2015	2015	4.2
R1 RD 00003	354	55	60	59	4	5	1	0	2	no	1998, 2001, 2003, 2007	1992	1987	-	1956	2014	2015	8.3
R1 RD 003a	107	65	72	69	4	7	1	0	1	yes	1997, 2002, 2005, 2010	1981	1974	-	1944	2012	2015	9.7
R1 RD 003b	107	-	-	-	-	-	-	-	-	-	-	-	-	-	-	-	-	-
R1 RD 03	270	45	48	48	3	3	0	0	2	yes	1978, 1984, 1987	-	-	-	1968	2015	2015	6.3
R1 RD 00004	-	-	-	-	-	-	-	-	-	-	-	-	-	-	-	-	-	-
R1 RD 04	380	28	28	28	0	0	0	0	0	yes	-	-	-	-	1988	2015	2015	0.0
R1 RD 00005	354	69	78	72	3	9	1	0	1	yes	1972, 1984, 2005	1992	1985	-	1938	2009	2015	11.5
R1 RD 05	460	63	69	65	2	6	0	0	1	no	2005, 2008	-	-	-	1947	2011	2015	8.7
R1 RD 00006	372	63	71	67	4	8	1	0	2	no	1984, 1987, 2003, 2007	1982	1974	-	1945	2011	2015	11.3
R1 RD 06	320	68	69	69	1	1	3	0	5	yes	1971	1973, 1977, 2000	1974, 1977, 2000	-	1947	2015	2015	1.4
R1 RD 00007	350	-	-	-	-	-	-	-	-	-	-	-	-	-	-	-	-	-
R1 RD 07	390	62	63	63	1	1	4	0	5	yes	1986	1986, 2008, 2010, 2013	1985, 2008, 2010, 2013	-	1953	2015	2015	1.6
R1 RD 00008	360	-	-	-	-	-	-	-	-	-	-	-	-	-	-	-	-	-
R1 RD 08	150	56	59	57	2	4	0	1	1	yes	1997, 2012	1983	-	1983	1957	2013	2015	6.8
R1 RD 00009	410	49	49	49	0	0	0	0	0	no	-	-	-	-	1967	2015	2015	0.0
R1 RD 09	430	40	47	42	2	7	0	0	4	yes	1993, 1998	-	-	-	1969	2010	2015	14.9
R1 RD 00010	390	-	-	-	-	-	-	-	-	-	-	-	-	-	-	-	-	-
R1 RD 10	420	-	-	-	-	-	-	-	-	-	-	-	-	-	-	-	-	-
R1 RD 00011	300	41	41	41	0	0	0	0	0	no	-	-	-	-	1975	2015	2015	0.0
R1 RD 11	230	65	69	69	4	4	0	0	2	no	1974, 1979, 1984, 1988	-	-	-	1947	2015	2015	5.8
R1 RD 12	270	35	40	36	1	5	0	0	1	yes	1983	-	-	-	1976	2011	2015	12.5
R1 RD 13	380	45	47	47	2	2	0	0	1	yes	2002, 2010	-	-	-	1969	2015	2015	4.3
R1 RD 14	130	53	54	54	1	1	1	0	4	yes	1980	2003	2003	-	1962	2015	2015	1.9
R1 RD 15a	180	54	59	55	1	5	1	0	4	yes	1996	2002	1998	-	1957	2011	2015	8.5
R1 RD 15b	180	37	39	39	2	2	0	0	2	yes	1982, 1994	-	-	-	1977	2015	2015	5.1
R1 RD 15c	180	54	55	54	0	1	0	0	3	yes	-	-	-	-	1961	2014	2015	1.8
R1 RD 15d	180	-	-	-	-	-	-	-	-	-	-	-	-	-	-	-	-	-
R1 RD 15e	180	45	45	45	0	0	0	0	0	yes	-	-	-	-	1971	2015	2015	0.0
R1 RD 16	340	67	67	67	0	0	0	0	0	yes	-	-	-	-	1949	2015	2015	0.0

Table 8. Cross-dating-data of the left levee of R1 (author 2017).

Sample name	Distance to the centre [m]	Age before cross-dating [a]	Age after cross-dating [a]	Age without refill years [a]	Missing ring (MR)	Total MR without PMR	PMR	Deleted rings	Group	Pith	MR-Years	PMR before cross-dating	PMR after cross-dating	deleted year-ring	birth-year	death-year cross-dating	death-year	MR percentage [%]
R1 RD 00001	178	65	69	69	5	5	0	0	2	no	1974, 1978, 1980, 1994, 2001	-	-	-	1947	2015	2015	7.2
R1 RD 001	320	42	47	43	1	5	0	0	1	no	1978	-	-	-	1969	2011	2015	10.6
R1 RD 01a	110	-	-	-	-	-	-	-	-	-	-	-	-	-	-	-	-	-
R1 RD 01b	110	77	83	81	4	6	0	0	2	yes	1978, 1984, 1987, 1994	-	-	-	1933	2013	2015	7.2
R1 RD 00002	288	77	77	77	0	0	0	0	0	no	-	-	-	-	1939	2015	2015	0.0
R1 RD 002	210	35	40	37	3	6	1	1	1	yes	1978, 1997, 2005	1995, 2000	1995	1995	1976	2012	2015	15.0
R1 RD 02	350	69	72	72	3	3	2	0	3	no	1971, 1977, 1979	1996, 2007	-	-	1944	2015	2015	4.2
R1 RD 00003	354	55	60	59	4	5	1	0	2	no	1998, 2001, 2003, 2007	1992	1987	-	1956	2014	2015	8.3
R1 RD 003a	107	65	72	69	4	7	1	0	1	yes	1997, 2002, 2005, 2010	1981	1974	-	1944	2012	2015	9.7
R1 RD 003b	107	-	-	-	-	-	-	-	-	-	-	-	-	-	-	-	-	-
R1 RD 03	270	45	48	48	3	3	0	0	2	yes	1978, 1984, 1987	-	-	-	1968	2015	2015	6.3
R1 RD 00004	350	-	-	-	-	-	-	-	-	-	-	-	-	-	-	-	-	-
R1 RD 04	380	28	28	28	0	0	0	0	0	yes	-	-	-	-	1988	2015	2015	0.0
R1 RD 00005	354	69	78	72	3	9	1	0	1	yes	1972, 1984, 2005	1992	1985	-	1938	2009	2015	11.5
R1 RD 05	460	63	69	65	2	6	0	0	1	no	2005, 2008	-	-	-	1947	2011	2015	8.7
R1 RD 00006	372	63	71	67	4	8	1	0	2	no	1984, 1987, 2003, 2007	1982	1974	-	1945	2011	2015	11.3
R1 RD 06	320	68	69	69	1	1	3	0	5	yes	1971	1973, 1977, 2000	1974, 1977, 2000	-	1947	2015	2015	1.4
R1 RD 00007	350	-	-	-	-	-	-	-	-	-	-	-	-	-	-	-	-	-
R1 RD 07	390	62	63	63	1	1	4	0	5	yes	1986	1986, 2008, 2010, 2011, 2015, 2010, 2011	-	-	1953	2015	2015	1.6
R1 RD 00008	360	-	-	-	-	-	-	-	-	-	-	-	-	-	-	-	-	-
R1 RD 08	150	56	59	57	2	4	0	1	1	yes	1997, 2012	1983	-	1983	1957	2013	2015	6.8
R1 RD 00009	410	49	49	49	0	0	0	0	0	no	-	-	-	-	1967	2015	2015	0.0
R1 RD 09	430	40	47	42	2	7	0	0	4	yes	1993, 1998	-	-	-	1969	2010	2015	14.9
R1 RD 00010	390	-	-	-	-	-	-	-	-	-	-	-	-	-	-	-	-	-
R1 RD 10	420	-	-	-	-	-	-	-	-	-	-	-	-	-	-	-	-	-
R1 RD 00011	300	41	41	41	0	0	0	0	0	no	-	-	-	-	1975	2015	2015	0.0
R1 RD 11	230	65	69	69	4	4	0	0	2	no	1974, 1979, 1984, 1998	-	-	-	1947	2015	2015	5.8
R1 RD 12	270	35	40	36	1	5	0	0	1	yes	1983	-	-	-	1976	2011	2015	12.5
R1 RD 13	380	45	47	47	2	2	0	0	1	yes	2002, 2010	-	-	-	1969	2015	2015	4.3
R1 RD 14	130	53	54	54	1	1	1	0	4	yes	1980	2003	2003	-	1962	2015	2015	1.9
R1 RD 15a	180	54	59	55	1	5	1	0	4	yes	1996	2002	1998	-	1957	2011	2015	8.5
R1 RD 15b	180	37	39	39	2	2	0	0	2	yes	1982, 1994	-	-	-	1977	2015	2015	5.1
R1 RD 15c	180	54	55	54	0	1	0	0	3	yes	-	-	-	-	1961	2014	2015	1.8
R1 RD 15d	180	-	-	-	-	-	-	-	-	-	-	-	-	-	-	-	-	-
R1 RD 15e	180	45	45	45	0	0	0	0	0	yes	-	-	-	-	1971	2015	2015	0.0
R1 RD 16	340	67	67	67	0	0	0	0	0	yes	-	-	-	-	1949	2015	2015	0.0

Table 9. Cross-dating-data of the right levee of R1 (author 2017).

APPENDIX C – CLIMATE DATA

Solda - Sulfen													
Cod. 06400MS		1907 m s.m./ü.M.					X_UTM 622375			Y_UTM 5152605			
Anno Jahr	I	II	III	IV	V	VI	VII	VIII	IX	X	XI	XII	ANNO JAHR
	med	med	med	med	med	med	med	med	med	med	med	med	med
1971	-5.6	-3.7	-5.0	4.1	7.0	7.9	12.1	12.6	7.6	6.8	0.2	0.2	3.7
1972	-5.4	-3.0	0.2	1.6	5.0	8.8	10.5	10.0	4.3	3.9	-0.2	-2.8	2.7
1973	-3.3	-5.0	-2.5	-0.6	7.6	10.2	10.5	13.9	10.5	4.3	1.5	-5.0	3.5
1974	-1.6	-3.4	-0.4	1.8	4.9	7.9	11.5	12.6	7.8	-1.7	-2.6	-2.3	2.9
1975	-2.5	-1.9	-3.4	1.7	7.0	7.7	11.5	11.5	10.1	4.2	-1.1	-2.3	3.5
1976	-3.0	-1.9	-1.6	2.8	7.3	10.7	11.5	9.2	5.9	4.7	-2.2	-6.4	3.1
1977	-6.2	-3.7	0.6	-0.4	5.3	8.4	9.8	8.6	7.0	4.6	-2.6	-3.1	2.3
1978	-5.8	-4.8	-2.0	-2.4	-4.4	4.3	9.7	8.8	8.0	4.8	1.5	-2.7	1.2
1979	"	"	"	"	"	"	"	"	"	"	"	"	"
1980	"	"	"	"	"	"	"	"	"	"	"	"	"
71-80	-4.2	-3.4	-1.8	1.1	5.0	8.2	10.9	10.9	7.6	3.9	-0.7	-3.0	2.9
1981	"	"	"	"	"	"	"	"	"	"	"	"	"
1982	"	"	"	"	"	"	"	"	"	"	"	"	"
1983	"	"	"	"	"	"	"	"	"	"	"	"	"
1984	"	"	"	"	"	"	"	"	"	"	"	"	"
1985	"	"	"	"	"	"	"	"	"	"	"	"	"
1986	"	"	"	"	"	"	"	"	"	"	"	"	"
1987	-6.3	-3.2	-5.4	1.9	3.6	7.8	12.4	11.5	11.2	4.8	-0.6	-1.0	3.1
1988	"	"	"	"	"	"	"	"	"	"	"	"	"
1989	-0.4	-0.5	1.4	0.9	6.3	7.7	11.5	11.3	7.8	5.6	-1.4	-2.4	4.0
1990	-3.1	-0.7	1.0	0.6	6.9	8.6	11.9	11.8	7.3	5.0	-1.9	-7.2	3.4
81-90	-3.3	-1.4	-1.0	1.1	5.6	8.0	11.9	11.5	8.8	5.1	-1.3	-3.5	3.5
1991	-4.4	-6.6	0.7	0.1	2.3	8.3	12.6	12.7	9.6	2.3	-2.4	-4.4	2.5
1992	-2.9	-3.5	-1.2	0.9	7.2	7.9	11.9	13.4	7.4	0.4	0.3	-3.8	3.2
1993	-3.1	-4.1	-3.1	1.7	7.1	9.0	9.7	11.3	5.6	2.4	-3.1	-4.0	2.5
1994	-4.0	-5.2	2.2	0.0	6.3	9.9	14.1	13.2	7.6	4.0	2.4	-2.2	4.0
1995	-7.3	-2.1	-4.0	1.7	5.8	7.9	14.1	10.7	5.3	7.7	-2.3	-5.4	2.7
1996	-3.8	"	"	"	"	10.7	11.0	10.2	5.1	3.7	-1.9	-4.8	"
1997	-2.9	-1.8	1.0	0.0	6.3	8.8	10.6	12.5	10.9	"	"	-4.5	"
1998	-4.3	0.4	-2.6	0.5	6.4	10.2	11.7	12.3	6.5	2.9	-4.3	-4.7	2.9
1999	-4.4	-6.1	-1.5	1.6	7.8	8.6	11.9	11.2	9.0	4.4	-3.6	-5.8	2.8
2000	-4.8	-3.2	-0.9	3.0	7.6	11.0	9.6	12.3	8.3	3.8	-2.6	-3.7	3.4
91	-4.2	-3.6	-1.1	1.0	6.3	9.2	11.7	12.0	7.5	3.5	-1.9	-4.3	3.0
2001	-6.7	-4.3	-0.3	-0.4	7.5	8.2	12.0	12.6	4.4	6.9	-1.0	-5.9	2.8
2002	-2.7	-2.3	-0.1	1.1	6.3	11.8	11.4	10.6	6.5	3.8	-0.8	-3.3	3.5
2003	"	"	"	"	"	"	"	"	"	"	"	"	"
2004	-6.7	-3.8	-3.3	1.2	4.6	9.8	11.4	11.5	8.6	4.6	-0.7	-3.3	2.8
2005	-5.3	-8.9	-2.1	1.6	7.2	11.4	11.7	9.4	8.6	5.0	-2.4	-7.1	2.4
2006	-6.5	-5.5	-4.7	1.4	6.1	10.8	14.4	8.6	11.2	6.0	0.5	-1.6	3.4
2007	-2.2	-2.3	-1.4	6.2	7.3	10.8	11.6	10.8	6.2	3.7	-2.2	-4.7	3.6
2008	-3.4	-1.8	-3.1	-0.1	6.8	11.0	11.2	11.7	6.5	4.7	-2.0	-5.3	3.0
2009	-6.5	-6.5	-2.8	2.8	8.3	9.7	11.9	13.0	8.8	3.4	-0.5	-7.6	2.8
2010	-7.9	-7.0	-4.0	0.8	4.1	9.2	12.9	10.6	7.1	2.4	-2.3	-8.1	1.5
2001	-5.3	-4.7	-2.4	1.6	6.5	10.3	12.0	11.0	7.5	4.5	-1.3	-5.2	2.9
2011	-5.5	-2.4	-0.7	4.5	8.0	10.0	10.2	12.9	10.2	4.1	2.3	-4.0	4.1
2012	-4.4	-7.0	1.8	1.0	6.9	11.5	12.3	13.3	8.2	4.6	0.0	-6.0	3.5
2013	-4.2	-7.4	-3.1	2.6	4.8	9.7	13.7	12.3	9.3	4.5	-1.5	-1.8	3.2
2014	-3.9	-4.1	0.6	3.5	"	"	"	"	"	"	"	"	"
2015	"	"	"	"	7.6	11.6	16.2	13.5	7.3	4.4	3.7	2.0	"
2016	-3.9	-2.7	-1.9	2.8	5.6	10.6	13.1	12.7	10.3	3.3	-0.8	-0.6	4.0
2017													
2018													
2019													
2020													
11-20	-4.4	-4.7	-0.7	2.9	6.6	10.7	13.1	12.9	9.0	4.2	0.7	-2.1	3.7

Table 10. Monthly average temperature in Sulfen (University of Bolzano 2017b).

Solda - Suldén														
Cod.	06400MS		1907			m s.m./ù.M.			X_UTM 622375			Y_UTM 5152605		
Anno	1	2	3	4	5	6	7	8	9	10	11	12	Anno	
Jahr	1	2	3	4	5	6	7	8	9	10	11	12	Jahr	
1925	2.2	110.7	42.2	100.4	69.8	47.2	63.1	141.0	57.3	40.0	60.0	57.3	791.2	
1926	25.0	32.3	55.8	71.5	131.4	149.4	142.4	61.6	58.2	224.0	57.0	19.7	1018.5	
1927	92.0	7.7	62.9	50.0	34.3	126.4	127.4	97.6	177.5	30.0	131.6	19.7	947.9	
1928	30.6	6.7	46.2	187.0	47.6	44.2	135.6	106.3	92.2	180.0	40.0	11.7	928.1	
1929	20.6	10.0	0.0	18.9	76.0	41.3	46.2	185.7	10.0	70.0	35.0	36.3	550.0	
1930	5.8	5.7	31.0	95.0	76.9	55.6	97.6	91.3	81.4	65.0	15.7	16.9	637.9	
21-30	29.4	28.9	39.7	87.1	72.7	77.4	102.1	113.9	79.4	101.5	56.6	23.7	812.4	
1931	25.6	55.0	35.0	25.0	85.7	40.9	82.5	149.8	38.1	53.0	23.6	2.4	616.6	
1932	2.1	2.5	9.7	47.7	60.2	31.0	75.2	8.9	55.9	50.3	8.3	21.0	372.8	
1933	11.5	11.8	23.2	16.8	85.3	111.9	72.0	67.4	35.3	75.3	78.5	24.1	613.1	
1934	"	"	"	"	"	"	"	"	"	"	"	"	"	
1935	6.1	55.0	0.0	20.3	69.7	8.7	37.0	135.9	36.4	107.1	74.7	25.3	576.2	
1936	26.9	47.6	45.0	46.2	98.9	31.4	59.1	30.4	41.3	10.9	44.1	44.8	526.6	
1937	"	"	"	"	"	"	"	"	"	"	"	"	"	
1938	"	"	"	"	"	"	"	"	"	"	"	"	"	
1939	"	"	"	"	"	"	"	"	"	"	"	"	"	
1940	"	"	"	"	"	"	"	"	"	"	"	"	"	
31-40	14.4	34.4	22.6	31.2	80.0	44.8	65.2	78.5	41.4	59.3	45.8	23.5	541.1	
1941	"	"	"	"	"	"	"	"	"	"	"	"	"	
1942	"	"	"	"	"	"	"	"	"	"	"	"	"	
1943	"	"	"	"	"	"	"	"	"	"	"	"	"	
1944	"	"	"	"	"	"	"	"	"	"	"	"	"	
1945	"	"	"	"	"	"	"	"	"	"	"	"	"	
1946	"	"	"	"	"	"	"	"	"	"	"	"	"	
1947	"	"	"	"	"	"	"	"	"	"	"	"	"	
1948	"	"	"	"	"	"	"	"	"	"	"	"	"	
1949	"	"	"	"	"	"	"	"	"	"	"	"	"	
1950	21.8	51.6	7.9	89.6	12.4	50.6	55.5	73.5	36.8	13.1	34.2	24.2	471.2	
41-50	21.8	51.6	7.9	89.6	12.4	50.6	55.5	73.5	36.8	13.1	34.2	24.2	471.2	
1951	40.2	72.1	56.7	38.9	36.0	46.1	70.8	79.3	51.7	20.1	102.3	5.8	620.0	
1952	5.3	5.3	15.0	23.9	24.3	45.8	30.5	79.6	57.9	80.4	17.1	20.1	405.2	
1953	1.2	1.3	0.0	34.6	5.6	67.1	92.4	55.0	56.5	79.2	0.0	3.5	396.4	
1954	6.7	12.5	37.6	42.9	55.4	81.7	30.5	121.5	60.3	26.3	16.1	137.1	628.6	
1955	24.0	122.0	18.0	7.4	85.1	114.5	88.3	80.2	86.7	41.6	13.0	14.8	695.6	
1956	7.7	0.6	6.7	53.0	69.0	104.8	91.3	147.0	83.5	24.3	1.9	0.5	590.3	
1957	2.3	11.8	18.1	39.7	98.8	159.0	132.5	149.6	35.1	10.2	52.0	2.2	711.3	
1958	9.9	24.0	2.5	27.6	46.0	116.4	124.2	100.2	58.7	81.2	38.9	36.7	666.3	
1959	0.6	0.0	14.1	47.9	95.6	79.1	80.5	60.0	14.4	47.3	13.7	18.9	472.1	
1960	4.5	10.3	12.3	23.5	55.9	90.9	123.2	146.6	175.8	204.9	33.2	30.2	911.3	
51-60	10.2	26.0	18.1	33.9	57.2	90.5	86.4	101.9	68.1	61.6	28.8	27.0	609.7	
1961	12.7	4.9	1.6	48.4	61.9	84.3	89.3	67.4	21.6	80.2	27.2	16.3	515.8	
1962	54.5	14.5	50.5	108.1	61.7	32.8	48.1	64.1	38.4	34.5	89.6	22.0	618.8	
1963	3.9	17.1	53.5	70.4	50.6	79.6	88.4	156.2	84.3	11.9	86.2	23.0	725.1	
1964	0.4	2.2	17.7	13.4	29.4	79.7	91.7	99.2	20.5	69.3	22.6	4.7	450.8	
1965	4.9	0.8	15.7	35.0	91.3	103.7	183.5	118.6	223.2	9.3	12.4	7.2	805.6	
1966	0.9	13.0	1.8	42.0	79.7	53.9	142.1	197.5	23.6	65.1	28.8	9.1	657.5	
1967	1.5	7.3	77.2	66.2	49.4	35.4	102.5	131.0	93.6	37.4	88.7	7.2	697.4	
1968	27.8	84.1	27.4	46.2	51.9	117.5	68.5	139.8	116.0	24.4	89.2	36.3	829.1	
1969	25.8	52.9	41.5	25.3	104.7	107.4	60.3	103.8	30.0	3.4	111.8	16.8	683.7	
1970	59.0	54.6	68.7	85.5	60.8	71.2	85.0	212.7	79.1	30.7	78.8	33.4	919.5	
61-70	19.1	25.1	35.6	54.1	64.1	76.6	95.9	129.0	73.0	36.6	63.5	17.6	690.2	
1971	27.6	41.0	71.3	29.3	86.5	125.6	77.2	138.7	23.9	8.3	65.7	10.3	705.4	
1972	21.4	61.1	38.2	102.9	57.4	152.9	196.4	48.9	80.6	18.5	32.3	22.7	833.3	
1973	47.2	9.2	20.5	32.9	98.2	58.5	137.1	108.8	124.8	117.3	11.9	29.8	796.2	
1974	8.8	45.9	53.4	64.3	96.8	167.3	78.7	81.4	110.1	58.7	44.8	5.1	815.3	
1975	20.3	9.4	55.3	49.7	109.6	94.6	145.6	139.8	133.8	102.2	23.1	55.6	939.0	
1976	7.0	19.7	8.2	39.2	64.1	16.5	185.7	83.2	265.0	188.5	80.2	39.4	996.7	
1977	123.3	123.1	90.0	96.5	207.0	69.9	81.5	212.1	26.6	53.2	41.1	28.0	1152.3	
1978	"	"	"	"	"	"	"	"	"	"	"	"	"	
1979	"	"	"	"	"	"	"	"	"	"	"	"	"	
1980	"	"	"	"	"	"	"	"	"	"	"	"	"	
71-80	36.5	44.2	48.1	59.3	102.8	97.9	128.9	116.1	109.3	78.1	42.7	27.3	891.2	
1981	"	"	"	"	"	"	"	"	"	"	"	"	"	
1982	"	"	"	"	"	"	"	"	"	"	"	"	"	
1983	"	"	"	"	"	"	"	"	"	"	"	"	"	
1984	"	"	"	"	"	"	"	"	"	"	"	"	"	
1985	"	"	"	"	"	"	"	"	"	"	"	"	"	
1986	"	"	"	"	"	"	"	"	"	"	"	"	"	
1987	29.2	61.0	27.0	96.6	110.8	151.8	193.2	105.4	112.8	109.6	53.8	18.2	1069.4	
1988	"	"	"	"	"	"	"	"	"	"	"	"	"	
1989	"	"	"	"	"	"	"	"	"	"	"	"	"	
1990	18.2	21.2	34.2	92.2	42.2	163.6	86.2	62.6	71.2	86.4	122.6	36.8	837.4	
81-90	23.7	41.1	30.6	94.4	76.5	157.7	139.7	84.0	92.0	98.0	88.2	27.5	953.4	
1991	19.0	18.0	93.8	58.8	64.8	117.0	97.4	53.4	93.8	86.8	54.0	52.8	809.6	
1992	11.0	11.2	26.2	154.8	35.2	153.8	93.0	69.4	85.0	216.2	47.4	111.0	1014.2	
1993	0.2	2.4	29.0	50.8	62.8	79.2	124.4	135.2	194.4	329.2	28.4	27.0	1063.0	
1994	88.2	16.0	33.2	63.0	135.2	112.2	114.2	108.6	214.2	30.4	65.8	20.0	1001.0	
1995	27.8	37.2	34.8	55.0	93.6	128.6	101.8	68.2	92.0	3.0	16.4	55.6	714.0	
1996	50.0	18.2	13.5	28.0	162.0	97.2	127.2	143.6	46.8	90.8	119.0	14.8	911.1	
1997	24.0	5.8	9.0	21.8	45.6	205.2	64.2	69.6	26.2	15.8	121.6	60.2	669.0	
1998	15.8	11.4	2.2	81.8	19.4	93.2	101.4	55.4	82.4	86.0	18.8	1.2	569.0	
1999	20.8	17.0	48.0	31.4	82.2	105.0	64.0	164.2	112.2	103.8	38.0	25.8	812.4	
2000	22.0	24.8	61.8	72.6	47.4	54.8	125.4	100.4	69.8	152.2	189.2	28.2	948.6	
91-2000	27.9	16.2	35.2	61.8	74.8	114.6	101.3	96.8	101.7	111.4	69.9	39.7	851.3	
2001	79.0	8.2	77.2	63.0	39.6	150.4	113.6	101.6	66.8	30.8	17.4	7.2	754.8	
2002	1.2	35.6	35.0	43.0	120.4	90.6	95.6	83.6	65.0	49.0	254.4	32.4	905.8	
2003	"	"	"	"	"	"	"	"	"	"	"	"	"	
2004	15.2	17.2	32.8	23.0	45.6	32.2	129.8	67.0	36.4	84.8	45.2	28.8	558.0	
2005	2.8	4.6	12.2	54.2	61.0	32.2	66.6	90.8	35.8	78.4	17.0	19.2	474.8	
2006	11.2	34.8	35.0	60.4	62.8	48.4	76.6	100.6	56.4	91.2	10.0	24.0	611.4	
2007	23.6	15.6	35.0	8.2	83.8	86.4	109.0	115.0	59.6	16.2	35.4	5.6	593.4	
2008	41.2	9.0	23.0	87.4	93.6	91.2	160.6	74.6	88.8	46.4	78.4	71.6	865.8	
2009	40.2	37.8	45.2	56.8	10.4	74.2	92.6	59.2	59.6	16.4	49.4	119.6	661.4	
2010	16.0	"	"	"	"	"	"	202.5	94.3	85.0	163.0	65.4	"	
2001-10	25.6	20.4	36.9	49.5	64.7	75.7	105.6	99.4	62.5	55.4	74.5	41.5	711.7	
2011	11.1	33.1	47.8	17.5	85.8	173.1	157.0	92.6	198.4	68.9	33.2	26.7	945.2	
2012	26.9	9.0	16.8	103.4	80.7	120.3	182.3	157.5	190.5	77.2	162.9	22.7	1150.2	
2013	40.5	24.7	59.5	95.										

APPENDIX D – CDI-VALUES OF R1 BEFORE AND AFTER CROSS-DATING

In the following tables the CDI-values before and after the cross-dating are displayed. The beige coloured values represent the CDI-values after the grouping and cross-dating took place. The white coloured cells shows the CDI-values just before the cross-dating. The samples are however already shifted to begin at the date of death, which the samples display after the cross-dating but before any refilling rings were added (see appendix B “death-year before cross-dating” in table 8. and 9.)

	R1 LD 004	R1 LD 05	R1 LD 08	R1 LD 11	R1 LD 19	R1 LD 21b	R1 LD 27b	MeanG I	MeanG II	MeanGIII
R1 LD 004		29	21	21	42	11	17	44	4	6
R1 LD 05	-		18	13	28	10	27	44	56	6
R1 LD 08	18	-		22	31	19	11	59	1	2
R1 LD 11	-	-	4		16	29	4	61	8	8
R1 LD 19	2	-	-	-		13	11	47	2	6
R1 LD 21b	-	-	12	11	-		12	62	3	4
R1 LD 27b	7	13	-	-	4	10		33	9	2
MeanGI	-	-	-	-	-	-	-		7	5
MeanGII	-	-	-	-	-	-	-	-		9
MeanGIII	-	-	-	-	-	-	-	-	-	

Table 12. CDI-values of group I R1LD (author 2017).

	R1 LD 001	R1 LD 02	R1 LD 03b	R1 LD 04	R1 LD 06	R1 LD 10a	R1 LD 18	R1 LD 23b	MeanG I	MeanG II	MeanG III
R1 LD 001		17	20	6	17	13	16	5	1	26	2
R1 LD 02	7		7	46	14	31	16	15	5	68	10
R1 LD 03b	-	20		5	7	13	18	5	9	42	10
R1 LD 04	-	-	-		9	14	10	8	8	52	4
R1 LD 06	-	23	-	2		11	13	2	2	37	15
R1 LD 10a	-	-	-	13	3		19	6	1	48	1
R1 LD 18	7	-	-	-	-	-		2	5	23	8
R1 LD 23b	11	-	-	-	-	-	-		4	27	4
MeanGI	-	-	-	-	-	-	-	-		7	5
MeanGII	-	-	-	-	-	-	-	-	-		9
MeanGIII	-	-	-	-	-	-	-	-	-	-	

Table 13. CDI-values of group II R1LD (author 2017).

	R1 LD 09	R1 LD 13	R1 LD 17	R1 LD 21a	R1 LD 26b	MeanG I	MeanG II	MeanG III
R1 LD 09		10	18	5	24	13	11	53
R1 LD 13	-		8	4	14	5	4	27
R1 LD 17	-	-		24	28	9	3	74
R1 LD 21a	16	-	-		12	11	4	32
R1 LD 26b	-	-	-	-		5	8	65
MeanGI	-	-	-	-	-		7	5
MeanGII	-	-	-	-	-	-		9
MeanGIII	-	-	-	-	-	-	-	

Table 14. CDI-values of group III R1LD (author 2017).

	R1 LD 002a	R1 LD 002b	R1 LD 03a	R1 LD 14	R1 LD 15	R1 LD 23a	R1 LD 27a	MeanG I	MeanG II	MeanG III
R1 LD 002a		8	9	4	1	4	3	6	2	2
R1 LD 002b	8		11	7	4	10	7	6	1	5
R1 LD 03a	-	11		6	4	2	5	12	6	8
R1 LD 14	4	-	6		5	1	1	5	8	2
R1 LD 15	-	-	-	5		2	2	2	3	5
R1 LD 23a	-	10	-	-	-		10	3	11	7
R1 LD 27a	-	-	-	-	-	10		2	3	7
MeanGI	-	-	-	-	-	-	-		7	5
MeanGII	-	-	-	-	-	-	-	-		9
MeanGIII	-	-	-	-	-	-	-	-	-	

Table 15. CDI-values of group 0 R1LD (author 2017).

	R1 RD 001	R1 RD 002	R1 RD 003a	R1 RD 00005	R1 RD 05	R1 RD 08	R1 RD 12	R1 RD 13	MeanG I	MeanG II	MeanG III	MeanG IV	MeanG V
R1 RD 001		22	23	10	14	16	18	9	44	4	14	4	7
R1 RD 002	3		27	7	17	9	11	3	38	2	4	8	5
R1 RD 003a	4	4		13	22	21	25	34	72	4	3	6	5
R1 RD 00005	5	7	7		14	16	7	1	31	9	2	2	7
R1 RD 05	19	1	4	1		18	24	10	37	2	2	1	3
R1 RD 08	1	2	20	1	7		11	15	53	4	7	4	4
R1 RD 12	11	4	6	5	5	6		8	40	5	4	4	5
R1 RD 13	4	1	3	7	7	3	7		28	7	3	5	6
MeanGI	-	-	-	-	-	-	-	-		4	5	5	5
MeanGII	-	-	-	-	-	-	-	-	-		4	3	10
MeanGIII	-	-	-	-	-	-	-	-	-	-		11	1
MeanGIV	-	-	-	-	-	-	-	-	-	-	-		3
MeanGV	-	-	-	-	-	-	-	-	-	-	-	-	

Table 16. CDI-values of group I R1RD (author 2017).

	R1 RD 00001	R1 RD 01b	R1 RD 00003	R1 RD 03	R1 RD 00006	R1 RD 11	R1 RD 15b	MeanG I	MeanG II	MeanG III	MeanG IV	MeanG V
R1 RD 00001		23	15	19	22	23	13	2	52	11	2	2
R1 RD 01b	4		13	66	17	16	20	3	60	2	5	11
R1 RD 00003	6	6		9	22	20	7	6	43	4	6	9
R1 RD 03	4	1	5		21	16	20	2	48	4	5	15
R1 RD 00006	12	8	6	19		31	12	2	48	3	4	13
R1 RD 11	8	11	5	8	5		13	1	62	2	5	12
R1 RD 15b	3	0	2	7	7	7		5	35	3	1	2
MeanGI	-	-	-	-	-	-	-	-	4	5	5	5
MeanGII	-	-	-	-	-	-	-	-		4	3	10
MeanGIII	-	-	-	-	-	-	-	-	-		11	1
MeanGIV	-	-	-	-	-	-	-	-	-	-		3
MeanGV	-	-	-	-	-	-	-	-	-	-	-	

Table 17. CDI-values of group II R1RD (author 2017).

	R1 RD 02	R1 RD 15c	MeanG I	MeanG II	MeanG III	MeanG IV	MeanG V
R1 RD 02		19	8	4	148	16	2
R1 RD 15c	10		3	5	46	3	3
MeanGI	-	-		4	5	5	5
MeanGII	-	-	-		4	3	10
MeanGIII	-	-	-	-		11	1
MeanGIV	-	-	-	-	-		3
MeanGV	-	-	-	-	-	-	

Table 18. CDI-values of group III R1RD (author 2017).

	R1 RD 09	R1 RD 14	R1 RD 15a	MeanG I	MeanG II	MeanG III	MeanG IV	MeanG V
R1 RD 09		14	21	4	4	2	69	3
R1 RD 14	5		18	4	6	8	43	10
R1 RD 15a	13	9		4	2	6	71	1
MeanGI	-	-	-		4	5	5	5
MeanGII	-	-	-	-		4	3	10
MeanGIII	-	-	-	-	-		11	1
MeanGIV	-	-	-	-	-	-		3
MeanGV	-	-	-	-	-	-	-	

Table 19. CDI-values of group IV R1RD (author 2017).

	R1 RD 06	R1 RD 07	MeanG I	MeanG II	MeanG III	MeanG IV	MeanG V
R1 RD 06		16	7	9	7	1	83
R1 RD 07	5		2	9	5	4	86
MeanGI	-	-		4	5	5	5
MeanGII	-	-	-		4	3	10
MeanGIII	-	-	-	-		11	1
MeanGIV	-	-	-	-	-		3
MeanGV	-	-	-	-	-	-	

Table 20. CDI-values of group V R1RD (author 2017).

	R1 RD 00002	R1 RD 04	R1 RD 00009	R1 RD 00011	R1 RD 15e	R1 RD 16	MeanG I	MeanG II	MeanG III	MeanG IV	MeanG V
R1 RD 00002		2	4	5	9	1	3	2	1	2	5
R1 RD 04	2		2	5	5	6	8	3	1	1	2
R1 RD 00009	4	2		5	8	3	3	5	4	9	1
R1 RD 00011	6	2	2		1	1	7	3	3	11	6
R1 RD 15e	9	5	8	15		1	3	12	7	9	3
R1 RD 16	1	6	3	1	1		3	13	10	3	5
MeanGI	-	-	-	-	-	-		4	5	5	5
MeanGII	-	-	-	-	-	-	-		4	3	10
MeanGIII	-	-	-	-	-	-	-	-		11	1
MeanGIV	-	-	-	-	-	-	-	-	-		3
MeanGV	-	-	-	-	-	-	-	-	-	-	

Table 21. CDI-values of group 0 R1RD (author 2017).

	r1 (middle)	r2 (left)	r3 (right)
r1 (middle)		70	68
r2 (left)	43		80
r3 (right)	55	50	

Table 22. CDI-values of multiple radii of R1 RD 003a (author 2017).

APPENDIX E – GLK-VALUES OF R1 BEFORE AND AFTER CROSS-DATING

The following tables shows analogously to appendix D the GLK-values before and after the cross-dating. The same criteria as the CDI-values and the same considerations as already described in appendix D were applied.

	R1 LD 004	R1 LD 05	R1 LD 08	R1 LD 11	R1 LD 19	R1 LD 21b	R1 LD 27b	MeanG I	MeanG II	MeanG III
R1 LD 004		73	78	71	82	71	71	83	61	45
R1 LD 05	-		74	66	28	71	82	82	58	47
R1 LD 08	63	-		67	69	81	64	89	49	42
R1 LD 11	-	-	71		73	60	58	74	53	65
R1 LD 19	63	-	-	-		73	68	79	55	51
R1 LD 21b	-	-	79	62	-		72	81	55	45
R1 LD 27b	65	56	-	-	67	53		78	59	43
MeanGI	-	-	-	-	-	-	-		58	51
MeanGII	-	-	-	-	-	-	-	-		57
MeanGIII	-	-	-	-	-	-	-	-	-	

Table 23. GLK-values of group I R1LD (author 2017).

	R1 LD 001	R1 LD 02	R1 LD 03b	R1 LD 04	R1 LD 06	R1 LD 10a	R1 LD 18	R1 LD 23b	MeanG I	MeanG II	MeanG III
R1 LD 001		78	70	73	63	66	61	56	65	74	63
R1 LD 02	60		68	76	70	81	75	63	58	91	54
R1 LD 03b	-	66		62	62	69	55	55	54	73	58
R1 LD 04	-	-	-		62	65	67	56	54	72	54
R1 LD 06	-	54	-	54		66	77	57	47	74	63
R1 LD 10a	-	-	-	54	58		62	66	49	80	54
R1 LD 18	63	-	-	-	-	-		58	57	70	67
R1 LD 23b	58	-	-	-	-	-	-		42	68	55
MeanGI	-	-	-	-	-	-	-	-		58	51
MeanGII	-	-	-	-	-	-	-	-	-		57
MeanGIII	-	-	-	-	-	-	-	-	-	-	

Table 24. GLK-values of group II R1LD (author 2017).

	R1 LD 09	R1 LD 13	R1 LD 17	R1 LD 21a	R1 LD 26b	MeanG I	MeanG II	MeanG III
R1 LD 09		63	69	59	65	57	56	76
R1 LD 13	-		70	66	73	52	54	82
R1 LD 17	-	-		68	68	56	56	79
R1 LD 21a	62	-	-		73	51	52	76
R1 LD 26b	-	-	-	-		44	52	80
MeanGI	-	-	-	-	-		58	51
MeanGII	-	-	-	-	-	-		57
MeanGIII	-	-	-	-	-	-	-	

Table 25. GLK-values of group III R1LD (author 2017).

	R1 LD 002a	R1 LD 002b	R1 LD 03a	R1 LD 14	R1 LD 15	R1 LD 23a	R1 LD 27a	MeanGI	MeanG II	MeanG III
R1 LD 002a		39	43	60	55	58	53	40	39	48
R1 LD 002b	39		42	44	53	35	44	46	41	54
R1 LD 03a	-	42		47	42	47	52	55	36	42
R1 LD 14	60	-	47		55	49	51	42	46	39
R1 LD 15	-	-	-	55		43	43	50	51	53
R1 LD 23a	-	35	-	-	-		61	43	60	51
R1 LD 27a	-	-	-	-	-	61		40	53	51
MeanGI	-	-	-	-	-	-	-		58	51
MeanGII	-	-	-	-	-	-	-	-		57
MeanGIII	-	-	-	-	-	-	-	-	-	

Table 26. GLK-values of group 0 R1LD (author 2017).

	R1 RD 001	R1 RD 002	R1 RD 003a	R1 RD 00005	R1 RD 05	R1 RD 08	R1 RD 12	R1 RD 13	MeanG I	MeanG II	MeanG III	MeanG IV	MeanG V
R1 RD 001		59	75	77	71	76	67	60	76	54	45	45	36
R1 RD 002	59		71	60	68	59	64	55	72	42	42	42	60
R1 RD 003a	41	31		58	71	68	83	74	80	29	43	52	46
R1 RD 00005	28	31	60		65	63	73	50	69	56	54	53	38
R1 RD 05	60	39	55	43		77	81	40	75	50	52	48	45
R1 RD 08	59	54	51	47	69		67	62	53	52	39	42	42
R1 RD 12	56	47	35	34	63	50		71	87	40	47	58	47
R1 RD 13	58	43	59	55	61	55	56		71	27	39	54	50
MeanGI	-	-	-	-	-	-	-	-		44	44	54	32
MeanGII	-	-	-	-	-	-	-	-	-		41	41	49
MeanGIII	-	-	-	-	-	-	-	-	-	-		62	44
MeanGIV	-	-	-	-	-	-	-	-	-	-	-		50
MeanGV	-	-	-	-	-	-	-	-	-	-	-	-	

Table 27. GLK-values of group I R1RD (author 2017).

	R1 RD 00001	R1 RD 01b	R1 RD 00003	R1 RD 03	R1 RD 00006	R1 RD 11	R1 RD 15b	MeanG I	MeanG II	MeanG III	MeanG IV	MeanG V
R1 RD 00001		62	59	69	68	72	64	40	62	51	47	56
R1 RD 01b	50		55	76	63	62	67	47	83	49	43	35
R1 RD 00003	43	42		52	55	62	63	41	69	42	42	50
R1 RD 03	59	49	44		67	68	72	44	76	57	49	47
R1 RD 00006	69	45	41	50		65	51	44	71	56	40	44
R1 RD 11	46	57	53	60	44		66	46	80	44	45	53
R1 RD 15b	46	56	64	56	42	64		54	76	55	58	47
MeanGI	-	-	-	-	-	-	-		44	44	54	32
MeanGII	-	-	-	-	-	-	-	-		41	41	49
MeanGIII	-	-	-	-	-	-	-	-	-		62	44
MeanGIV	-	-	-	-	-	-	-	-	-	-		50
MeanGV	-	-	-	-	-	-	-	-	-	-	-	

Table 28. GLK-values of group II R1RD (author 2017).

	R1 RD 02	R1 RD 15c	MeanG I	MeanG II	MeanG III	MeanG IV	MeanG V
R1 RD 02		73	48	54	87	71	46
R1 RD 15c	69		39	50	90	55	47
MeanGI	-	-		44	44	54	32
MeanGII	-	-	-		41	41	49
MeanGIII	-	-	-	-		62	44
MeanGIV	-	-	-	-	-		50
MeanGV	-	-	-	-	-	-	

Table 29. GLK-values of group III R1RD (author 2017).

	R1 RD 09	R1 RD 14	R1 RD 15a	MeanG I	MeanG II	MeanG III	MeanG IV	MeanG V
R1 RD 09		66	73	49	45	50	83	54
R1 RD 14	35		72	38	47	59	75	61
R1 RD 15a	64	64		48	53	65	87	54
MeanGI	-	-	-		44	44	54	32
MeanGII	-	-	-	-		41	41	49
MeanGIII	-	-	-	-	-		62	44
MeanGIV	-	-	-	-	-	-		50
MeanGV	-	-	-	-	-	-	-	

Table 30. GLK-values of group IV R1RD (author 2017).

	R1 RD 06	R1 RD 07	MeanG I	MeanG II	MeanG III	MeanG IV	MeanG V
R1 RD 06		73	38	44	46	54	83
R1 RD 07	57		34	52	44	53	90
MeanGI	-	-		44	44	54	32
MeanGII	-	-	-		41	41	49
MeanGIII	-	-	-	-		62	44
MeanGIV	-	-	-	-	-		50
MeanGV	-	-	-	-	-	-	

Table 31. GLK-values of group V R1RD (author 2017).

	R1 RD 00002	R1 RD 04	R1 RD 00009	R1 RD 00011	R1 RD 15e	R1 RD 16	MeanG I	MeanG II	MeanG III	MeanG IV	MeanG V
R1 RD 00002		44	47	48	27	59	48	49	58	40	47
R1 RD 04	44		28	43	52	44	65	52	33	44	52
R1 RD 00009	47	28		59	49	43	44	56	61	47	53
R1 RD 00011	51	46	50		62	33	54	52	45	55	43
R1 RD 15e	27	52	49	59		45	51	58	45	61	36
R1 RD 16	59	44	43	41	45		45	52	61	41	58
MeanGI	-	-	-	-	-	-		44	44	54	32
MeanGII	-	-	-	-	-	-	-		41	41	49
MeanGIII	-	-	-	-	-	-	-	-		62	44
MeanGIV	-	-	-	-	-	-	-	-	-		50
MeanGV	-	-	-	-	-	-	-	-	-	-	

Table 32. GLK-values of group 0 R1RD (author 2017).

	r1 (middle)	r2 (left)	r3 (right)
r1 (middle)		70	68
r2 (left)	43		80
r3 (right)	55	50	

Table 33. GLK-values of multiple radii of R1RD 003a (author 2017).

APPENDIX F – GSL-VALUES OF R1 BEFORE AND AFTER CROSS-DATING

The following tables shows analogously to appendix D the GSL-values before and after the cross-dating. The same criteria as the CDI-values and the same considerations as already described in appendix D were applied.

	R1 LD 004	R1 LD 05	R1 LD 08	R1 LD 11	R1 LD 19	R1 LD 21b	R1 LD 27b	MeanG I	MeanG II	MeanGIII
R1 LD 004		***	***	**	***	***	***	***	*	-
R1 LD 05	-		**	**	***	***	***	***	-	-
R1 LD 08	-	-		*	**	***	*	***	-	-
R1 LD 11	-	-	**		***	-	-	***	-	*
R1 LD 19	*	-	-	-		***	**	***	-	-
R1 LD 21b	-	-	***	*	-		***	***	-	-
R1 LD 27b	*	-	-	-	**	-		***	-	-
MeanGI	-	-	-	-	-	-	-		-	-
MeanGII	-	-	-	-	-	-	-	-		-
MeanGIII	-	-	-	-	-	-	-	-	-	

Table 34. GSL-values of group I R1LD (author 2017).

	R1 LD 001	R1 LD 02	R1 LD 03b	R1 LD 04	R1 LD 06	R1 LD 10a	R1 LD 18	R1 LD 23b	MeanG I	MeanG II	MeanG III
R1 LD 001		***	**	**	-	*	-	-	*	**	-
R1 LD 02	-		**	***	***	***	***	*	-	***	-
R1 LD 03b	-	*		*	*	**	-	-	-	***	-
R1 LD 04	-	-	-		*	**	**	-	-	***	-
R1 LD 06	-	-	-	-		**	***	-	-	***	*
R1 LD 10a	-	-	-	-	-		*	**	-	***	-
R1 LD 18	-	-	-	-	-	-		-	-	**	**
R1 LD 23b	-	-	-	-	-	-	-		-	**	-
MeanGI	-	-	-	-	-	-	-	-		-	-
MeanGII	-	-	-	-	-	-	-	-	-		-
MeanGIII	-	-	-	-	-	-	-	-	-	-	

Table 35. GSL-values of group II R1LD (author 2017).

	R1 LD 09	R1 LD 13	R1 LD 17	R1 LD 21a	R1 LD 26b	MeanG I	MeanG II	MeanG III
R1 LD 09		*	***	-	**	-	-	***
R1 LD 13	-		***	*	***	-	-	***
R1 LD 17	-	-		**	**	-	-	***
R1 LD 21a	-	-	-		**	-	-	***
R1 LD 26b	-	-	-	-		-	-	***
MeanGI	-	-	-	-	-		-	-
MeanGII	-	-	-	-	-	-		-
MeanGIII	-	-	-	-	-	-	-	

Table 36. GSL-values of group III R1LD (author 2017).

	R1 LD 002a	R1 LD 002b	R1 LD 03a	R1 LD 14	R1 LD 15	R1 LD 23a	R1 LD 27a	MeanGI	MeanG II	MeanG III
R1 LD 002a		-	-	-	-	-	-	-	-	-
R1 LD 002b	-		-	-	-	-	-	-	-	-
R1 LD 03a	-	-		-	-	-	-	-	-	-
R1 LD 14	-	-	-		-	-	-	-	-	-
R1 LD 15	-	-	-	-		-	-	-	-	-
R1 LD 23a	-	-	-	-	-		*	-	-	-
R1 LD 27a	-	-	-	-	-	*		-	-	-
MeanGI	-	-	-	-	-	-	-		-	-
MeanGII	-	-	-	-	-	-	-	-		-
MeanGIII	-	-	-	-	-	-	-	-	-	

Table 37. GSL-values of group 0 R1LD (author 2017).

	R1 RD 001	R1 RD 002	R1 RD 003a	R1 RD 00005	R1 RD 05	R1 RD 08	R1 RD 12	R1 RD 13	MeanG I	MeanG II	MeanG III	MeanG IV	MeanG V
R1 RD 001		-	***	***	**	***	*	-	***	-	-	-	-
R1 RD 002	-		**	-	*	-	*	-	**	-	-	-	-
R1 RD 003a	-	-		-	***	**	***	***	***	-	-	-	-
R1 RD 00005	-	-	-		**	*	**	-	***	-	-	-	-
R1 RD 05	-	-	-	-		***	***	-	***	-	-	-	-
R1 RD 08	-	-	-	-	**		*	-	***	-	-	-	-
R1 RD 12	-	-	-	-	-	-		**	***	-	-	-	-
R1 RD 13	-	-	-	-	-	-	-		**	-	-	-	-
MeanGI	-	-	-	-	-	-	-	-		-	-	-	-
MeanGII	-	-	-	-	-	-	-	-	-		-	-	-
MeanGIII	-	-	-	-	-	-	-	-	-	-		*	-
MeanGIV	-	-	-	-	-	-	-	-	-	-	-		-
MeanGV	-	-	-	-	-	-	-	-	-	-	-	-	

Table 38. GSL-values of group I R1RD (author 2017).

	R1 RD 00001	R1 RD 01b	R1 RD 00003	R1 RD 03	R1 RD 00006	R1 RD 11	R1 RD 15b	MeanG I	MeanG II	MeanG III	MeanG IV	MeanG V
R1 RD 00001		*	-	**	**	***	*	-	***	-	-	-
R1 RD 01b	-		-	***	*	*	*	-	***	-	-	-
R1 RD 00003	-	-		-	-	*	-	-	**	-	-	-
R1 RD 03	-	-	-		**	**	**	-	***	-	-	-
R1 RD 00006	**	-	-	-		**	-	-	***	-	-	-
R1 RD 11	-	-	-	-	-		*	-	***	-	-	-
R1 RD 15b	-	-	*	-	-	*		-	***	-	-	-
MeanGI	-	-	-	-	-	-	-		-	-	-	-
MeanGII	-	-	-	-	-	-	-	-		-	-	-
MeanGIII	-	-	-	-	-	-	-	-	-		*	-
MeanGIV	-	-	-	-	-	-	-	-	-	-		-
MeanGV	-	-	-	-	-	-	-	-	-	-	-	

Table 39. GSL-values of group II R1RD (author 2017).

	R1 RD 02	R1 RD 15c	MeanG I	MeanG II	MeanG III	MeanG IV	MeanG V
R1 RD 02		***	-	-	***	***	-
R1 RD 15c	**		-	-	***	-	-
MeanGI	-	-		-	-	-	-
MeanGII	-	-	-		-	-	-
MeanGIII	-	-	-	-		*	-
MeanGIV	-	-	-	-	-		-
MeanGV	-	-	-	-	-	-	

Table 40. GSL-values of group III R1RD (author 2017).

	R1 RD 09	R1 RD 14	R1 RD 15a	MeanG I	MeanG II	MeanG III	MeanG IV	MeanG V
R1 RD 09		*	***	-	-	-	***	-
R1 RD 14	-		***	-	-	-	***	*
R1 RD 15a	*	*		-	-	*	***	-
MeanGI	-	-	-		-	-	-	-
MeanGII	-	-	-	-		-	-	-
MeanGIII	-	-	-	-	-		*	-
MeanGIV	-	-	-	-	-	-		-
MeanGV	-	-	-	-	-	-	-	

Table 41. GSL-values of group IV R1RD (author 2017).

	R1 RD 06	R1 RD 07	MeanG I	MeanG II	MeanG III	MeanG IV	MeanG V
R1 RD 06		***	-	-	-	-	***
R1 RD 07	-		-	-	-	-	***
MeanGI	-	-		-	-	-	-
MeanGII	-	-	-		-	-	-
MeanGIII	-	-	-	-		*	-
MeanGIV	-	-	-	-	-		-
MeanGV	-	-	-	-	-	-	

Table 42. GSL-values of group V R1RD (author 2017).

	R1 RD 00002	R1 RD 04	R1 RD 00009	R1 RD 00011	R1 RD 15e	R1 RD 16	MeanG I	MeanG II	MeanG III	MeanG IV	MeanG V
R1 RD 00002		-	-	-	-	-	-	-	-	-	-
R1 RD 04	-		-	-	-	-	-	-	-	-	-
R1 RD 00009	-	-		-	-	-	-	-	-	-	-
R1 RD 00011	-	-	-		-	-	-	-	-	-	-
R1 RD 15e	-	-	-	-		-	-	-	-	-	-
R1 RD 16	-	-	-	-	-		-	-	*	-	-
MeanGI	-	-	-	-	-	-		-	-	-	-
MeanGII	-	-	-	-	-	-	-		-	-	-
MeanGIII	-	-	-	-	-	-	-	-		*	-
MeanGIV	-	-	-	-	-	-	-	-	-		-
MeanGV	-	-	-	-	-	-	-	-	-	-	

Table 43. GSL-values of group 0 R1RD (author 2017).

	r1 (middle)	r2 (left)	r3 (right)
r1 (middle)		***	**
r2 (left)	-		***
r3 (right)	-	-	

Table 44. GSL-values of multiple radii of R1RD 003a (author 2017).

ACKNOWLEDGMENTS

First of all I would like to thank my supervisors Holger Gärtner and Markus Egli for their great help and guidance during my master thesis. A big thank you goes to my family members Mauro, Rossella and Anna Fontana, for their encouragement, support in the field and in the logistic. Also I'm very grateful to the employees of the WSL Birmensdorf, in particular Anne Verstege and Loic Schneider, who helped me with their knowledge during the sample preparation and the data evaluation. I also thank the Swiss Federal Institute for Forest, Snow and Landscape Research WSL for allowing me to absolve my work at the WSL facilities in Birmensdorf. I would like to express my gratitude to Claudio Mutinelli of the University of Bolzano for providing the climate data of Sulden. Further I express my appreciation to the students of the field course 2016 in Sulden for their help in collecting part of the samples. Not least a big thank goes to Rahel Aus der Au, Nancy Bolze, Michael Holborn, Jasmin Bertschi, Christelle Bovier and Richard Peters for their helpfulness.

PERSONAL DECLARATION

Personal declaration: I hereby declare that the submitted thesis is the result of my own, independent work. All external sources are explicitly acknowledged in the thesis.

Date

Signature

Giulia Fontana